THE UNIVERSITY *of* EDINBURGH

The role of tetrahydrobiopterin in biological NO synthesis

Ben Gazur

Doctor of Philosophy

University of Edinburgh

2012

I solemnly declare that the work in this thesis is entirely my own, except where otherwise stated and referenced. This work has not been previously been submitted for any other degree, though it may have been published.

Ben Gazur

For my Mum and Dad

A scholar ther was of Maidenhead also,
That un-to logik hadde longe y-go.
As lene was his hors as was a rake,
And he nas nat right fat, I undertake;
But loked holwe, and ther-to soberly.
Ful thredbar was his overest courtepy;
For he had geten him yet no benefyce,
Ne was so worldly for to have offyce.
For him was lever have at his beddes heed
Twenty bokes, clad in black or reed,
Of Aristotle and his philosophye,
Than robes riche, or fithele, or gaye sautrye.
But al be that he was a philosophre,
Yet hadde he but littel gold in cofre.
But al that he mighte of his freendes hente,
On bokes and on lerninge he it spente,
And bisily gan for the soules preye
Of hem that yaf him wher-with to scoleye.

Figure 0.1- adapted from Chaucer *et al* (1388)

Acknowledgements

I would first like to thank Simon Daff for giving me the opportunity to work in his lab and in particular on this fascinating/infuriating project (delete as appropriate to the day). Thanks also to Steve Chapman and Chris Mowat for their advice and toleration. Graeme Reid was also kind and easy going with my usurpation of his lab space.

Davide and Chiara trained me in the basics of this project and gave me a bedrock of data on which to build this thesis. Sarah cleverly got me into the lab rhythm. Thanks also go to Borran, Fei, Sally, and Sidong for making the time in the lab fun. George, Martin and Fanny have been a pleasure to work with and too nice to get angry at my meddling in their projects. Laura has been a crystallographic marvel.

Much of the work in this thesis resulted from collaboration with Craig McInnes and Colin Suckling of Strathclyde. Thanks for the analogues on demand!

My project students/slaves did lots of helpful work in many areas. I thank Angela and Aden, and Omar and Jillian for providing the comic relief to my work and I wish them all the best in the future.

Finally I need to thank my friends and family. My friends have given me hot meals when I forget to feed myself and a glass of wine, which St Paul says is good for the stomach. My family have been ever supportive and listened to long and incomprehensible rants regarding pterins, electrons and mutants. Anna, Luke, Ella and Aden, thanks. None of this would be possible without Mum and Dad, so thanks for the germplasm, food packages and all the laughter.

Friends

Following complaints, and in no particular order…

Anna Calvert for her tea, parties, and many a roaring rendition of ‘God Save the Queen!’

Han and Jam for the most comfortable floor in Edinburgh.

Iain and Vladimir. ABC Forever!

Sal and mighty Hrothgar for all the laughter in the world and the Gazur Duelling Girdle.

Nic for lightsabre battles, party rings and too long on the N64.

Beth and Matt, and Alfie and Aslan, for much support and roast chicken.

Olly and Jess for perudo, pubs and public bickering. And Jason.

Ben for much the nerdiest coffees in town.

Abstract

Nitric oxide synthase (NOS) catalyses the production of nitric oxide (NO). A cytochrome P450-like oxygenase, it uses two monooxygenation steps to convert L-arginine (L-arg) first to N^{ω}-hydroxy-L-arginine (NOHA), a stable intermediate, and then to L-citrulline and NO. Mammalian NOSs are homodimeric enzymes. Each monomer is composed of an oxygenase domain (containing the L-arg binding site, a heme ligated by a cysteine thiolate, and a tetrahydrobiopterin (H_4B)) and a reductase domain (binding NADPH, FAD, and FMN). NOS substrates are O_2, L-arg, and NADPH. NADPH is the source of electrons required for oxygen activation. H_4B is a vital cofactor that aids dimerisation and acts as a reducing/oxidising agent. Controversy still exists as to the final oxygenating species in the NOS mechanism, but the general reaction scheme is known. The ferric heme is reduced to the ferrous state by an electron from the reductase domain. Then oxygen binds to form the oxy-ferrous species. Then H_4B donates an electron to form a peroxy-ferric species. It is likely this then forms a compound 1 ($Fe(IV)^{+\cdot}=O$) species that is the final oxygenating species.

This thesis probes the mechanism of NOS to further define the mechanistic intermediates involved. The role of H_4B in NO synthesis has been probed in both normal turnover conditions and special case reactions.

To elucidate this mechanism further a mutant with a residue capable of stabilising the activated oxygen species was created, G586S, where glycine 586 of nNOS was replaced with a serine. This serine was within hydrogen bonding distance of the oxy-heme. A stabilised intermediate was observed by stopped flow reaction in the presence of H_4B, but not aH_4B (an inactive pterin analogue). Here single turnover reactions, each following either the reaction of L-arg to NOHA or NOHA to citrulline, were performed on the mutant using an external source of electrons. The reaction products were observed by HPLC. The mutant appears capable of the conversion of NOHA to citrulline, but not L-arg to NOHA. The WT enzyme appears capable of both. The intermediate is observed with either L-arg or NOHA bound, suggesting both reactions proceed via the same active oxygenating species. The inability of the mutant to catalyse the conversion of L-arg to NOHA may be due to protonation of the substrate hindering reaction such that the active oxygenating species decays before reaction can occur. This mutation, in allowing separation of the two monooxygenation steps, deserves further study.

H_4B binds at the dimer interface of NOS. Here the π-systems of the pterins are only 13Å apart. This is within allowed distances for efficient electron transfer. Electron transfer between hemes, via the pterins, would allow a route for the breakdown of a dead end, ferrous-NO, species. Stopped flow monitoring of the decay of the ferrous-heme NO complex with nNOSoxy dimers with varying proportions of the hemes in the ferrous heme-NO complex showed no electron transfer between hemes of the dimer. The rate of decay of

the ferrous heme-NO complex in oxygenated buffer is 0.12 s^{-1} for all conditions tested here.

H_4B-deficiency leads to several diseases. H_4B makes a poor drug due to instability and cost, the search for druggable analogues of it is ongoing. H_4B analogues blocked at the 6,7-positions in the dihydropterine-form have been screened here for catalytic activity. Several have shown comparable ability to catalyse NO production *in vitro*. Structure function analysis of these analogues has revealed the extent extension is tolerated at the C6 and C7 positions of the pterin.

Content

List of figures

Chapter 3- nNOSG586S

Chapter 4- Inter-pterin electron transfer

Chapter 5- Analogues of H_4B

Abbreviations

Standard amino acid abbreviations are used throughout, e.g. Tryptophan is Trp or W.

Mutations are referred to by single letter amino acid codes and location within the protein. Thus a mutation the glycine at position 586 in the nNOS protein to a serine would be called G586S.

A	Absorbance
Al	Autoinhibitory Loop
aH_4B	4-amino-tetrahydrobiopterin
ATP	Adenosine triphosphate
CaM	Calmodulin
cGMP	Cyclic guanosine monophosphate
cNOS	Constitutive nitric oxide synthase
CO	Carbon monoxide
Da	Dalton
DMSO	Dimethyl sulphoxide
DTT	Dithiotheitol
ε	Molar extinction coefficient
EDRF	Endothelial relaxation factor
EDTA	Ethylenediametetraacetic acid
EGTA	Ethyleneglycoltetraacetic acid
eNOS	Endothelial nitric oxide synthase
EPR	Electron paramagnetic resonance
FAD	Flavin adenine dinucleotide
FMN	Flavin mononucleotide
FNR	Ferredoxin−$NADP^+$ reductase
FPLC	Fast protein liquid chromatography
sGC	Soluble guanylate cyclase
GSH	Glutathione
GTP	Guanosine tripohosphate
H_4B	Tetrahydrobiopterin
HEPES	4-(2-hydroxyethyl)-1-piperazineethanesulfonic acid
HPLC	High pressure liquid chromatography
iNOS	Inducible nitric oxide synthase
IPTG	Isopropyl-β-D-thiogalactoside
K_d	Dissociation constant
KPi	Potassium phosphate buffer
L-arg	L-Arginine
LB	Luria/Bertani
MES	2-(*N*-morpholino)ethanesulfonic acid
MW	Molecular weight
NADPH	Nicotinamide adenine dinucleotide phosphate
NMR	Nuclear magnetic resonance

nNOS	Neuronal nitric oxide synthase
NO	Nitric oxide
NOHA	N-hydroxy-L-arginine
NOS	Nitric oxide synthase
NOSoxy	Nitric oxide synthase oxygenase domain
NOSrd	Nitric oxide synthase reductase domain
OPA	*o*-phthaldialdehyde
PAGE	Polyacrylamide gel electrophoresis
PDB	Protein database
PDZ	Postsynaptic density-95 discs large/ZO-1
PEG	Polyethylene glycol
PMSF	Phenylmethylsulfonyl fluoride
SOC	Super optimal catabolite
SOD	Superoxide dismutase
SDS	Sodium dodecyl sulphate
TB	Terrific broth
Tris	Tris (hydroxymethyl) aminomethane
UV	Ultraviolet
VIS	Visible
WT	Wild type

Chapter One

Introduction

1.1 Nitric oxide

Nitric oxide (NO) is a diatomic radical molecule. NO was, prior to the discovery of its place in physiology, considered a gaseous pollutant. NO is, however, now known as a signalling molecule that is involved in a plethora of physiological processes and vital to the complexity of life (1, and references therein).

Furchgott, Ignarro and Murad were awarded the Nobel Prize in Physiology or Medicine in 1998 for their work in identifying the role of NO as a relaxing agent of blood vessels (2, 3). A previously observed but uncharacterized Endothelial Relaxation Factor (EDRF) was known to relax smooth muscle, particularly in blood vessels. Clues to the identity of the EDRF came from the inhibition of EDRF action by superoxide anions generated by methylene blue. However a key finding was that acidified rather than neutral sodium nitrite produced transient relaxations of the aorta. NO gas was then found to produce similar results. Then Guanylyl-cyclase activation by EDRF was found to be heme dependent, a further link to NO, a fine binder of hemes (4).

Now NO is clearly established as playing a vital role in life. Its physiological roles range from that of being a cytotoxic agent during immune response acting in a cell destructive way, to a neurotransmitter diffusing between synapses to reinforce signal transmission. It is also involved in nitrosylation of proteins, modulating their activity (5). Its ability to fulfill these roles simultaneously is due to its chemical properties. As a small molecule it is able to diffuse rapidly across hundreds of microns. As an uncharged molecule it is able diffuse across lipid membranes and so enter cells. As a radical molecule it is unstable and reactive. It readily forms complexes with transition metals as well as reacting with protein

residues. All of these chemical properties allow NO to play so many varied roles physiological roles. These roles will be discussed further in relation to the biological process of NO formation.

As a diatomic signalling molecule it was a great novelty and research into its production and roles began at once and continued and continues at great pace. Papers are published in great profusion on NO every year. Here the roles of NO will be discussed.

1.2 Nitrosylation

Nitrosylation is a post-translational modification of proteins directly analogous to phosphorylation. Nitrosylation is able to alter the activity of a protein dramatically. The most well known nitrosylation, although not the only possible, is S-nitrosylation, mechanism shown in Figure 1.1 (6).

a) $2\,NO + O_2 \longrightarrow 2\,NO_2$

b) $NO_2 + NO \longrightarrow N_2O_3$

c) $N_2O_3 + RSH \longrightarrow RSNO + HNO_2$

Figure 1.1- This is the generally accepted route for S-nitrosylation. Here R is a cysteine residue to be nitrosylated. To achieve nitrosylation the three distinct steps shown above occur.

S-nitrosylation is the reaction of reactive NO-products with certain cysteine residues in a protein. This can occur randomly, but there are also enzymes which catalyse the reaction specifically. It has also been suggested that S-nitrosylated proteins may act as carriers of NO to prolong its activity and preserve it from the reactive species found physiologically

(7). For example, red blood cells release S-nitrosothiols under low oxygen concentration leading to blood vessel relaxation presumably by NO release from the nitrosothiols (8). Targets of this modification can be proteins with essential roles such as hemoglobin and serum albumin. Misplaced protein nitrosylation and denitrosylation have been associated with pathologies such as myocardial ischemia, atherosclerosis, inflammation, and cancer (9). Clearly these are topics of research interest and therefore NO remains at the forefront of medical science.

1.3 Interaction with Guanylyl Cyclase

The most important enzyme targeted by NO is soluble Guanylyl Cyclase (sGC), the enzyme that catalyses the conversion of guanosine triphosphate (GTP) to cyclic guanosine monophosphate (cGMP), Figure 1.2.

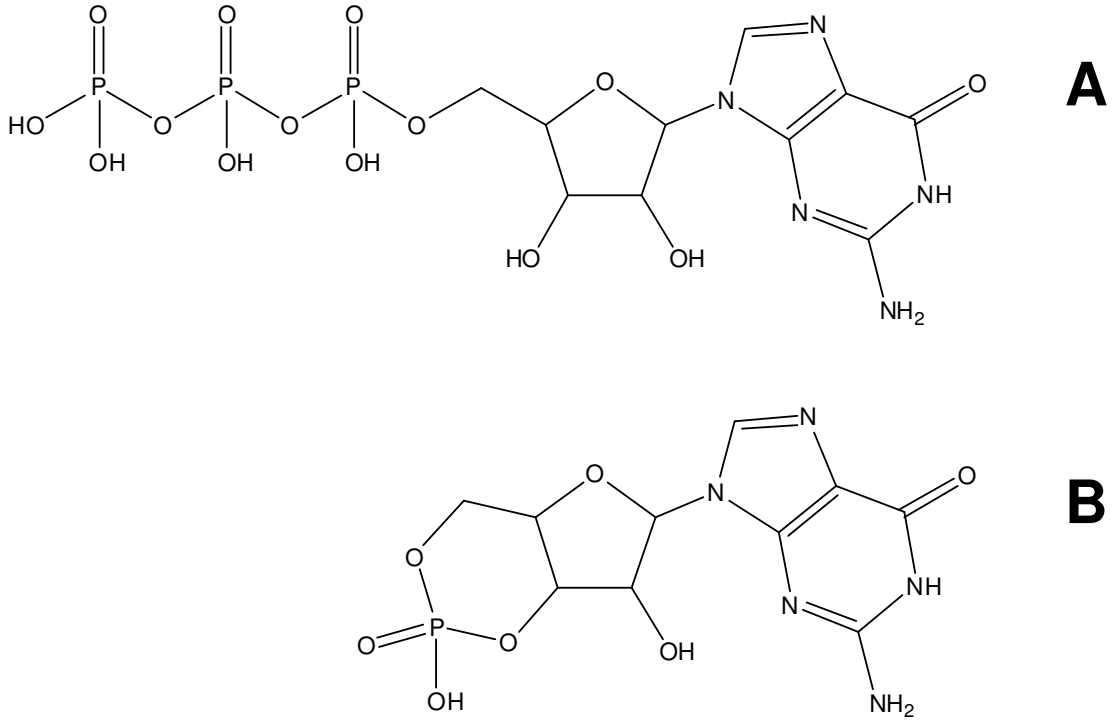

Figure 1.2- Structures of GTP, A, and cGMP, B.

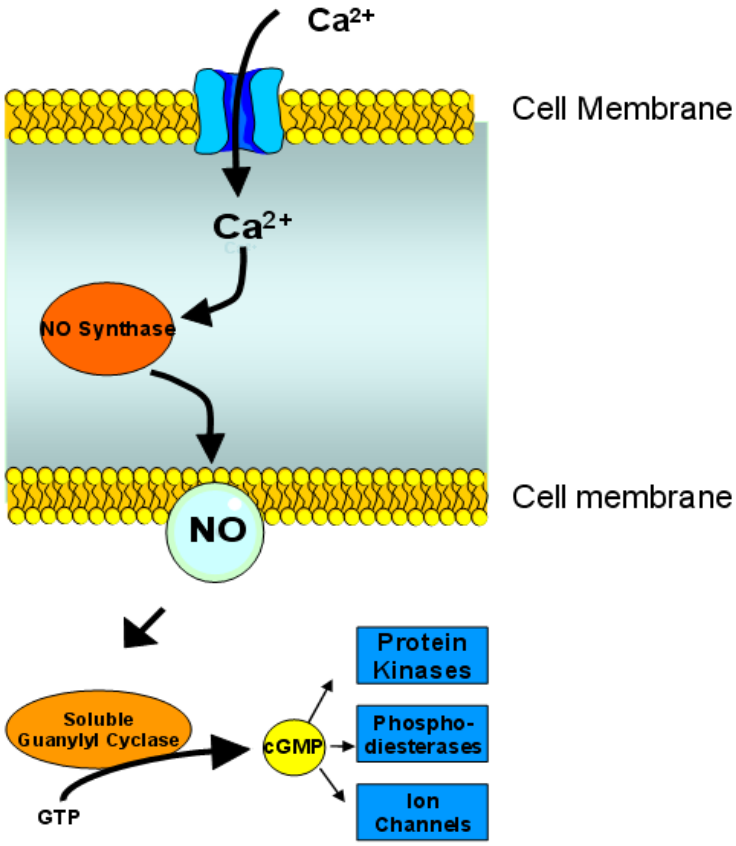

Figure 1.3 - Showing the role NO plays linking Ca^{2+} concentrations to final outcomes. The NO produced by constitutive NOSs in response to increased Ca^{2+} levels may affect intracellular events, or as shown here diffuse between cells. NO activates sGC and promotes production of cGMP. cGMP activates protein kinases, phosphodiesterases and ion channels giving a range of physiological responses. (Adapted from Papale, 2008)

sGC is, in fact, the only known receptor of NO. By NO binding to the heme of sGC a proximal histidine ligand is dissociated and the protein activated. NO binding increases the activity of the enzyme by 300 times (10). This interaction of NO with sGC derives its importance from the huge number of processes in which cGMP has a role. It acts in smooth muscle relaxation, regulation of synaptic transmission and platelet aggregation inhibition. These, and other processes, are controlled through the action of cGMP-

dependent enzymes, such as protein kinases, phosphodiesterases and ion channels. NO production is sensitive to the increase of calcium concentration as will be discussed later. Therefore NO links calcium concentration and the production of cGMP. Figure 1.3 shows the pathway of NO and cGMP (11,12).

1.4 Chemical properties of NO

Some of the most interesting features of NO are due to its radical nature. The unpaired electron of NO, which makes it such a versatile molecule, is in a π^* orbital, Figure 1.4.

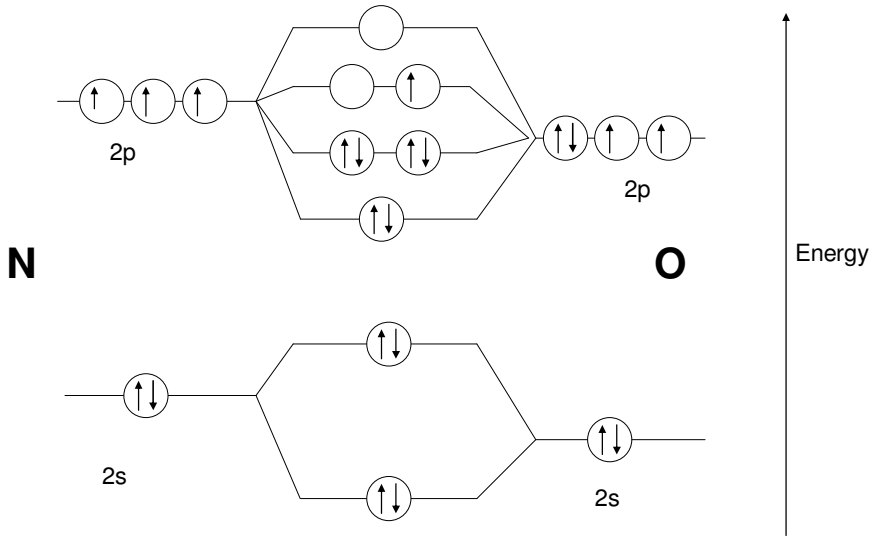

Figure 1.4- Molecular-orbital energy-level diagram for nitric oxide.

The unpaired electron is positioned in an antibonding orbital and is shielded from the nucleus by the inner electrons, allowing it to be easily lost and giving rise to the formation

of NO^+. When complexed with metals, NO can be considered to be either an electron donor or acceptor, binding as either NO^+ (nitrosonium cation) in a linear geometry or as NO^- (nitroxyl anion) in a bent geometry, both via the nitrogen. The relatively small difference in electronegativity between oxygen and nitrogen gives the bond a very limited polar character, with the electrons being more probably found around the oxygen atom. NO can be described as an almost non-polar molecule, allowing it to act as an efficient messenger molecule across the lipid membrane of cells. Being a radical molecule NO is unstable, giving it a limited diffusion range and so localizing the effects of NO production.

What is fascinating is that when in solution NO, unlike other nitrogen and carbon radicals, does not dimerise but remains in the active monomer form (13).

As already said the most significant biological role of NO is in the reaction with the heme group of sGC. How then does NO coordinate with a heme iron?

Unlike other ligands (such as CO and O_2) NO will bind to hemes in either the ferric or ferrous states (as will cyanide and water). The binding of NO to ferric heme is rapidly reversible. It can be considered in either of two states; Fe^{III}-NO or Fe^{II}-NO^+ (14).

NO is a superb ligand for the ferrous heme. This is because of the donation of electrons from the NO to the heme iron and the overlap of the iron d-orbitals and the antibonding orbitals of NO. The ferrous heme-NO complex is such a tightly bound complex that, as shall be seen in the mechanism of NOS, it can be considered a dead-end complex.

1.5 Biological electron transfer

The transfer of electrons underpins all chemical reactions (15). Animals must extract energy stored in chemical bonds in a useful form. This is achieved by a process of gradual oxidation. Oxidation here does not necessarily mean the direct reaction of a molecule with oxygen but the loss of electrons by transfer, often catalysed by proteins. In this thesis protein mediated electron transfer will prove key to the understanding of NOS mechanism. There is a long electron transfer distance to be made in the reductase domain of NOS, and the mechanism of reaction at the active site relies on electron transfer from several sources. To understand this the general theory of electron transfer must be discussed before applying it to biological systems.

The rate of the electron transfer depends upon ΔG^*, the change in energy in the system under standard conditions, according to the following equation,

$$k' = k'_0 \exp [- \Delta G^* / kT] \qquad \textbf{(Eqn. 1)}$$

where k' is the observed electron transfer rate, k'_0 is the rate of electron transfer when ΔG^* is zero, T is the temperature in Kelvin and k is the Boltzmann constant. Generally the rate of electron transfer will increase with ΔG and temperature. However there is an optimal ΔG at which electron transfer is 'activationless' (16).

From orbital theory we see that an electron transfer reaction in a biological system must involve movement of an electron from a donor orbital to an acceptor orbital. This requires the electron to 'tunnel' through the intervening medium, which is of higher

energy, and the extent of the tunnelling necessary is dependent upon the amount of overlap of the electronic wavefunctions of the orbitals involved. The greater the overlap then the faster the rate of electron transfer. It is known from quantum mechanical theory that the energy of electronic wavefunctions decreases exponentially with distance, and therefore it follows that the rate of electron transfer will also decrease exponentially with distance. The strength of the electronic coupling between the donor and acceptor orbitals is given by H_{AB}, the tunnelling matrix element. The value of k'_0 is directly proportional to H_{AB}, which is defined in-

$$\boldsymbol{H_{AB} = H^0_{AB} \exp [-\tfrac{1}{2}\beta (d - d^0)]} \qquad \textbf{(Eqn. 2)}$$

$\boldsymbol{H^0_{AB}}$ is the electronic coupling at close contact ($\boldsymbol{d^0}$), and $\boldsymbol{\beta}$ is the rate of decay of coupling (in $Å^{-1}$) over distance $\boldsymbol{d}$. In a vacuum the value of β is typically about 2.8 $Å^{-1}$, implying that electron transfer can only occur over relatively short distances (17). Long distance electron transfer in biological systems requires that the value of β for the intervening medium be smaller than that observed *in vacuo*, and a value of 1.4 $Å^{-1}$ has been suggested for a protein medium (18). Practically, this value means that a 10-fold decrease in the rate of electron transfer is observed with an increase in distance between the redox centres of 1.7 Å. This general value of β for proteins means that the intervening medium can be thought of as a homogeneous 'organic glass'. Although this approximation may be acceptable for systems optimised for electron transfer, reactions with a more heterogeneous intervening medium require more careful consideration. The explanation for such situations involves tunnelling pathways through covalent bonds, hydrogen

bonds, and direct through-space jumps (19). This complicates consideration of electron transfer in biological systems, where redox centres are normally surrounded by a protein medium. In such cases many differing pathways may be possible routes for electron movement and it is possible that stabilisation of electronic wavefunctions may be greatest in a longer pathway, and electron transfer may therefore occur at a greater rate than it would via the shortest pathway.

1.6 Biological NO synthesis

NO is produced biologically by means of the enzyme nitric oxide synthase (NOS) shown in Figure 1.5 (20). This was the first example of an enzymatic hydroxylation of the L-Arginine (L-Arg) guanidinium group (21).

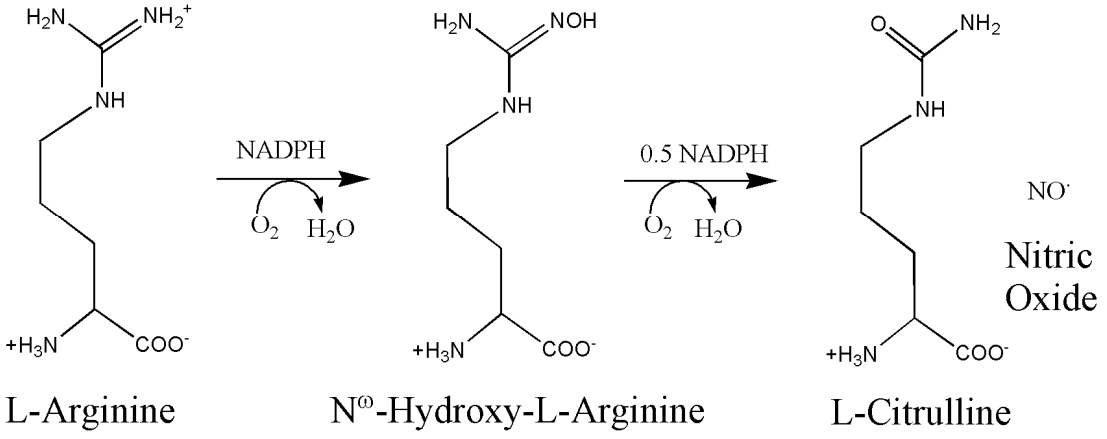

Figure 1.5 - Enzyme catalyzed production of NO showing the two monooxygenation steps performed by nitric oxide synthase.

L-Arginine, once bound into the catalytic site of NOS, can undergo a first oxidation, that, with the consumption of molecular oxygen and 2 electrons, leads to the formation of N^{ω}-

Hydroxy-L-Arginine (NOHA) and water. This reaction intermediate stays bound to the catalytic site and undergoes a second monooxygenation, performed with the consumption of 1 electron equivalent and 1 molecule of oxygen. This leads to the production of water, L-citrulline and nitric oxide. Of course each step can be further broken down into several stages. This more complex reaction scheme is still hotly debated amongst researchers and will be discussed further in the section on the catalytic cycle of nitric oxide synthases.

1.7 NO from Nitrate and Nitrite

There is a second path for NO production that is only now being closely studied (22, 23). Nitrite (NO_2^-) and nitrate (NO_3^-) are the end products of NO oxidation in the body. They are also taken in from the diet. While the NOS derived NO production requires oxygen, NO from the reduction of nitrite does not require oxygen, and is in fact favoured by anoxia. It has been found that as levels of oxygen fall in the blood there is an increase in NO production from nitrite and nitrate (24). Mammals lack specific nitrate and nitrite reductases, but several routes have been suggested. Nitrate must be reduced to nitrite first, it has been suggested that commensal bacteria perform this conversion, and then the stable nitrite must be converted to NO. There are several pathways that can achieve this: involving haemoglobin (25), myoglobin (26), xanthine oxidoreductase (27), ascorbate (28), polyphenols (29) and protons (30). However none of these pathways produces NO at a satisfactory rate under physiological conditions and so the route of NO from nitrite remains an open question.

Under conditions of acidosis or hypoxia the rates of nitrite reduction increase greatly and NO is produced at physiologically relevant rates. This makes physiological sense as under hypoxia the vasodilator effects of NO would be beneficial to increase blood flow to the aeschemic area. The use of nitrite as a therapeutic agent in the case of stroke or anoxia may soon become more common. A truly effective treatment for transient aeschaemic attacks would be aided if a specific and efficient pathway of nitrite reduction was elucidated.

1.8 Nitric Oxide Synthase

The group of enzymes that specifically produce nitric oxide in eukaryotes and in some prokaryotes are called Nitric Oxide Synthases (31). The mammalian NOSs are dimeric proteins in which each subunit is made of two domains, with a specific connecting region between the two that binds calmodulin, Figure 1.6.

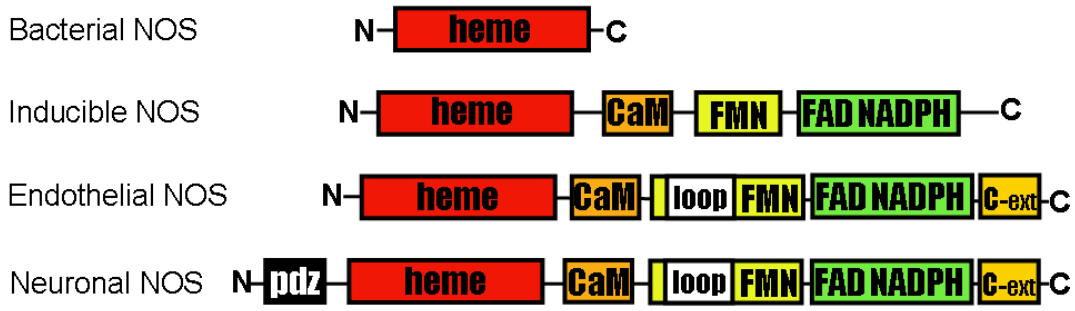

Figure 1.6 - Modular composition of the different NOS isoforms, showing their overall structural similarity though with extensions and inserts leading to isoform speciality. An autoinhibitory loop present in the FMN domain of eNOS and nNOS confers strict control of catalysis to CaM binding.

The N-terminal domain is called the oxygenase or heme domain and binds the cysteine-thiol ligated heme, the substrate L-Arginine, the cofactor (6R)-5,6,7,8-Tetrahydrobiopterin (H_4B) and forms the active site of the enzyme. The C-terminal portion is called the reductase domain and has the function of providing electrons to the heme domain derived from NADPH and transferred to the heme by sequential reduction of FAD and FMN. The connecting region is a flexible domain of approximately 20 amino acid residues capable of binding the small protein calmodulin (CaM) (32). This binding of CaM is possible only when CaM has Ca^{2+} bound to it. The CaM then binds primarily to an alpha-helix linking the reductase and oxygenase domains. The binding of CaM is thought to introduce a degree of motion within the reductase domain allowing the passage of electrons from one domain to the other, Figure 1.7 shows the effect of CaM on electron transfer in the dimer (33). The reductase domain is structurally similar to cytochrome P450 reductases, leading to another interesting link with these mono-oxygenating cytochromes to be further outlined later. In nNOS there is an N-terminal region which forms a PDZ domain. This region interacts with other proteins or intracellular structures in the organization of signal transduction complexes. Specifically the PDZ domain binds to PSD (Post Synaptic Density protein) and targets nNOS to synaptic sites in the brain and skeletal muscle, mediating the membrane association of nNOS in neurons (34).

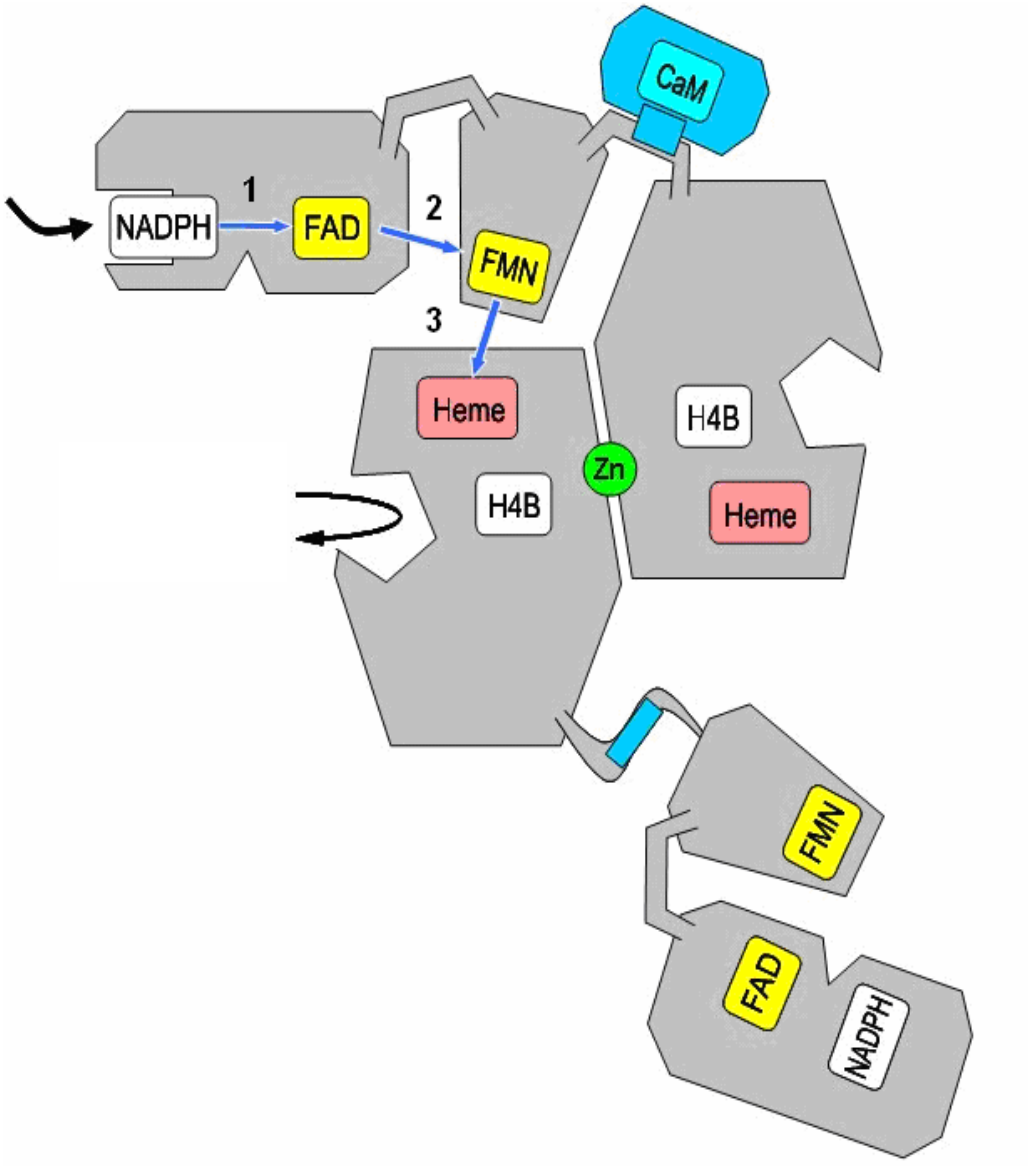

Figure 1.7 - Showing path of electrons through the NOS dimer. 1 is the transfer of a hydride from NADPH to FAD. 2 is the transfer of an electron from FAD to FMN. 3 is the final electron transfer, from FMN to heme. Note that electrons derived from one subunit are passed to the oxygenase domain of the other subunit where NO synthesis occurs. This passage of electrons only occurs when CaM is bound.

All NOSs are functional homodimers. The dimer is formed by a large interface involving the heme domains of each monomer, resulting in a quasi-globular enzyme. Bacterial NOSs are equivalent to the oxygenase domain of mammalian NOSs, lacking

some of the complex control regions, but most importantly the reductase domain and therefore requiring an external source of electrons. The dimer of the mammalian NOSs is supported through interactions involving the H_4B. Each subunit interacts with the H_4B and protein expressed without H_4B exists mainly in the monomer (31). Also supporting the dimer is a Zn^{2+} ion which binds to two cysteines from each subunit, though mutational studies have shown it not to be necessary or sufficient for dimerisation.

In animals three distinct isoforms of NOSs have been identified with a sequence identity of 50 to 60% between them. These are neuronal NOS (nNOS), inducible NOS (iNOS) and endothelial NOS (eNOS), or, respectively, NOS I, II and III (though these terms are rapidly falling into disuse as confusing, and not a moment too soon). The three isoforms can be divided in two other groups; nNOS and eNOS are the two constitutively produced enzymes whose activity is regulated by the binding of CaM. In the other group, iNOS has such a high affinity for CaM that CaM will bind even without the presence Ca^{2+}. It binds irreversibly. The inducible form is therefore primarily regulated at the level of its expression, as once produced it will bind CaM and remain active until the protein is dismantled.

The length of the polypeptide chains of the two main domains are quite similar within the mammalian NOS isoforms, with the heme domain of about 500 residues and the reductase domain of about 700 (from residue 221 to 724 and from 743 to 1429 in nNOS respectively). The overall mass of a neuronal NOS dimer is consequently of about 160 kDa. The X-ray crystal structures of the isolated heme domains are available for all isoforms in a number of conditions (e.g. binding substrates or other ligands into the catalytic site) and for many bacterial NOSs (133, 134, 135, though weekly searches of the

protein database reveal more structures). The structure of the isolated neuronal NOS reductase domain has also been determined (33). On the other hand the structure of an entire mammalian NOS enzyme has not been achieved yet, due to the large size of the protein and the flexibility of portions of it.

1.9 Reductase domain

The NOS reductase domain (Figure 1.8 shows the structure of the reductase domain) is the source of the electrons required for catalysis. It is composed of two subdomains; one binding FMN, and one binding FAD and NADPH. There is a cleft in the FAD/NADPH subdomain that accommodates the FMN subdomain, with the two subdomains connected by a flexible linker region. As we shall see flexibility is key to the functioning of the reductase domain.

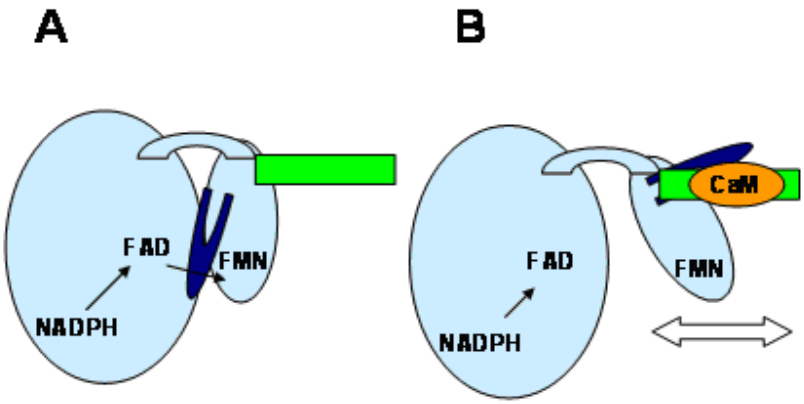

Figure 1.8 - Diagram of the reductase domain and subdomains. In A no CaM is bound. The autoinhibitory loop (dark blue) favours the close association of the FMN subdomain to the NADPH/FAD subdomain. Electrons may transfer to the FMN. When CaM (orange) binds, B, the autoinhibitory loop is rearranged and the FMN subdomain is capable of motion. It may now move towards the oxygenase domain and transfer an electron to the heme. Structure A may be observed in crystal structures (PDB 1TLL, Ref 35), B is inferred from mutagenic studies destabilizing the ionic interactions between the FAD and FMN subdomains and deletion of the autoinhibitory loop (36, 37).

As will be discussed in the section on the heme domain there is no structural resemblance between the heme domain and cytochrome P450s, but a strong resemblance in mechanism. Here we will see there is a strong similarity between the NOS reductase domain and P450 reductases, to the extent that chimaeras of P450 BM3 and the NOS reductase domain are catalytically functional (38). There is a strong structural and functional relationship between the NOSrd and other diflavin reductases. The reductase domain is thought to have been created by a fusion of the genes that coded for proteins that resembled the FMN subdomain and NADPH/FAD subdomain. The FMN subdomain is strongly related to flavodoxin and the NADPH/FAD subdomain to ferredoxin $NADP^+$ reductases.

The domain's function as an electron delivery system is derived from its ability to bind NADPH, Figure 1.9, and the cofactors FAD and FMN, Figure 1.10, being able to shuttle electron through the protein (39). The flavin cofactors have stable partially reduced states that allow temporally controlled single electron delivery to the heme. This, as we shall see in the mechanism section, is vital as the delivery of two electrons at once, as would be derived from direct NADPH oxidation, would be futile. The route of electron delivery, NADPH→FAD→FMN, can be seen in Figure 1.7, and the reductase cofactors in Figures 1.9 and 1.10. The partially reduced states of the flavins and their role in single electron delivery is seen in Figure 1.8.

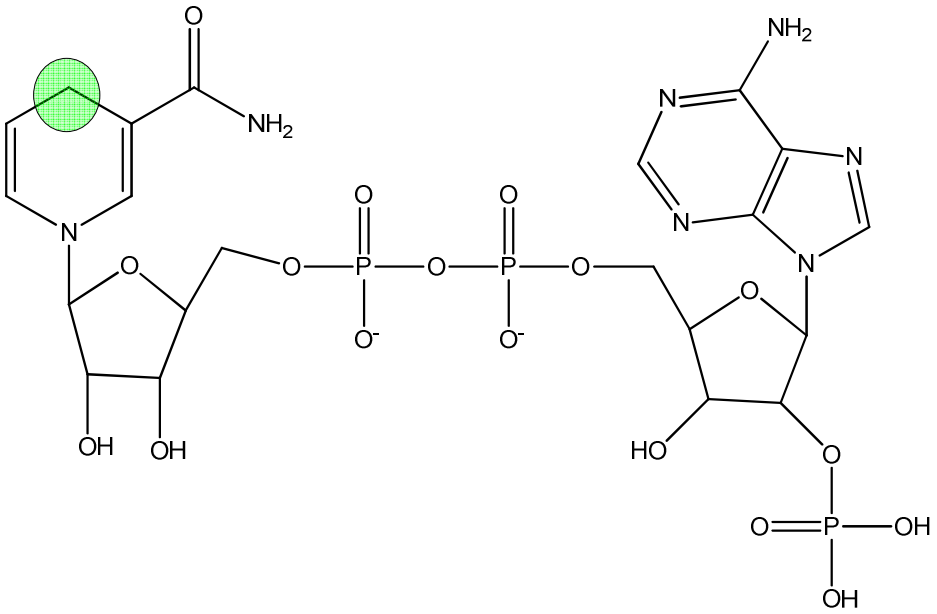

Figure 1.9- NADPH structure. The source of the hydride is circled in green.

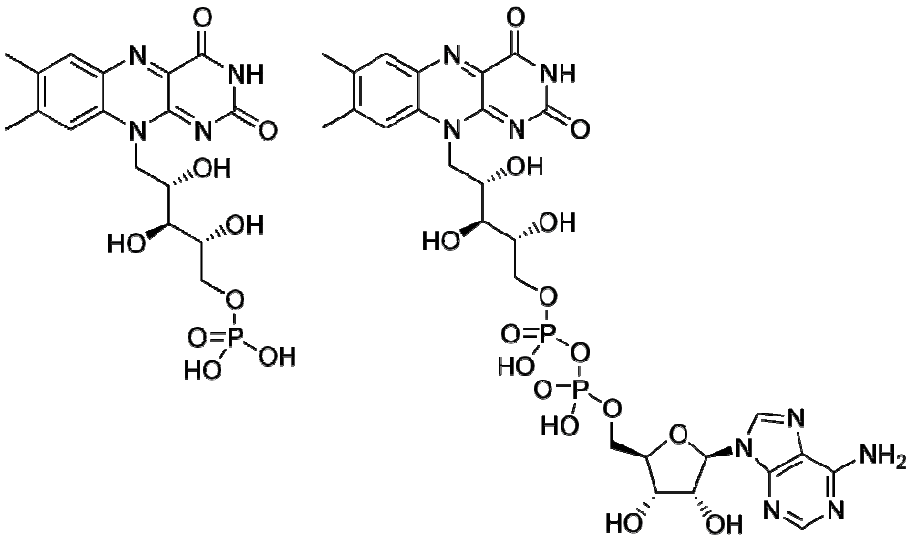

Figure 1.10*:* Diagram of oxidized Flavin Mononucleotide (FMN) and Flavin Adenine Dinucleotide (FAD) showing the common part and the isoalloxazine ring which support the different oxidation states of the cofactors.

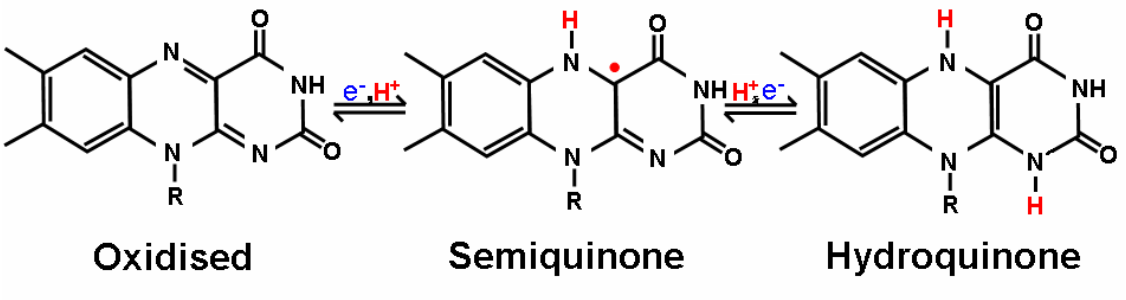

Figure 1.11*:* Different oxidation states assumed by the isoalloxazine rings of FAD and FMN.

1.9.1 Reductase domain electron transfer

The electron delivery mechanism of NOSrd has been studied in depth through the use of truncated constructs of the subdomains and electron acceptors other than the heme domain (40). For example, ferricyanide is a small smolecule and therefore capable of fitting close to either FAD or FMN and being reduced by them. Cytchrome *c*, a protein of sufficient size to be unable to reach FAD, is capable of only accepting electron from FMN (41). Recall, the flow of electrons in the reductase domain is NADPH→FAD→FMN. The reduction rates derived are useful in informing our understanding of electron transfer. Also useful is the ability to follow the oxidation states of the flavins by UV/VIS.

The first step in electron transfer in NOSrd is the transfer of a hydride from the NADPH to the N5 of the bound FAD (41). To allow this transfer to occur the NADPH must move from a non-productive conformation to one that allows π-stacking with the isoalloxazine ring of FAD, Figure 1.12.

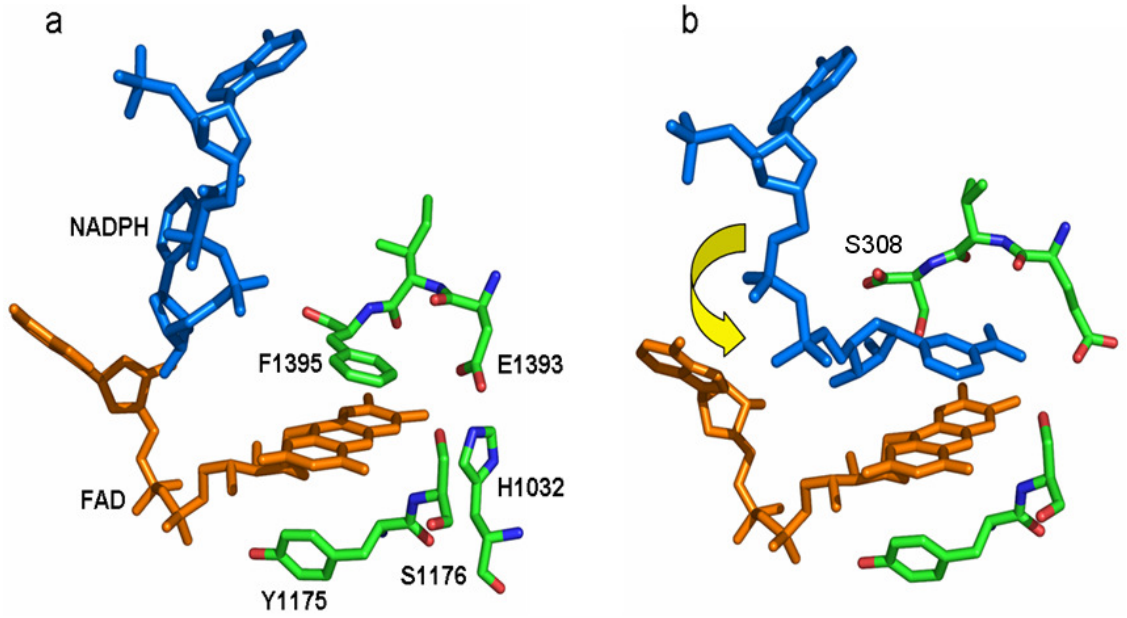

Figure 1.12 - This figure shows how NADPH may bind in a productive (a) or unproductive (b) orientation. The reaction is hydride transfer from NADPH (blue) to FAD (orange): a) is the NADPH/FAD domain of rat nNOS (33) and b) FNR Y308S mutant (38, 42), showing NADPH binding in unproductive and productive conformations respectively. The mutation engineered on FNR, by removal of the tyrosine residue that controls binding in the productive mode, enhanced the stacking of the nicotinamide on FAD achieving a much more ordered structure. The F1395 residue of nNOS, which corresponds to Y308 of FNR, must move before productive binding can occur.

The isoalloxazine ring of FAD must be stacked either with the nicotinamide ring or with a conserved phenylalanine residue (F1395 in rat nNOS), and the mechanism of displacing each other partitions the enzyme into an active or inactive state as a consequence. This mechanism, as well as the secondary structure of the NADPH and FAD binding portion, is shared by the large family of ferredoxin–$NADP^+$ reductase (FNR) proteins.

An equilibrium exists within the reductase domain between NADPH bound in the productive and non-productive states, Figure 1.12. This equilibrium helps to slow the delivery of hydrides and allows for single electron delivery to occur to the heme. Once bound in the productive state a hydride is transferred to the FAD, putting it in the

hydroquinone state, a double reduction. The FAD is held close to the FMN domain, with both buried within the protein. The two subdomains are held in proximity by a conserved electronegative patch on the FMN domain and a corresponding electropositive patch of residues on the FAD domain (43). Held by these salt bridges the domains bring the isoalloxazine rings of the flavins 5Å apart and efficient electron transfer can occur. The domains of the flavins support electron transfer by stabilising the semiquinone forms (45). A conserved serine, Ser1176 in rat nNOS, stabilises the FAD semiquinone via a hydrogen bond to the N5, supporting single electron transfer from the double reduced FAD. Before a second cycle of FAD reduction can occur the proton from the hydride transfer must be removed from the FAD and a series of residues is thought to act a proton transfer pathway between FAD and solvent.

The FMN semiquinone is extremely stable, with Phe809 and Tyr889 in nNOS stacking either side of the isoalloxazine ring. The peptide backbone also forms a hydrogen bond with the N5 of the FMN. These interactions help to prevent the complete oxidation of FMN. This facilitates the single electron transfer to the heme.

No full structure of the holoenzyme exists but studies have undertaken to fit all the structures of the isolated domains together (33). This has yielded the suggestion that the distance between the FMN and the heme it is to deliver electrons to may be as great as 70Å, much beyond the limit of efficient electron transfer. There must be a conformational change in the protein to bring the FMN a reasonable distance from the heme.

Passage of electrons to the heme in NOS is controlled by the binding of CaM. This is true of all NOS isoforms. Without CaM bound the rate of heme reduction is extremely slow. However the rate of flavin reduction without CaM bound is sufficient to allow

turnover of the enzyme, but no products are detected. This suggested that CaM controlled the passage of electrons to the heme. It has also been noted that CaM binding increases the rate of hydride and electron transfer within the reductase domain (37).

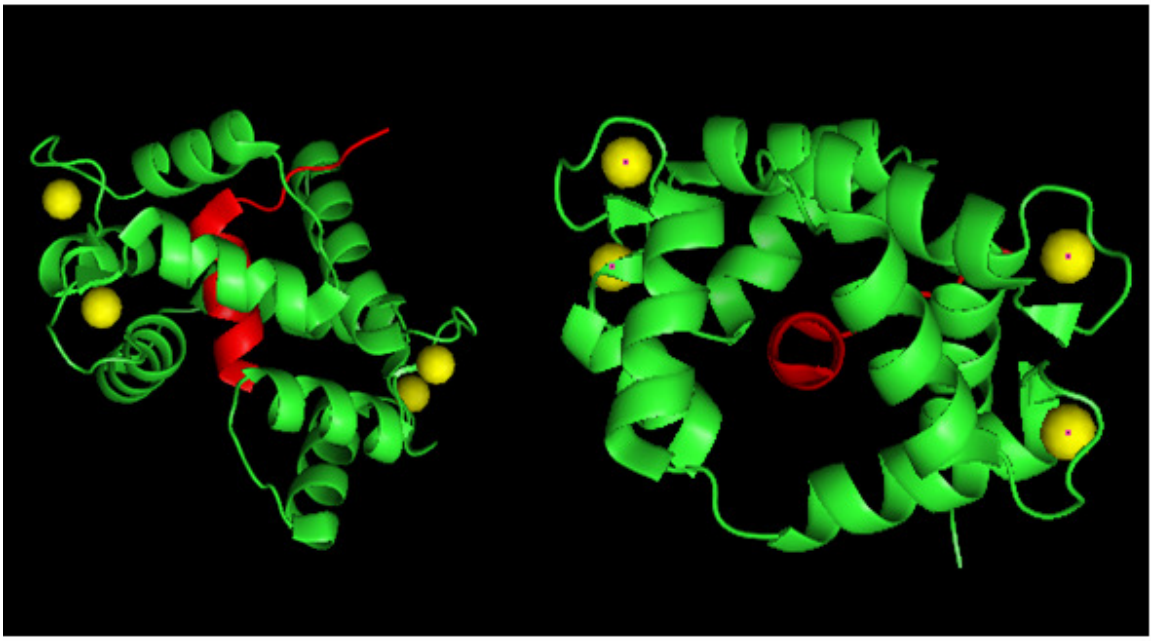

Figure 1.13 - Structure of Calmodulin, green, binding 4 atoms of Ca^{2+}, yellow spheres, while bound to the CaM binding helix of nNOS, red. Shows the CaM protein completely surrounding the helix. This binding opens the structure of the reductase domain. (PDB file 3GOF)

Binding of CaM was shown to occur by the protection of a cleavage site from trypsinolysis in the presence of CaM (45). CaM is a small protein (less then 17 KDa) formed by 4 helix-loop-helix Ca^{2+} binding regions arranged in a double globular structure, Figure 1.13. In the presence of a Ca^{2+} atom, two helices are held in perpendicular to one another resulting in the exposure of hydrophobic residues, which are capable of interacting with recognition sites on NOS. Structures derived from x-ray crystallography and solution NMR show that CaM changes its shape completely on the binding of Ca^{2+}

(46). The binding of CaM to NOS has different features and effects depending on the isotype of NOS. The main difference being between iNOS and constitutive NOSs (cNOSs), eNOS and nNOS. The latter have an affinity for the CaM-Ca^{2+} complex in the range of nM, while that of iNOS is ten fold higher (K_d= 0.1 nM). iNOS is also able to bind CaM in the absence of Ca^{2+} and binds it irreversibly (47).

The different affinities of constitutive NOSs and inducible NOS for CaM rely not only on a different CaM-binding region sequence. There are at least two elements that differentiate the structure of the various isoforms reductase domains: these are an autoregulatory region which is positioned within the FMN-binding subdomain of cNOSs and a C-terminal extension of various lengths. Both elements exert their regulatory role with a mechanism that involve the interaction with CaM and its binding to NOS (48). Due to the flexibility of at least a portion of both elements none of the reductase domain structures yet published tell us about the exact position they have in the different functional conformations of NOS.

The autoregulatory region, or autoinhibitory loop, is an insert of 40-50 amino acids that lowers the affinity of constitutive NOSs for CaM with the result of making the enzyme sensitive to intracellular changes in Ca^{2+} concentration. The insert is in fact in a competition with CaM to bind the region between the two flavin domains. In addition, a role for the autoregulatory insert as a suppressor of electron flow to the heme domain apart from CaM involvement has been inferred: a truncated form of NOS lacking the insert, showed in fact a suboptimal production of NO even in CaM free condition, differently from the WT which has none. The C-terminal extension is present in all the three isoforms of NOS but has a different length, being 21, 33 and 42 residues long in the

inducible, neuronal and endothelial forms respectively. The deletion of the extension produces an enzyme with higher reductase efficiency in the absence of CaM; the deletion mutant activity has no difference with that of the WT when CaM is present. The role of the tail is consequently that of an interflavins electron-flow repressor in the CaM-free NOS. Though studies have shown a complexity in the role of this c-terminal tail (49, 50, 51).

Further investigations analyzing a NOS reductase domain mutant lacking both the insert and C-terminal extension have been made; on the basis of this work a model relying on the concerted interaction of the two elements with CaM has been proposed (52). According to the model two different conformations are assumed by the reductase domain: a locked one where electron flow is allowed within the reductase domain, and an open one which lets electron flow to the heme domain. The switch between the different conformations is determined by the oxidation state of NADP(H): when oxidised $NADP^+$ is released and no longer interacting with the C-terminal extension, which in turn is no longer capable to contact the autoregulatory insert. The loss of this contact determines the conformational change that arranges the reductase domain in order to donate electrons to the heme domain (open).

Activation of electron transfer by CaM binding is independent of the heme domain as CaM is has an activating effect on the isolated reductase domain. CaM binding doesn't affect the reduction potentials of FAD and FMN, indicating that the triggering effect is based on a deep structural rearrangement that shortens the distance from FMN to heme, probably by inducing a degree of conformational mobility (53).

1.10 Heme domain

The heme domain of NOS (Figure 1.14) consists of the approximately 400 N-terminal residues of the protein, though nNOS also has a preceding PDZ-binding domain. The heme domain, or oxygenase domain, as the name suggests, binds a b-type heme via a cysteine thiol linkage to the heme iron. All the NOS heme domains share a strong sequence homology, ~50%, and also share an overall tertiary structure.

Figure 1.14 - A nNOS heme domain dimer showing the heme (red) and H_4B (blue and green). The H_4Bs lie within the dimer interface, which is approximately vertical in the above diagram (PDB file: 1OM4, unpublished paper).

The quasi-globular structure of the heme domain is fairly rigid and has very few flexible portions. This has allowed for successful crystallography of the isolated heme domain. The largest portion of the domain, it would be hard to describe any subdomains as in NOSrd, is formed from the residues that compose the binding site of the substrate. These residues are highly conserved as the substrate must be specific and maintained in both the correct orientation to the heme iron and at the correct distance from it. Figure 1.15 shows the active site heme and residues.

The second important portion of the domain consists of the helical region below the heme concerned with the binding of H_4B and dimerisation. This region contacts both with the H_4B in its domain and the H_4B of the partner domain in the dimer. This shared binding structure of H_4B gives it a key role in the dimerisation of the enzyme.

The heme is held by a proximal thiolate linkage, from Cys415 in rat nNOS. This leaves little space on the proximal side of the heme, but a relatively large binding pocket exists on the distal that forms the active site (54). On the rim of the heme are several hydrophobic residues that further stabilise binding, particularly Leu424, Leu559, Trp587, Met589, Val649, Phe704 and Tyr706 in rat nNOS. There are also stacking interactions from Phe584, on the distal heme, and Trp409, on the proximal. Trp409 also interacts with Cys415 and so may also have a role in modulating the electron density of the heme iron via the thiolate.

The active site binding pocket is formed by a large β-sheet whose residue side chains radiate into the active site, particularly Val567, Pro565, Tyr588 and Ile593 in rat nNOS.

1.10.1 The active site

The active site of NOS is relatively large, externally, but narrows towards the heme (55).

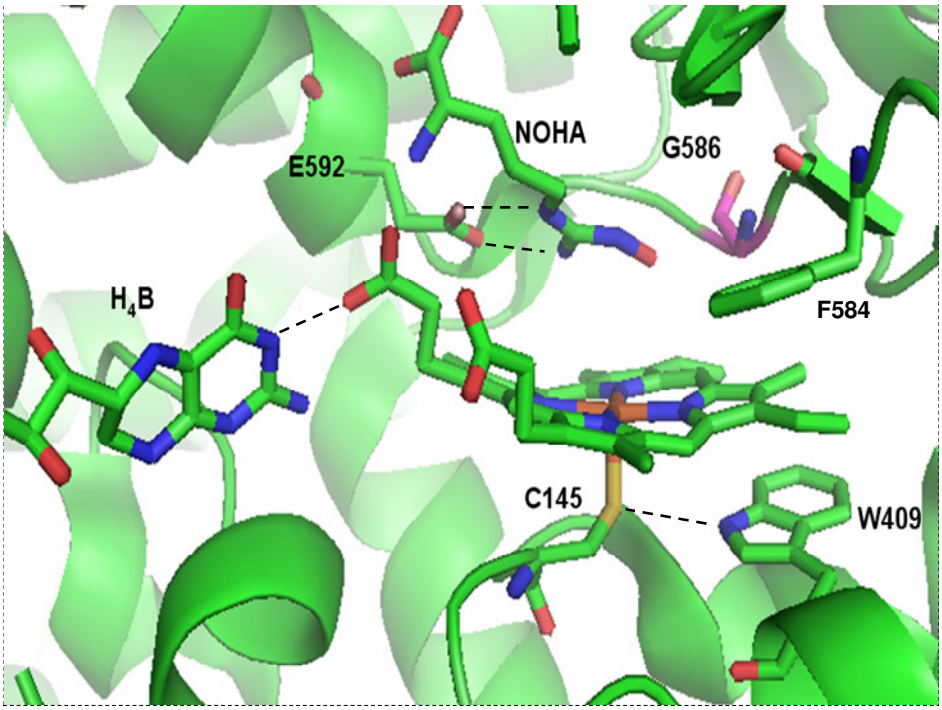

Figure 1.15- Active site of nNOS. Below the heme plane is Trp409, which has stacking interactions with the heme, but also hydrogen bonds (dashed lines) to the cysteine thiol ligand. Above the heme is Phe584, with more stacking interactions. Gly586, the subject of mutation in this work is shown in the background in pink. To the left is Glu592, which via two hydrogen bonds to the substrate guanidinium positions the substrate over the heme iron. The substrate here in NOHA. H_4B is shown in its position hydrogen bonded to the heme. (PDB 3HSN, Ref 56)

This allows easy diffusion in and out of the site, but make for tightly controlled binding near the heme. The specificity of binding is important in NOS as the reaction of L-Arg to citrulline and NO happens asymmetrically. Both monooxygenation reactions occur on a single nitrogen of the guanidinium group. It is therefore important that this nitrogen be always held in close proximity to the heme iron, the site of reaction. The main interaction between the substrate and the active site in this positioning is a pair of hydrogen bonds

between Glu592 and the guanidinium group, Figure 1.15. This Glu is conserved in all mammalian NOSs. There is also a hydrogen bond between the non-heme orientated guanadinyl nitrogen and the peptide bond of Trp587, further strengthening this precise positioning.

The active site is limited in the size of compounds it can accept by Pro565, Val567 and Phe584 in rat nNOS. The binding pocket can only accept L-amino acids, due to the position of the α-carbon of the substrate. The H bonds formed between the protein and the terminal α-carbon of the substrate involve the hydroxyl of Tyr588, the carboxylates of Asp597, Lys478 and a water molecule held by Arg603 with the carboxylate of the substrate; the α amino-group on the other hand interacts with the previously mentioned Glu592 and a heme propionate.

Work on inhibitors for NOS must, if they are competitive inhibitors, take into account all of these interactions. Many inhibitors simply do not mimic the interactions of the α–groups of the natural substrate. But they must in some ways be comparable to L-Arg if they are to bind in close proximity to the heme, mainly via the interactions with Glu592.

1.11 Pterins

All mammalian NOSs have an absolute requirement for H_4B, Figure 1.16. This is unusual as H_4B is not a very common cofactor. As we shall see later though, its role in NOS as a cofactor in monooxygenation is not unique.

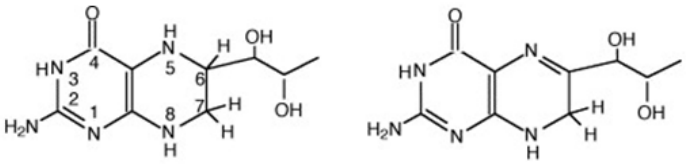

Figure 1.16 - Structures of H_4B, showing the ring numbering system used throughout this work, and H_2B (57).

The binding of H_4B leads to dimerisation of the protein (58). On dimerisation there are various changes in conformation of the enzyme, in both the heme domain (59) and the reductase domain. The C-terminal portions of the heme domain are flexible and can change conformation depending on whether the protein is dimerised or not. When H_4B is bound there are several residue interactions that stiffen these portions and aid in dimerisation. The binding site of H_4B is on the dimer interface and both the protein partners interact with both H_4Bs, strengthening the dimerisation Figure 1.17.

H_4B is bound at the dimer interface by hydrophobic interactions and stacking interactions by Trp678 and Phe690. The reduced tetrahydro-form of the pterin is deeply unstable (60) and readily undergoes a double oxidation to the inactive dihydro-form in solution. Since the role of H_4B in NOS catalysis is as a one electron donor/acceptor the bound pterin must be stabilised to avoid a two electron oxidation to be of use. The bound H_4B is far more stable than that in solution. The interactions of the protein with the pterin must therefore support the tetrahydro-form. The stacking of Trp678 is believed to stabilize the H_4B radical by a π interaction. Mutagenesis of this residue allowed the formation of the pterin radical, but at a far reduced rate and stopped complete turnover of the enzyme. Phe690,

contributed from the other subunit, also stacks with H_4B, stabilizing the dimer and also likely stabilizing the pterin. Vital to the mechanism is the ability of H_4B to support a radical. Here again the residues that support binding also support the stability of this radical (61).

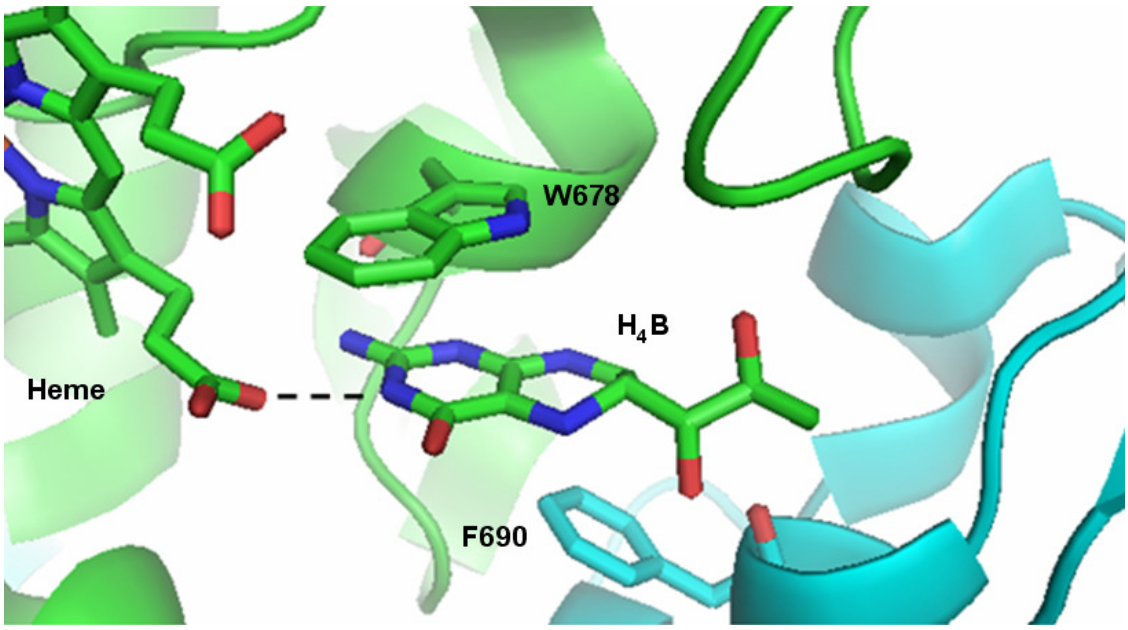

Figure 1.17 - H_4B, buried in the dimer interface, is stacked by a tryptophan (678) and a phenylalanine (690) from the facing monomer. The two subunits of the dimer are differentiated by being shown as blue and green. The heme propionate H-bonds with the 3N of the pterin ring. (1OM4, Unpublished paper)

There are H-bonds from the nitrogen atoms of H_4B to surrounding residues, further aiding binding and leading to a binding constant in the high nanomolar range. The most important interaction, however, is between the N3 of H_4B and heme propionate. This is considered to be the path of electron transfer from H_4B to the heme-bound oxygen and, as will become clear when the mechanism is discussed, is vital to the turnover of NOS (62). Aiding the activity of NOS is the preferential binding of H_4B over the oxidized and inactive H_2B form. This is because, on oxidation, the C6 on the second ring assumes a

trigonal planar geometry that clashes with the environment. Thus, should the bound pterin become fully oxidized it would be replaced by a reduced pterin. Also the steric hindrance experienced by H_2B in the binding site would stabilise any H_4B already bound.

All of these interactions must be considered in the design of H_4B analogues. The design of analogues will be discussed further in the section of the mechanism directly related to H_4B.

1.12 Aromatic Amino Acid Hydroxylases

H_4B has an important role in another class of enzymes, the aromatic amino acid hydroxylases (63): phenylalanine hydroxylase (PheH), tyrosine hydroxylase (TyrH), and tryptophan hydroxylase (TrpH). These enzymes catalyse the reactions shown in Figure 1.18 and are dependent on H_4B for activity.

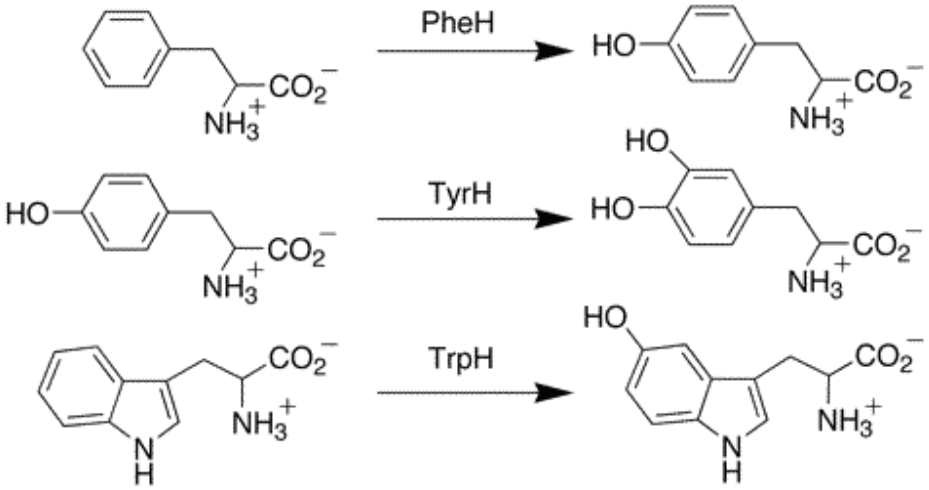

Figure 1.18 - The reactions catalysed by the aromatic amino acid hydroxylases (63).

As discussed the most common, and therefore the most studied, mechanisms for hydroxylation in biology are the cytochrome P-450–dependent hydroxylases and the flavoprotein phenol hydroxylases. These are also easy to study with spectrophotemetry due to the bound cofactor heme or flavin. The aromatic amino acid hydroxylases are harder to study because they lack easy spectral changes to follow during the reaction, as they lack heme or flavin cofactors, relying on an iron-sulphur cluster.

What can be said with certainty is that the amino acid hydroxylases perform monooxygenation reactions, attaching one oxygen atom from dioxygen to the substrate and reducing, via two electrons, the other oxygen atom to water. In this overall reaction these hydroxylases are therefore very similar to each half step catalysed by NOS.

When the mechanism is observed though, the role of H_4B is found to differ greatly between NOS and the aromatic amino acid hydroxylases. H_4B in NOS donates electrons to the heme for oxygen activation, but is in turn reduced, finishing a catalytic cycle in the same state at which it started. In the amino acid hydroxylases H_4B is consumed by the reaction, donating two electrons and ending the cycle as dihydroxypterin (64). This dihydroxypterin then must dissociate from the enzyme. In solution it will dehydrate to a quinonoid dihydropterin and must be converted back to the tetrahydro-form by dihydropteridine reductase.

Structures are available for all three enzymes with a pterin bound, allowing a close study of the binding of H_4B. Figure 1.19, shows the major interactions of H_4B in PheH.

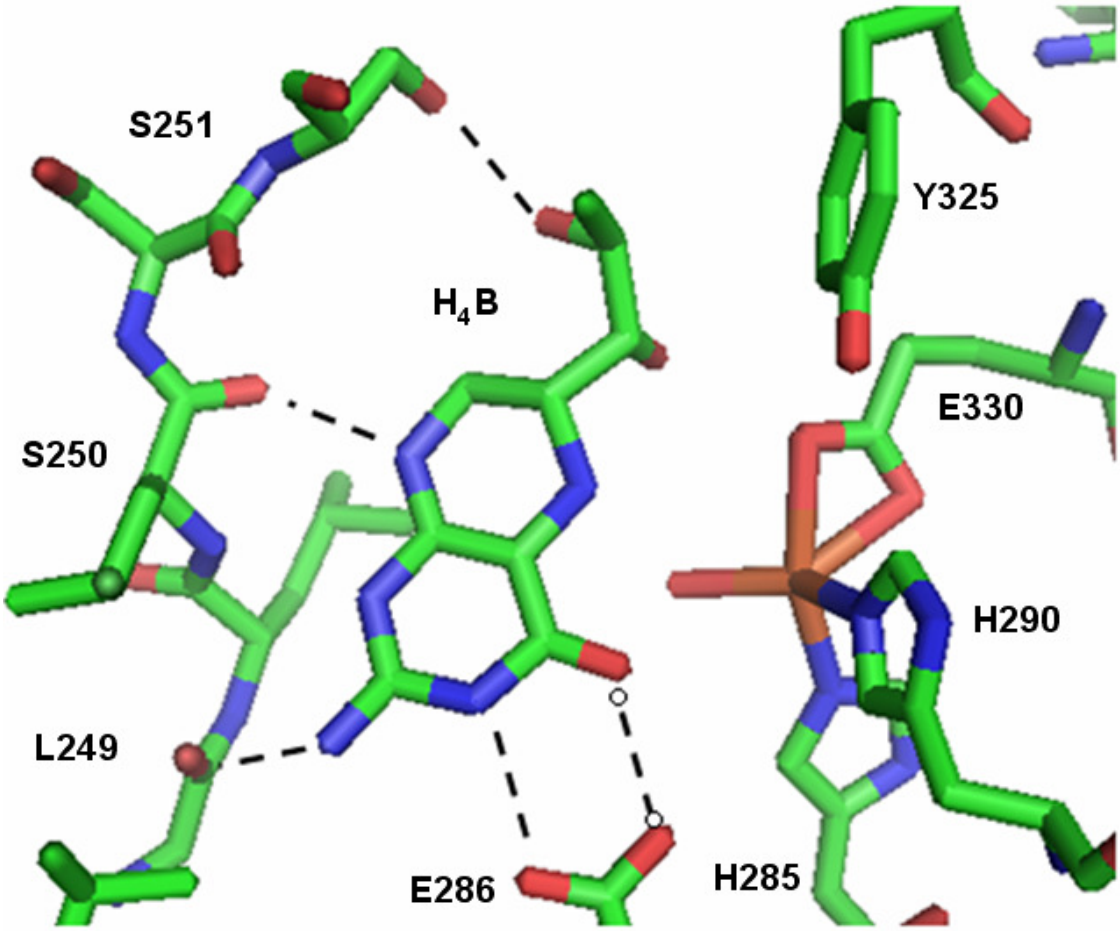

Figure 1.19- Binding of H_4B in PheH. Three hydrogen bonds exist between the nitrogens of the pterin and the protein backbone. These may alter on NADPH binding. Water mediated hydrogen bonds exist between the pterin and the iron (Orange). (PDB 1MMT, Ref 65)

As can be seen most of the interactions are between the pyrimidine ring of the pterin, with the N1 and N8 of the pterin hydrogen bonding to a flexible loop of PheH. Interestingly only Ser251 interacts via the side chain, all the other interactions are via the peptide backbone (65). Ser251 hydrogen bonds to the dihydroxypropyl side chain of H_4B. Since this residue is not conserved in TyrH or TrpH, this interaction does not seem to be key to the mechanism. However it must be taken into account in modelling of possible analogues that may wish to target specifically the PheH pterin binding site.

Site directed mutagenesis has confirmed the importance of the electrostatic interaction between H_4B and the carboxylate of Glu286. The dense series of interactions is also supported by a stacking interaction with Phe254. The complexity of all these interactions suggests the importance of H_4B to the mechanism, but does it also confer a strong specificity for H_4B over analogues?

Much work has been done on substituting the dihydroxypropyl side chain of the pterin (66), position 6, Figure 1.18. Replacing the side chain with a methyl group, 6-$MePH_4$, gives a functional analogue in all three enzymes. Phenyl, ethyl, hydroxymethyl, and trihydroxypropyl side chains at the 6 position also yield functional analogues. A carboxylate side chain is not tolerated by the hydrophobic binding pocket and therefore is not functional. 2,4-Diamino-6,7-dimethyl-tetrahydropterin is reported to be a substrate for PheH suggesting that some expansion in the 7 position is tolerated, at least by PheH (67). All studies show that the pyrimidine ring is critical for function.

The mechanism of these enzymes, Figure 1.20, shows how different the role of H_4B is here in comparison to in NOS (68).

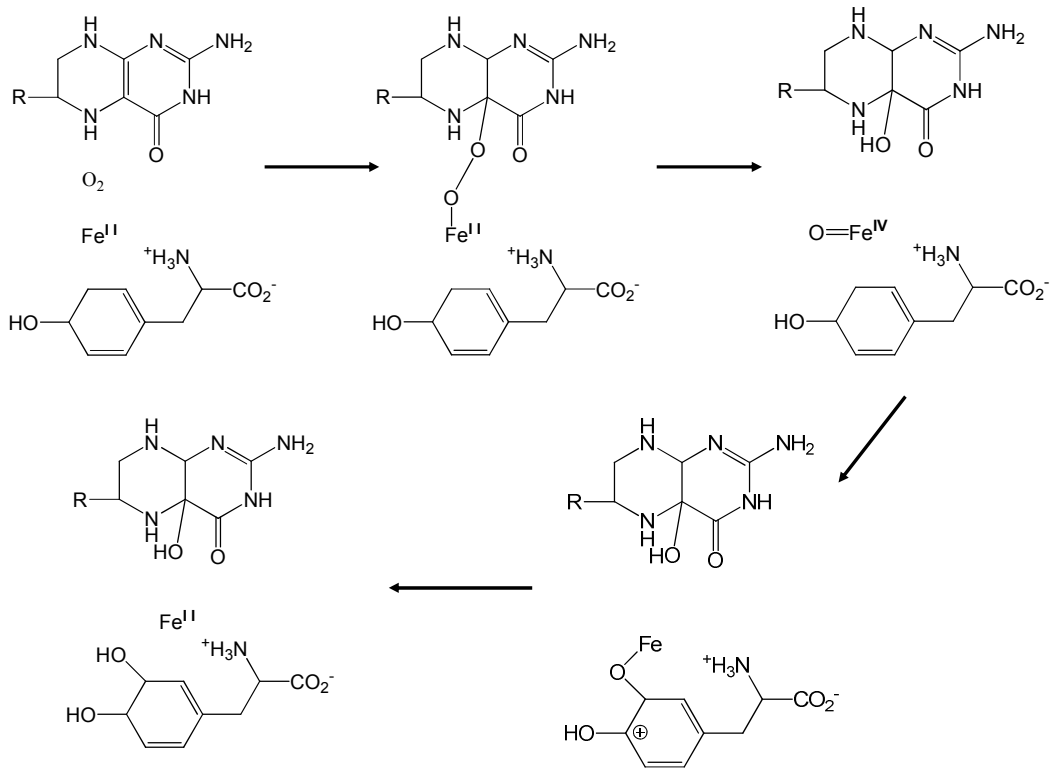

Figure 1.20- Mechanism of aromatic amino acid hydroxylases, shown here for TyrH (68).

In these enzymes there is direct chemical reaction between H_4B and oxygen, something not observed in NOS. The roles of H_4B cannot seemingly be directly compared then. It is tantalising that both these enzyme families use H_4B for oxygen activation but the aromatic amino acid hydroxylases utilise a far less subtle mechanism.

For the design of analogues of H_4B the roles and interactions of H_4B with all these enzymes must be considered to ensure activity and specificity.

1.13 Cytochromes P450

Any discussion of NOS mechanisms invariably begins with a comparison to cytochromes P450. This is because NOS mechanism is based on two monooxygenation steps. Each of the monooxygenation steps resembles the full reaction mechanism of a P450 cyytochrome, as we shall see in this section. The P450 cytochromes are a large family of enzymes that usually perform mono-oxygenation reactions, Figure 1.21 (69). Dioxygen is bound at the heme, activated by reduction and an atom of oxygen is inserted into the substrate. These words could very well be used to describe the mechanism of NOS, but further similarities will also render comparison of NOS to the P450s edifying.

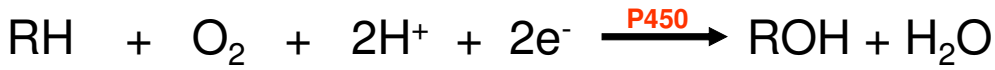

Figure 1.21 - The generic mono-oxygenation reaction catalyzed by P450s.

P450s have an active site based around a b-type heme that is thiol ligated from the iron to a cysteine residue. The strong electron donating nature of the thiolate is thought to activate molecular oxygen bound to the ferrous heme iron. This is also directly analogous to NOS. It would be tempting to say, given the similarities of heme and function that NOS and P450s are evolutionarily related, but no sequence analysis bares this out nor does structural comparison. It would seem to be a case of convergent evolution of mechanism.

P450s have been studied closely and much detail is known about their mechanism. Following the discovery of NOS it has been useful to compare their mechanisms. Let us

therefore consider the P450 mechanism. But first it must be noted the P450s generally lack a fused reductase domain to supply electrons and must therefore rely on an external source. Class 1 P450s use a complex two step delivery system involving ferredoxin reductase, which accepts electrons from NADH dehydrogenation, and uses FAD as a cofactor to accept the hydride. Ferredoxin reductase then reduces a second protein (containing an iron-sulphur cluster), ferredoxin. From ferredoxin the electrons are passed to the class 1 P450 heme. This complex system is most commonly found in bacteria and mitochondria. Class 2 P450s have a specific redox partner, Cytochrome P450 reductase. This reductase resembles the reductase domain of NOS closely as it derives electrons from NADPH, and uses FAD and FMN to traffic them on to the heme. While this may give some insight into the evolution of the NOSrd it is in the monooxygenation reaction of the P450s themselves that we may garner more knowledge of NOS mechanism (70).

The mechanisms of P450s are so elegant in their details as to seem to transcend the phenomenological and enter the sublime. For the monooxygenation of hydrophobic substrates to occur molecular oxygen must be activated. Otherwise molecular oxygen in its triplet state would be unable to react with the substrate, typically in the singlet state. Transition metal ions are often used by enzymes for this purpose. In the case of P450s iron is used to activate oxygen due to its redox chemistry and ability to support highly reactive species. Once oxygen is bound to the heme iron two electrons, delivered sequentially, are required for reaction. The sequential delivery of these electrons gives rise to a number of intermediates which will prove useful in characterizing the intermediates

of the NOS mechanism. Figure 1.22 shows a general and widely accepted P450 mechanism.

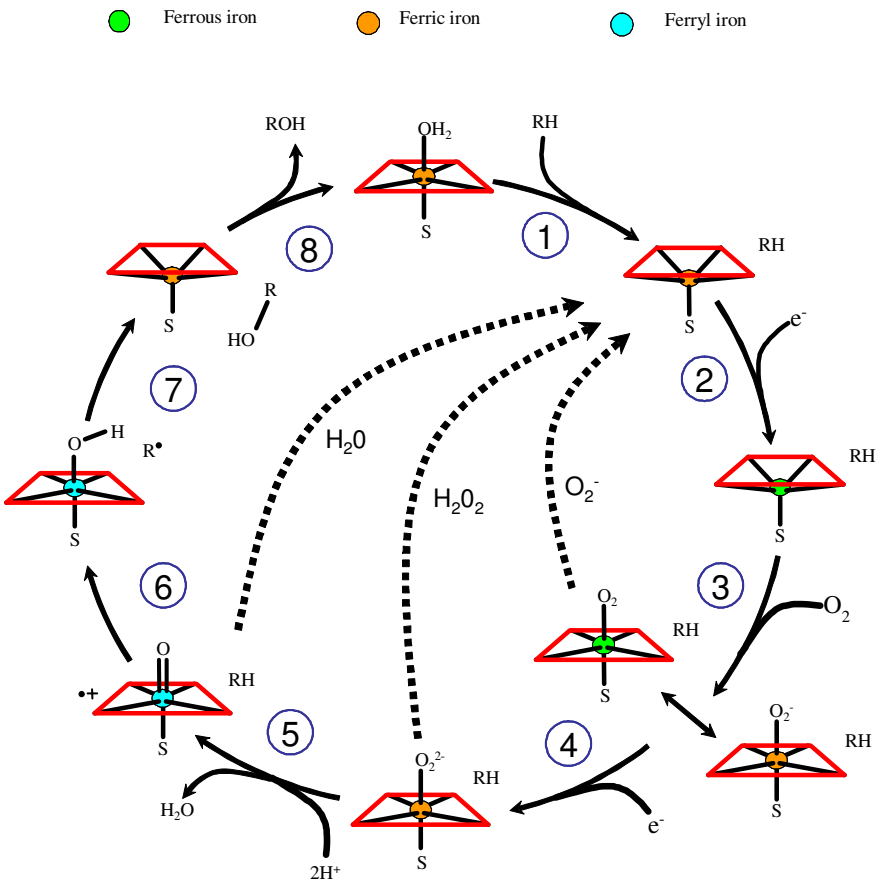

Figure 1.22 - A generalized P450 mechanism: 1- Substrate binding. 2- First electron transfer. 3- Oxygen binding. 4- Second electron transfer. 5- Formation of an oxy-ferryl species. 6 & 7- Rebound mechanism for oxygen insertion. 8- Product dissociation. Electron uncoupling leads to the production of superoxide, peroxide and water. (Adapted from Papale 2008)

Following this mechanism step by step will help in later unraveling the NOS mechanism.

1- Binding the substrate. The first step of the reaction is the binding of the substrate. This may seem an obvious first step, but in P450s the binding of the substrate often, though not always, involves the displacement of a loosely associated water molecule (71).

Here, as in NOS, the binding of the substrate changes the iron from a low to a high spin state. This change is easily seen spectroscopically. Unlike in NOS, the displacement of the water destabilizes the ferric form of the enzyme. Electrospectrometry shows a positive heme reduction shift on the binding of the substrate in P450 enzymes, by changes in the iron spin state. Binding the substrate therefore makes heme reduction far easier.

2- First electron transfer. As noted previously the electrons required for the reaction are supplied by a redox partner, derived ultimately from NADH or NADPH. Some P450 enzymes undergo structural rearrangement on heme reduction that bring the substrate closer to the heme (72). This could be to ensure that electron delivery is tied to productive reaction and not the futile uncoupled reactions that generate reactive oxygen species such as superoxide or hydrogen peroxide.

3- Oxygen binding. Molecular oxygen only has a strong affinity for the ferrous heme and binds rapidly to it. The iron-oxygen species could be described either as oxy-ferrous (Fe^{II}-O_2) or as the superoxy-ferric form (Fe^{III}-O_2^-).

4- Second electron transfer. The second electron donation from the redox partner to the heme leads to the formation of a peroxy-ferric species (Fe^{III}-OO^{2-}).

5- Protonation. The mechanism then proceeds via a double protonation, the first of which produces a hydroperoxy-ferric intermediate (Fe^{III}-OOH^-). The hydroperoxy-ferric compound has also been suggested to be in some cases the reactive species, being reactive enough to perform the oxygenation especially when the second protonation is slow. However it is generally accepted that the hydroperoxyferric species is protonated and subsequently decays by loss of a water molecule to form a highly reactive carbocationic oxy-ferryl species (Fe^{IV+}=O), known as Compound I, with a heme based radical (73). The

Compound I has now been directly observed by EPR and Mossbauer spectroscopy in, and found to be catalytically competent in, the P450 CYP119 (74). Compound I has therefore been shown to be capable of performing a reaction we shall see occurring in NOS.

6 and 7- Oxygen insertion. The oxy-ferryl compound is thought to remove a hydrogen atom from the substrate. This forms a substrate radical and a hydroxyferric heme species. Radical recombination would then rapidly occur to create a ferric heme and the final product. This is termed the radical rebound mechanism (75).

8- Product dissociation. The hydroxylated product is released from the ferric heme which binds a new molecule of water as sixth ligand. This mechanism is fairly simple and very elegant.

This mechanism took several years to elucidate but is now generally accepted. Under physiological conditions only the steps up to generation oxyferrous species can be observed by stopped flow reactions. The other intermediates required delicate work with Electron Paramagnetic Resonance (EPR), Electron-nuclear Double Resonance (ENDOR) and Raman spectroscopy to detect (76, 77). Work on stabilizing the intermediates involved mutagenesis and low temperature work, and gave direction on similar work on NOS. Compound I was observed by artificially generating it by the reaction of CYP119 with *m*-chloroperbenzoic acid in stopped flow reactions. This allowed UV-VIS spectra to be taken, and also preparation for EPR and Mossbauer spectroscopy (74).

Applying this chemistry to both steps of the NOS reaction gives us a good starting position from which to consider the mechanism.

1.14 NOS catalytic cycle

Now we can apply the knowledge of the P450 mechanism to the NOS mechanism. The conversion of NO from L-Arginine takes place in two steps: the monooxygenation of L-Arginine to L-NOHA and then the monooxygenation of L-NOHA to L-Citrulline and NO. Both of these steps can be considered monooxygenations but could be more properly described as first the hydroxylation of L-Arginine and then an oxidative scission of L-NOHA to L-Citrulline. Each step requires molecular oxygen to be activated by reduction while bound to the heme. Here we shall consider what is known of the NOS mechanism and how it was elucidated.

Figure 1.23 shows a proposed mechanism for NO synthesis. Here the two steps are shown to be identical in terms of intermediates for simplicity, but they will be discussed further. Steps 1-5 are reciprocated in steps 6-11.

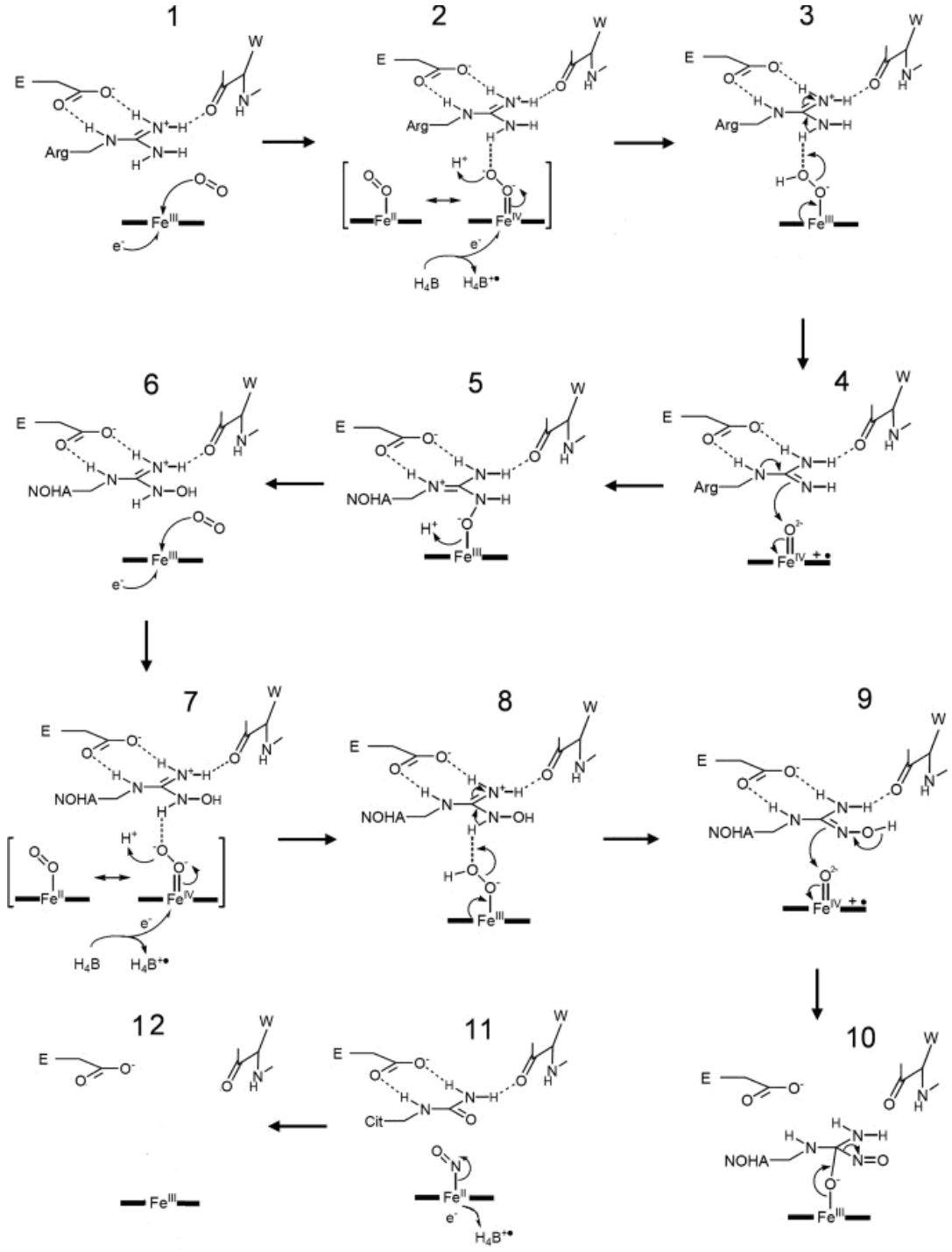

Figure 1.23 - Overall scheme of the NOS catalysed reaction here shown with a Compound I final species and both monooxygenation reactions following the same mechanism. This is not a universally accepted mechanism.

As seen in P450s the binding of substrate to NOS changes the heme high from a low or mixed spin state, to a high spin state, due to the displacement of a weakly associated water at the distal sixth position. This can be seen in the shift of the NOS Soret peak from 400nm to 394nm. Unlike in P450s there is no shift in the reduction potential of the heme iron on substrate binding (78).

As we saw in the section in the reductase section the electron transferred from the FMN shuttling between the reductase domain and the heme domain reduced the ferric heme to the ferrous. Again, this step can be followed spectroscopically with a shift of the Soret peak from 394nm to 414nm. There is a change in the alpha/beta bands, a wide peak forms at 560nm replacing two very slight peaks at 530nm and 650nm. The band at 650nm disappears completely on reduction to the heme. The complete flattening of the peak at 650nm is typically used to judge complete reduction of the heme to the ferrous state. Oxygen has a far greater affinity for the ferrous heme and it is after reduction that oxygen binds in the sixth axial position to form the oxy-ferrous species (79). This can be observed by UV/VIS as a shift in Soret peak to 425nm and sharpening of the 560nm band. This is only true for the substrate bound enzyme. In the absence of substrate there is no build up of the oxy-ferrous species, one only observes oxidation of the heme. This points to a stabilizing effect of substrate on the oxy-ferrous species

While discussing this first electron transfer it is useful to consider what happens in the uncoupled enzyme. The uncoupled transfer of electrons occurs when substrate or pterin, or both, is absent. In this condition electrons are delivered to the heme but without production of product. When substrate is absent the oxy-ferrous species will undergo

auto-oxidation and superoxide anions will be released (80). As has been seen the substrate stabilises the oxy-ferrous species, oxy-ferrous decay being seen at rates of $200s^{-1}$, $22s^{-1}$, and $4s^{-1}$ for the substrate free, Arginine-bound, and NOHA-bound nNOSoxy respectively. By control with CaM-binding the enzyme stops uncoupling by inhibiting the passage of electrons from the reductase domain to the heme domain.

After the oxy-ferrous species none of the other steps in the NOS mechanism can be viewed with UV/VIS under physiological conditions. This is due to the transient nature of these intermediates and they can only be detected with the techniques discussed for P450s and at low temperature.

Important insights into the second electron delivery have been gained from ENDOR characterization of intermediates at 77K by γ-irradiation of the oxy-ferrous species. The species formed was found to be a peroxy-ferric species, with a hydrogen bond to a water molecule (81).

However the identification of where the second electron comes from proved more tricky, as the second electron was delivered far more rapidly than the reductase domain was capable. The unusual and absolute requirement of NOSs for H_4B made it a tempting source of this second electron. This hypothesis was given strength when a H_4B radical ($H_4B^{\cdot}$) was detected after Rapid Freeze Quenching when arginine-bound Ferrous NOS was mixed with oxygen (82). Indeed the radical formed at the same rate as oxy-ferrous decay. This evidence was again strengthened by repeating the experiment with amino-H_4B, an analogue of H_4B competent to dimerise the protein but unable to donate an electron to the mechanism. Here, no radical was detected and the oxy-ferrous decay was seen at a very slow rate. The experiment was again repeated with 5-methyl-H_4B, an

analogue capable of donating electrons, the enzyme retains its capability to perform hydroxylation in a single turnover cycle and a pterin radical was detected. The rate of radical formation was three times faster then with H_4B, and the rate of oxy-ferrous decay was also three times faster. At this point it would seem proven that H_4B here acts as an electron donor, certainly in the reaction with arginine (83).

Proving the role of H_4B in the second reaction step has been harder still. Detection of the pterin radical has been much harder. When it was detected it was found in much smaller amounts (3% compared to 75%, of heme content) (82). This could be due to the transient nature of the radical in the reaction with NOHA, being rapidly reduced.

In the first stage of the mechanism it is likely that the radical is reduced by an electron delivered from the reductase domain (83). This is a relatively slow affair and therefore the radical persists in the first step for longer. However after NOHA has been converted to citrulline the heme species that remains is a ferrous heme-NO complex. The ferrous heme-NO complex is so stable that it is considered a dead-end complex and NO will not be released. The H_4B radical is a strong oxidizing agent and is assumed to oxidize this to a ferric heme-NO complex, thus regenerating a neutral pterin and the ferric heme. The ferric heme-NO complex will not long endure and NO is rapidly released. At this point the mechanism is complete and another cycle may begin.

So we can view H_4B as a transient electron donor and acceptor, a totally unique role for the pterin and one much different from its role seen in the aromatic amino acid hydroxylases.

Prior to the discussion of the role of H_4B we were up to the oxy-ferrous species in the mechanism. Now that we have seen H_4B donating electrons to form the peroxyferric

species we can continue with some of the controversies of the mechanism.

It has been suggested by some that the final reactive species may be the peroxy-ferric (85). It is possible that it may be reactive directly with arginine or NOHA. But by comparison with P450s it is generally accepted that the peroxy-ferric species undergoes a double protonation and, via the loss of a water molecule, forms an oxy-ferryl species, Compound I (86). The evidence for this species, never directly detected, is that of the formation of a heme-substrate adduct, detected after two protonations and the loss of a water molecule in cryoreduction experiments (86). Here the substrate is coordinated to the ferric iron through the oxygen of the hydroxyl, having already undergone hydroxylation. The double protonation weakens the O-O bond, breaks it and produces the water molecule. This would, necessarily, lead to the formation of an oxy-ferryl species capable of reacting with the arginine nitrogen to produce the adduct. Further evidence comes from the formation of an adduct of NOHA and the heme. Once citrulline is then formed the NO remains bound to the ferrous heme until reduced by H_4B as discussed in the section on the role of H_4B.

1.15 Aims of this project

The physiological roles of NO make its production and regulation in the body vital. As this introduction has hopefully demonstrated the production of NO is sublime in its complexity and this work will help to explain some of the steps. The focus of this work is the mechanism of arginine hydroxylation and the role of the pterin in it.

Can we characterize the stabilised intermediate of the NOS reaction formed by the G586S mutant?

Previous study of a mutant with a serine introduced to the active site gave evidence of a stabilized intermediate in oxyferrous decay. The G568S mutant introduces a hydrogen bond to the substrate, stabilizing the binding of the substrate in the active site (See specific introduction to chapter 3). This intermediate, formed by the G586S mutant, forms after the donation of an electron from H_4B. This points to the stabilised intermediate being the active oxidant in the mechanism. However, it has not been demonstrated that this stabilised intermediate in the G586S mutant nNOS is catalytically relevant or whether it is an artifact of mutation. By studying the mutant spectroscopically, by EPR, crystallographically with NOHA bound and the products of single turnover reactions by HPLC more light may shed on the mechanism of NOS and the role of H_4B.

Can H_4B act to rescue NOS from the ferrous heme-NO complex?

The pterins in the NOS dimer are held with their conjugated π-systems only 13 Å apart. This has led to the suggestion that there may be electron transfer between the pterins, and therefore possibly between hemes in the NOS dimer. This would be of particular importance in releasing a heme from the dead-end ferrous heme-NO complex. However, no studies have ever been undertaken to study whether effective electron transfer does occur between the pterins. Here, we aim to correct that oversight.

Can we find analogues of H_4B that are both active and more stable to oxidation than H_4B itself?

The importance of NO, and therefore the importance of H_4B to biological NO synthesis, means that H_4B is a crucial target for drug design. Some people suffer from a deficiency of H_4B. The unique qualities of H_4B that make it so fascinating a molecule also make it unfit for oral administration. It is also unstable in the blood stream. It would be useful to find an analogue that could activate NOS and was more stable in solution than H_4B. The creation of novel analogues of H_4B would also be of scientific use in furthering our knowledge of the role of H_4B in NO synthesis.

Chapter two

Materials and Methods

All chemicals were purchased from Sigma, unless where otherwise stated. H_4B and aH_4B were purchased from Schircks lab (Switzerland).

2.1 Preparation of cell lines

All plasmids had previously been constructed. The full length nNOS gene (from *Rattus norvegicus* (Appendix 1)) in plasmid pcWori was kindly donated by Dr T. Shimizu (Tohoku University, Sendai, Japan). All nNOS heme domain constructs were created by Dr. Caroline S. Miles (Institute of Cellular and Molecular Biology, University of Edinburgh). The NOS G586S heme domain mutant characterised was generated by site-directed mutagenesis. The *E.coli* strain BL21 was used for the expression of both wild type and G586S mutant constructs. During the creation of both wild type and G586S constructs, an N-terminal histidine tag was added to the C-terminus of the gene to allow purification by nickel affinity. To get correct protein folding in the bacteria the plasmid pGroESL was also transformed along with the nNOS plasmids (87). pGroESL codes for the mammalian chaperonin proteins.

Cell cultures for line-maintenance were prepared for the wild type full length, WT and G586S mutant nNOSoxy. Small amounts of cells were picked from the colonies on LB-agar plates with a sterile wire loop and dispersed into 30 ml of autoclaved TB media with 25 μg/ml carbenicillin, selective for pcWori, and 35 μg/ml chloramphenicol, selective for pGroESL, in sterelin tubes. This inoculated culture was then grown overnight at 37°C

while being shaken at 150 rpm in an orbital incubator. DMSO stocks for long term storage at -80°C were made by taking 930µl of this culture and adding 70µl DMSO before freezing. DMSO stocks were then used for future large growths. DMSO stocks were regularly remade to ensure cell line integrity.

For all growths the media used were prepared to the recipes in table 2.1.

Growth Media and Agar	
LB Media	For 1 litre: 10 g Bacto Tryptone 5 gYeast Extract 5 g NaCl
TB Media	For 1 litre: 20 g Bacto Tryptone 10 gYeast Extract 4 ml Glycerol 2.6 g KH_2PO_4 4.3 g K_2HPO_4
LB Agar Plates	15 gL^{-1} agar dissolved in LB by autoclaving Antibiotics were added to the liquid agar once the agar was cool to the touch.

Table 2.1- Guide to bacterial media preparation. All were made with MiliQ ultrapure water and sterilised by autoclave.

2.2 Expression

Starter cultures were created by inoculating small volumes of TB media with bacteria from DMSO stocks. These were then incubated overnight at 37°C and 150 rpm in an orbital incubator. Aliquots of 2ml from the starter cultures were inoculate in each flask containing larger quantity of TB media: typically 20 x 450ml TB augmented with 25

μg/ml carbenicillin and 35 μg/ml chloramphenicol in 1 litre baffled flasks were used. The flasks were kept at 37°C and 150 rpm in an orbital incubator until the optical density of the culture was approximately 0.5 – 0.8 (~6 hours). IPTG (24 μg/ml) and ATP (113 μg/ml) were then added to induce overexpression. The temperature of the incubator was lowered to 20°C for a period of 24 hours.

The cells were then harvested by centrifugation at 15000 rpm for 15 minutes at 4°C (Sorvall RC-5B centrifuge with a SLA 3000 head). Cell pellets were collected and stored at -20°C until required.

2.3 Extraction and Purification

For composition of the buffers used in purification see table 2.2. The collected cells pellets were defrosted and resuspended in Resuspension/Lysis buffer allowing approximately 4ml buffer per 1g of cell pellet. The thoroughly resuspended cells were lysed by ultrasonication with a Sanyo Soniprep 150. A typical preparation would use 5 small glass beakers each containing 40ml of resuspended cells. Each beaker would receive 8 sonications of 30s each at 13 microns. Between sonication steps the beakers would remain on ice to prevent overheating of the sample and thoroughly mixed to ensure complete lysis of cells. After sonication the solution would be centrifuged at 20000 rpm for 50 min using a Sorvall RC-B5 centrifuge with a SS34 head. This would pellet the cellular debris. The nNOS protein remains in the supernatant. Supernatant was then kept on ice for isolation of nNOS by column chromatography.

Purification Buffers	
Resuspension/Lysis Buffer	50 mM Tris-HCl (pH 7.5) 0.5 mM EDTA 10% glycerol 0.3 M NaCl 20 mM imidazole *20 µM H_4B** *1 mM dithiothreitol* *25 mM phenylmethylsulfonyl fluoride (PMSF)* *0.1mM L-Arginine* *Protease inhibitor (1 tablet/50ml buffer)*
Elution Buffer	50 mM Tris-HCl (pH 7.5) 0.5 mM EDTA 10% glycerol 150 mM imidazole 0.3 M NaCl *20 µM H_4B** *1 mM dithiothreitol* *0.1mM L-Arginine*
Gel Filtration Buffer	50 mM Tris-HCl (pH 7.5) 0.1 M NaCl *20 µM H_4B** *1 mM dithiothreitol*

Table 2.2- Protein preparation buffers. Chemicals shown in *italics* were added just prior to buffer use. *Or left out of preparation where analogues were to be used later.

2.3.1 Purification of nNOSoxy

All protein purification steps were carried out in a cold-room at 4^{o}C using gel filtration buffer with additions as stated below. The purification process for the WT and G586S nNOSoxy proteins were the same.

The first step used a Ni^{2+} Sepharose (Sigma) column. This column material is composed of agarose beads linked to nickel ions by chelating groups. This purification step exploits the high affinity and extreme selectivity of the hexa-His tag cloned into the nNOSoxy constructs for Ni^{2+}. This affinity allows for easy separation of tagged proteins from the lysate. Using a gravity feeding system the supernatant from the sonication step was loaded onto the nickel sepharose. The colour changes associated with loading, washing and elution can be seen in Figure 2.1.

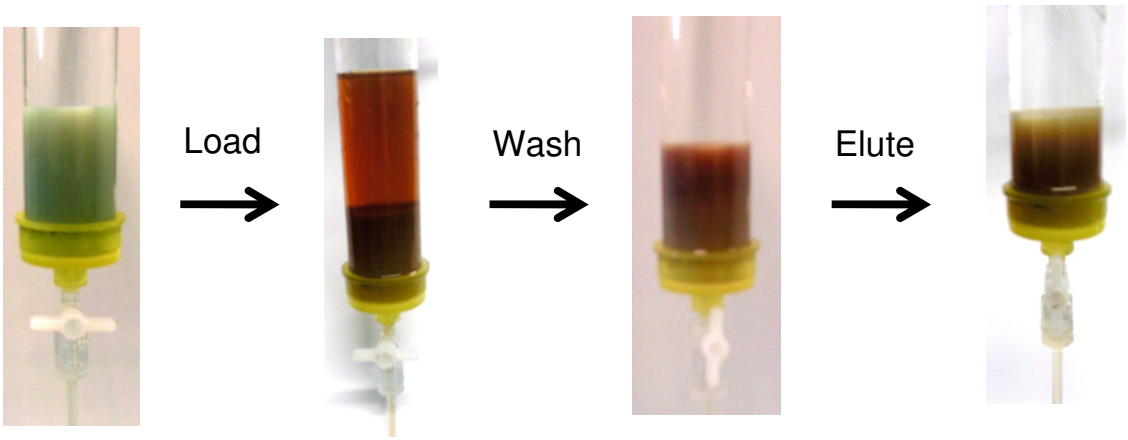

Figure 2.1- The purification of nNOSoxy with N-terminal hexa-His tag by affinity with a nickel sepharose.

The column was then washed with two column volumes of gel filtration buffer. The bound nNOSoxy leaves the column a dark red/brown colour. The protein is then eluted from the column using elution buffer. The high imidazole concentration displaces the hexa-His tag from the nickel. The eluting protein is then collected and concentrated using concentrators with a 30000MW cut off membrane (Vivascience).

Imidazole removal is performed by G-25 size exclusion chromatography. Excess imidazole must be removed as it has a high affinity for heme and will affect the protein's performance in other experiments. Size exclusion uses column beads with pores of specific sizes to separate molecules based on size. Molecules small enough to enter the pores, such as imidazole, will take a longer path through the material and will be eluted last. Molecules too large to enter the pores will take a shorter path through the column and be eluted first. Figure 2.2 shows the passage of nNOSoxy through a G25 column. Elution was simply by the addition of more gel filtration buffer to the top of the column.

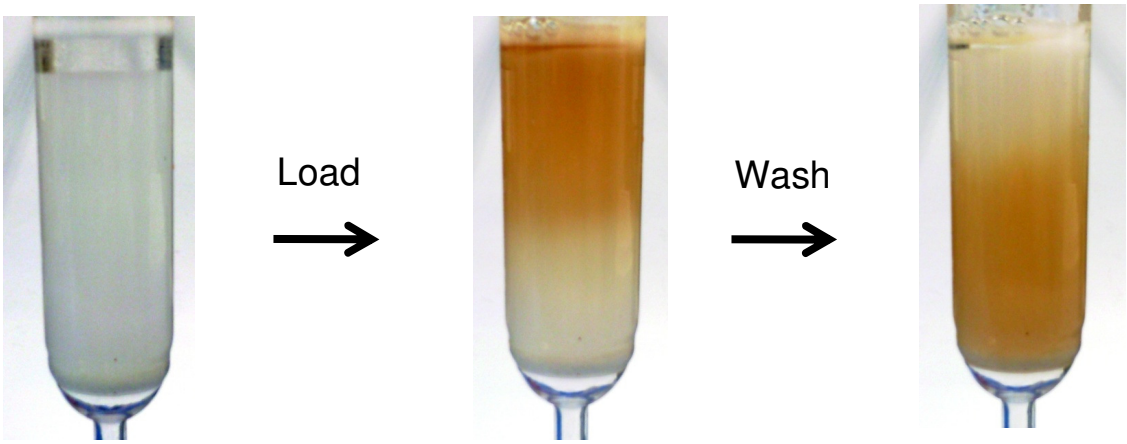

Figure 2.2- Removal of imidazole from nNOSoxy by size exclusion chromatography.

Eluted protein was then concentrated and frozen for later use. The protein was concentrated by centrifugation at 2000 rpm in Vivaspin concentrators with a membrane size of 30000 MW. Protein concentration was calculated as described below and concentrating was ceased when the protein was at the desired concentration. Aliquots of ~250-500µl of the concentrated, imidazole-free, protein were taken and flash frozen in liquid nitrogen. The samples of protein were then stored at -80^{o}C until required.

2.3.2 Purification of full length nNOS

The previously constructed plasmid containing full length WT nNOS (T. Shimizu, Sendai) did not include a His tag. Purification of the full length protein relies on different affinity chromatography from the heme domain.

Sonication and centrifugation steps are the same as for the nNOSoxy proteins. The first step of purification for the full length enzyme is loading of the protein onto a CaM-agarose column (Sigma). This column material has agarose beads cross-linked to calmodulin molecules. Here separation of the nNOS relies on its affinity for CaM.

Prior to loading the supernatant onto the column it is necessary to equilibrate the column with gel filtration buffer augmented with 1mM of $CaCl_2$. This ensures the CaM is saturated with Ca^{2+} ions, necessary for binding to nNOS. The supernatant is also augmented with $CaCl_2$ to a final concentration of 1mM.

After loading the column is washed with two column volumes of gel filtration buffer. This removes all proteins with no affinity for CaM.

Elution is by gel elution buffer with 5mM of EGTA. EGTA is a chelating agent with a specific affinity for Ca^{2+} ions. By removal of the Ca^{2+} ions from CaM, the CaM loses the ability to bind nNOS and the protein is eluted.

The protein is then passed down a G25 size exclusion column equilibrated with gel filtration buffer. This removes excess EGTA, as it would interfere with turnover assays.

Protein was then concentrated and frozen as previously described for nNOSoxy.

2.4 Protein characterisation

Purity of the protein collected after chromatography was determined by Sodium Dodecyl Sulfate-PolyAcrylamide Gel Electrophoresis (SDS-PAGE). Reagents used for SDS-PAGE are shown in table 2.3. SDS-PAGE was performed using NuPAGE Novex 4-12 % Bis-Tris pre-cast polyacrylamide gels. Size of proteins on the gel was judged by comparison with SeeBlue Plus 2 molecular weight markers. Protein samples for use in gel electrophoresis were prepared as shown in table 2.3. The samples were then boiled for 3 minutes to denature the proteins and allow SDS binding. SDS binding is always one SDS molecule per two residues. This gives a constant charge ratio to the protein and so migration through the gel is dependent entirely on the protein mass. Use of pre-stained standards allows protein size estimation from the gel.

SDS PAGE buffers and stains

Sample Preparation	25 µl NuPAGE® LDS 4x Sample preparation buffer pH 8.4 25 µl diluted protein sample (>1 µM) 50 µl dH_2O
Running Buffer	NuPAGE® MES SDS 20x Running buffer pH 7.0
Coomassie Stain	50 ml dH_2O 40 ml Methanol 10 ml Acetic Acid 1 ml Coomasie Brilliant Blue
Destain	50 ml dH_2O 40 ml Methanol 10 ml Acetic Acid

Table 2.3- Sample preparation and buffers for SDS-PAGE.

After preparation of the samples they were allowed to cool to room temperature for ease of loading. The pre-cast gel was placed in the running tank and running buffer added until the wells at the top of the gel were covered. To the first well pre-stained standard was added. Aliquots of protein sample were then added to subsequent wells. An electric field of 150V, 120mA and 60W was applied to the gel, and the gel left running until the dye reached the bottom. This allows for maximum separation and ease of size identification. After running the gel was stained in coomassie stain for 20 min and destained in destain

buffer for 1 hr. Protein presence on the gel is indicated by the areas where coomassie dye remains on the gel, Figure 2.3 gives an example gel.

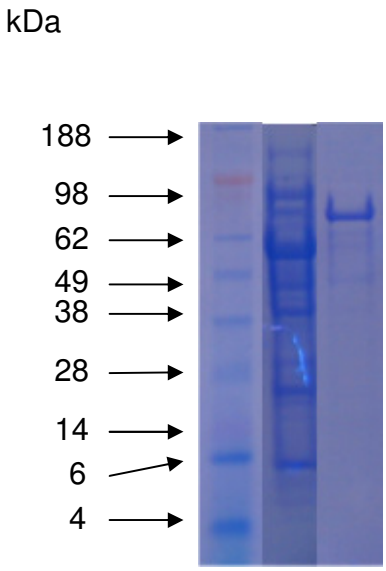

Figure 2.3- Coomassie stained SDS-PAGE of the elution from the Nickel column. In the first lane there are size markers (SeeBlue® Plus2 Protein Standard, Invitrogen). In the second there is a sample of flowthrough from the washing step. The final lane is the protein collected on elution of the column. nNOSoxy was the major component collected, band at approximately 80kDa. (Lanes edited together for ease of viewing)

2.5 Concentration determination

Calculating the concentration of nNOS was achieved by using the absorbance difference between the ferrous and ferrous-CO spectra of the enzyme. The extinction coefficient of this difference has been determined to be $\varepsilon_{444\text{-}467}$ = 55, 000 $M^{-1}cm^{-1}$ (80). Figure 2.4 shows the spectra for each state. The UV/VIS spectra were recorded over the range 250 – 800 nm with a Shimadzu UV-2101PC spectrophotometer. Sodium dithionite was used to

reduce the protein. Once fully reduced, as judged by Soret peak position and absorbance at 650nm, CO gas was bubbled through the sample for several seconds. The spectrum for the ferrous-CO complex was then recorded. The ferrous spectrum was then subtracted from the ferrous-CO spectrum. Peak heights were then taken at 444nm and 467nm of this subtraction spectrum. Using the Beer-Lambert law allows calculation of the concentration of the protein.

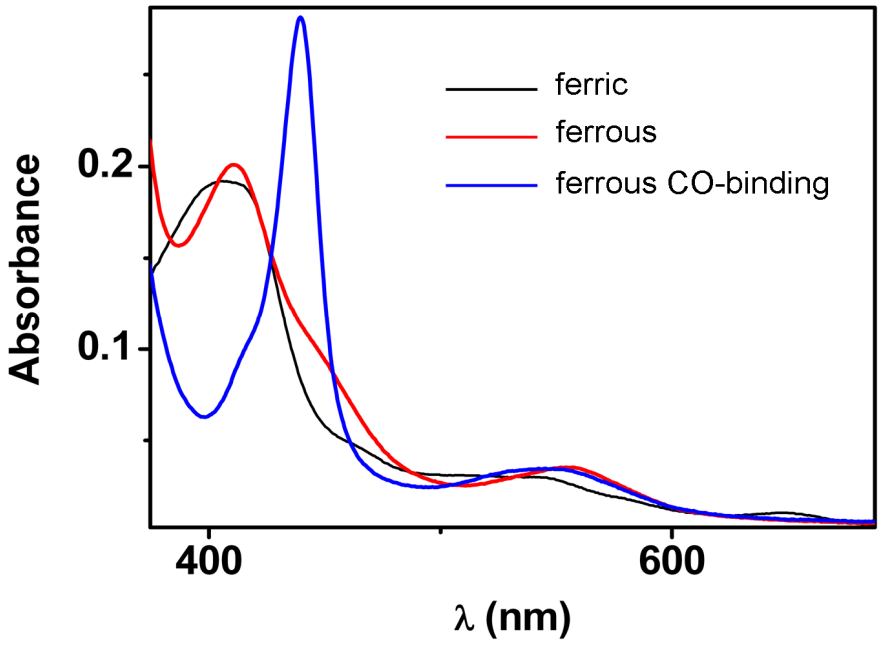

Figure 2.4- UV-Vis spectra of oxidised (black), reduced (red) and reduced CO-binding (blue) nNOSoxy. Ferric (substrate free) nNOS Soret peak has an absorbance maximum at 400nm, ferrous nNOS at 412nm and ferrous-CO nNOS at 444nm. These are the same in WT and G586S nNOSoxy.

2.6 Crystallography

The general crystallographic approach used in this thesis will be discussed in the following pages with specific conditions for crystallography discussed in the relevant results chapters. The full range of conditions used in each trial can be found in appendix

2. Crystallography was attempted for the WT nNOSoxy with various H_4B analogues and for G586S nNOSoxy with NOHA bound. When these substrates and cofactors were required they were used throughout the preparation and kept at constant excessive concentrations.

2.6.1 Trypsin digest

Trypsin agarose (Sigma) was used to cleave the PDZ domain from nNOSoxy proteins. This protease digestion is necessary for crystallography as the PDZ domain is mobile and impedes crystallography. Trypsin agarose, in a ratio of 1:100 (trypsin agarose: nNOSoxy) by weight, was added to the sample. The sample was left to digest at 4ºC for 24 hours under gentle stirring. To stop the digest the trypsin agarose was removed by filtration. The completion of the digest was judged by SDS-PAGE, Figure 2.5.

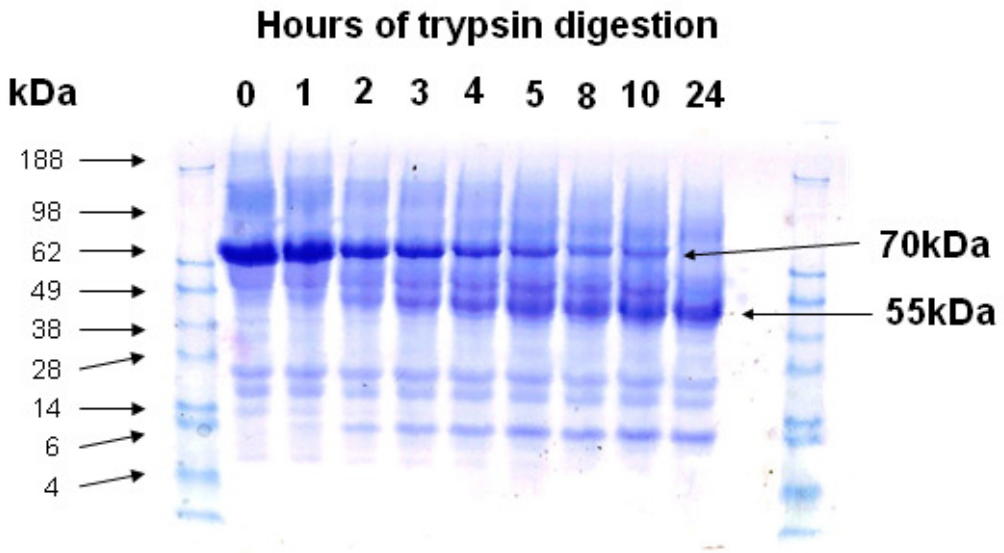

Figure 2.5- Trypsin digest of nNOSoxy followed by SDS-PAGE. The first and last lane are markers (SeeBlue® Plus2 Protein Standard, Invitrogen) used to judge fragment size. From left to right of the sample lanes are times of digestion of 0, 1, 2, 3, 4, 5, 8, 10, 24 hours. After 24 hours the oxygenase domain without PDZ domain predominates. It must be further purified by FPLC before use in crystallography.

2.6.2 Åkta separation of digestion products

A Sephadex 200 size-exclusion column is used to separate the products of the trypsin digest on the basis of size. It separates the PDZ domain, undigested nNOSoxy and digested nNOSoxy domain. The elution of protein was followed by monitoring at 280nm. Heme was detected by measuring at 400nm. Fractions were collected and SDS-PAGE was run to identify proteins in it and the purity of the fractions. Those containing oxygenase domain without the PDZ were pooled and concentrated using Vivaspin concentrators with a 30000 MW cut off membrane. Concentrated protein was flash frozen and stored for later use.

2.6.3 Protein crystallization

Crystallization of the digested nNOSoxy domains (either WT or G586S) was carried out by hanging drops, using 24 well Linbro® plates, respectively (Hampton Research). Hanging drops (4 µl volume) were prepared by adding 2 µl of 7-9 mg/ml protein 2µl of well solution. The particular well solution used for each protein sample will be discussed in the relevant chapter.

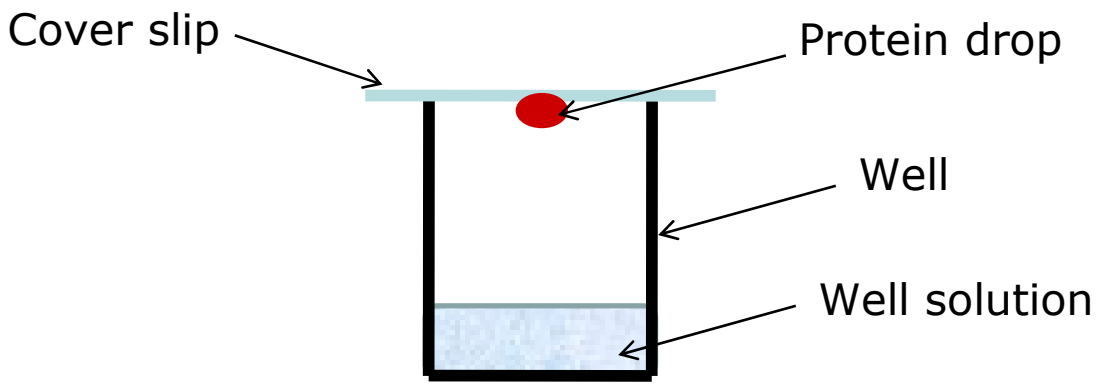

Figure 2.6- The set up of a hanging drop crystallography well.

2.7 Pre-Steady-State Kinetics

Pre-steady-state kinetic measurements were all carried out at 10 or 25^{o}C using an Applied-Photophysics stopped-flow spectrophotometer (SX.17MV) connected with a diode-array detector. All stopped flow measurements were recorded under a nitrogen atmosphere in an anaerobic glove box (Belle Technology; [O_2] < 5 ppm).

2.7.1 Oxy-ferrous decay

For studies of oxyferrous decay the formation of the oxyferrous complex was achieved by mixing ferrous enzyme with an oxygenated buffer. Oxyferrous decay was followed spectrophotometrically. All buffers used in the anaerobic box were bubbled with pure nitrogen before introduction to the box then allowed to equilibrate with the nitrogen atmosphere of the box for at least a day before use. Protein samples for use in stopped flow experiments was passed down a G25 column pre-equilibrated with degassed gel filtration buffer. This removed any oxygen from the sample and was used to introduce

any substrate or cofactors required for specific experiments. Protein was generally diluted to approximately 10 μM. Ferrous nNOSoxy was generated by titration with sodium dithionite. Reduction of the protein was monitored by UV/VIS spectral changes in the heme absorbance. Titration with sodium dithionite was carefully performed so that no excess reductant existed in the protein sample.

For oxyferrous decay measurements the system was cooled to 10°C with ice.

Ferrous protein was then loaded into syringe A of the stopped flow machine. Oxygenated buffer (air saturated, ~200 μm O_2) was loaded into syringe B. The two liquids were then rapidly mixed in the detector head and 400 spectra recorded over a time length of generally 1s. Experiments were repeated several times at several time lengths and data pooled. Data were analyzed using Pro-Kineticist 4.21 software (Applied Photophysics) software.

2.7.2 Ferrous heme-NO decay

The ferrous heme-NO complex of nNOS is considered a dead-end complex. It is tight binding and will only slowly decay without outside reactants. In reaction with oxygen it leaves a ferric heme and nitrate. These changes can be measured spectrophotometrically. All reactions were measured at 25°C.

WT nNOSoxy was treated as above for stopped flow reactions. After careful reduction with dithionite NO was titrated in. A 20ml sample of degassed gel filtration buffer was saturated with NO by bubbling with NO gas for 10min, this was used for NO titration.

Differing amounts of NO were titrated into samples of reduced protein. An excess of NO was used on the first titration so as to gauge a maximal absorbance for the ferrous heme-NO complex. This was measured for the formation of the peak at 436nm.

The proportion of ferrous-NO heme to ferrous heme was calculated by comparing absorbances at 436nm and, once the stopped flow reaction was completed, 426 nm, the oxyferrous absorbance region.

Samples of nNOSoxy with varying amounts of NO titrated in were then reacted with oxygenated buffer. This then led to three reactions in the sample. The first was oxyferrous formation. This then decayed, in the second reaction. The third reaction was the reaction of the ferrous heme-NO complex with oxygen. As these occur on different time scales (the oxyferrous decay being three orders of magnitude faster than the ferrous-NO decay) they could easily be modeled by Pro-Kineticist 4.21 software (Applied Photophysics) software.

2.8 Turnover assay

This assay for detection of the production of NO by NOS works on the shift in UV/VIS spectrum of hemoglobin when NO reacts to convert oxyhemoglobin to methemoglobin.

Oxyhemoglobin is prepared from bovine methemoglobin. A saturated hemoglobin solution is created by gentle stirring of solid hemoglobin over several hours in gel filtration buffer. This is then filtered to remove any debris. To this solution 20mM sodium dithionite is added. The reduced hemoglobin is then passed down a G25 size exclusion column. This removes excess dithionite and allows the reaction of the ferrous

hemoglobin with oxygen. As the hemoglobin reacts to form oxyhemoglobin there is a visible colour change, the protein should become vibrant red. The oxyhemoglobin is collected and flash frozen for later use.

A reaction mixture of 1ml is created containing a final concentration of: 50mM Tris/HCl buffer, pH7.5, 10μM oxyhemoglobin, 0.1mM NADPH, 10 units/ml superoxide dismutase, 100 units/ml catalase, 10μg/ml CaM, 250nM nNOS (prepared in the absence of any pterin cofactor), and pterin at desired concentration. Pterins are prepared for use from solid, under a nitrogen atmosphere, in a buffer containing 1mM dithiothreitol, and stored on ice. The reaction mixture is incubated at 25°C for ~1 min to allow for dimerisation of the enzyme and binding of the analogue.

The cuvette containing the reaction mixture is inserted into the spectrophotometer, set to 401nm, and zeroed. Measurement is started. Due to uncoupled reactions there may be a slight decrease in absorbance measured. The turnover reaction is then started by the addition of L-Arg to a concentration of 1mM. If the pterin is an active cofactor then NO will be produced. Figure 2.6 shows the sort of trace produced by these experiments.

NO converts oxyhemoglobin to methemoglobin. The rate of NO production is then calculated from this conversion. Methemoglobin minus oxyhemoglobin has ε_{401nm}= 49mM^{-1} cm^{-1}.

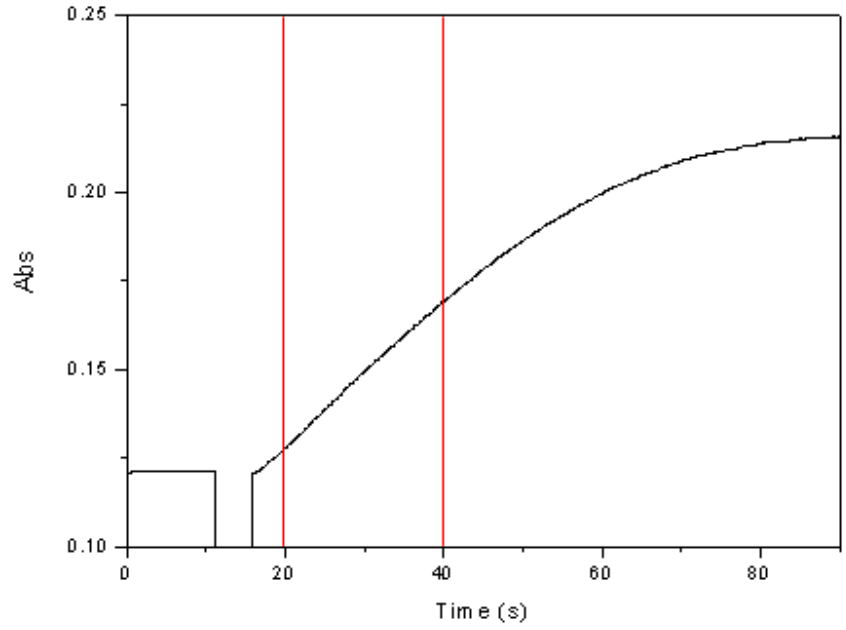

Figure 2.7- Results for a turnover assay for an analogue of H_4B. Absorbance is measured at 401nm. Rate of NO production is calculated from the linear portion of the graph, demarked in red.

2.9 Peroxide shunt reaction

It has been noted before that nNOSoxy can produce NO from NOHA if also in the presence of hydrogen peroxide (88), this is referred to as the shunt reaction, and is well demonstrated in cytochromes p450. However nNOSoxy will not perform the first monooxygenation step of L-Arg to NOHA. Also the product of the peroxide driven shunt reaction of NOHA leads to the formation of NO with L-citrulline and cyanoornithine in equal quantities. Under normal turnover conditions only L-citrulline is produced. The shunt reaction was attempted with both nNOSoxy WT and G586S.

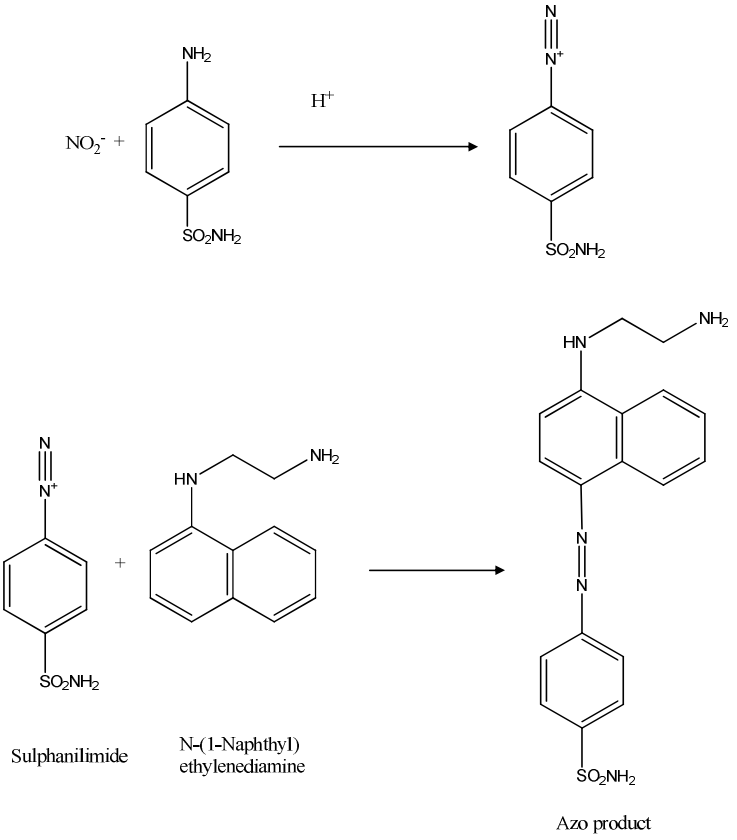

Figure 2.8 - The Griess reaction used in the detection of nitrite. The λ_{max} of the azo product is 540nm.

Direct detection of NO is difficult so nitrite (a rapidly produced breakdown product of NO with O_2) production by wild-type and G586S nNOSoxy was determined using the Greiss reagents (89) sulfanilamide and *N*-(1-naphthyl)ethylenediamine following the peroxide shunt assay. The product of the Griess reaction, a pink azo-dye, was measured by taking the absorbance at 540nm, Figure 2.8 shows the Griess reaction. The assay mix consisted of a 100µl reaction mixture prepared in 50mM Tris buffer pH7.5 with either 250nM nNOSoxy WT or nNOSoxy G586S, 0.1-1000 µM H_4B, 1mM NOHA, 0.5mM

DTT, 10units/ml SOD and 0.5mg/ml BSA. The reaction was initiated by the addition of hydrogen peroxide added to a final concentration of 30mM. The reaction was incubated at 25˚C for 10 mins and quenched with the addition of 1500 units of catalase.

At the beginning of each set of experiments a concentration curve for standard nitrite solutions reacted with the Griess reagents was derived to allow accurate concentration measurement.

2.10 Single turnover

To test the catalytic activity of the G586S mutant without creating the full length mutant single turnover reactions using the heme domain were used (90). These single turnover reactions mimic normal turnover exactly except they use dithionite as the external source of electrons instead of the reductase domain and they are only capable of performing a single monooxygenation step (either L-Arg to NOHA, or NOHA to citrulline).

nNOSoxy (WT or G586S) was introduced to a nitrogen atmosphere within an anaerobic box. Oxygen was removed from the sample by passing down a G25 size exclusion column pre-equilibrated with degassed 50mM Hepes buffer, 0.1M NaCl, 1μM H_4B, pH 7.5. The protein was reduced by careful titration with sodium dithionite, complete reduction being judged by a destruction of absorbance at 650nm.

Samples of 1ml protein, of approximately 50 μM, had either L-Arg or NOHA added to a concentration of 150μM. Samples were then removed from the anaerobic box and exposed to atmospheric oxygen for several minutes. The reaction solution was

separated from the protein by centrifuging the reaction sample in Millipore filters with 10000 MW cutoffs.

The reaction solution was then either used directly for derivatisation of amino acid products or frozen for later use (91). *o*-phthaldialdehyde (OPA) reagent (1mM OPA, 10 v/v methanol, 1v/v β-mercaptoethanol) was prepared and stored at 4˚C for up to 48hrs. 80µl of sample was mixed with 20µl of OPA reagent for 1 minute before use in HPLC. OPA derivitised amino acids are detectable by fluoroscopy. After derivatisation a 20µl sample was injected onto a Phenomenex hypersil 250 x 10.00 mm column, 5 micron particle size. The column was eluted under the following conditions. Buffer A= 5% acetonitrile, 15mM sodium borate with 0.1 v/v trifluoracetic acid, pH 9. Buffer B= 50% acetonitrile, 8mM sodium borate, 0.1 v/v trifluoroacetic acid, pH9. The solvent gradients were linear and as follows; Flow rate 1.5 ml/min. 0-10 min= 0-12% buffer B. 15-26 min= 12-85% buffer B. 31-36 min= 85-0% buffer B. 36-50 min at 2 ml/min, 100% buffer A. OPA-derivatised citrulline, NOHA and arginine eluted at 30.8, 31.2, and 32.2 min respectively as easily resolved peaks. Fluorescence was detected by excitation at 360nm and emission at 455nm using a Gilson 122 fluorometer. Each reaction was run in duplicate and each reaction analysed in duplicate.

2.11 EPR

WT and G586S nNOSoxy protein was prepared as described above. It was then passed down a G25 size exclusion column pre-equilibrated with a standard phosphate buffer (KPi 0.1M, pH 7.4, no Glycerol, no salt) to exchange the buffer. The resulting protein

in phosphate buffer was concentrated to 150 μM. No substrate, L-arg or NOHA was added to the protein at a concentration of 300 μM depending on the conditions to be tested. The protein was then reduced carefully with sodium dithionite so as to leave no excess. After reduction of the protein sample NO gas was bubbled through the sample for several seconds and the sample sealed. The protein was then flash frozen in liquid nitrogen and sent to Jerome Santolini and Pierre Dorlet (Institut de Biologie et de Technologies de Saclay, Saclay, France) who recorded the spectra shown in Figure 3.5. The 9.4 GHz (X-band) EPR spectra were recorded on a Bruker ELEXSYS 500 spectrometer equipped with a standard TE cavity (Bruker) and an Oxford Instrument continuous flow liquid helium cryostat and a temperature control system. Simulations were performed by using the Easyspin software package.

Chapter three

nNOS G586S

3.1 Introduction

(Previous work on G586S mutant by Davide Papale and Chiara Bruckman)

As stated in the introduction there is still much discussion on the details of the mechanism of NOS. Argument hinges on the active species of the heme capable of performing the monooxygenation. An oxyferryl heme radical cation (Compound I), as is found in the mechanism of cytochromes P450, seems a sound candidate and DFT calculations support its role in NOS (92). No direct detection of this intermediate has been made in NOS however.

It must also be remembered that NOS carry out two monooxygenations; the first on L-Arg and the second on NOHA. Most research assumes that the two steps are different in mechanism, favouring a peroxy ferrous active species for the second monooxygenation (93). Certain portions of both steps are known. For instance, a pterin radical is formed for both substrates. After the binding of an oxygen molecule to the ferrous heme then both steps proceed via the donation of an electron from H_4B. Both steps then continue via a peroxo ferric complex. It is after this point in the mechanism, steps 2 and 7 in Figure 3.9, that remains unclear and the role of H_4B must be defined.

The residues of the distal active site of nNOS act to stabilise and activate the oxygen species formed on the heme iron via positioning of the substrate. They aid in promoting oxygen binding and cleavage of the O-O bond. They do this by the precise positioning of the substrate guanidinium group (21). However, there are no hydrogen bonds directed at the space where substrate and oxygen react. Cytrochromes P450 do have hydrogen bonds in the active site which interact with heme-bound oxygen, usually stabilizing water

molecules in the active site to act as a proton transfer pathway (94). Protons are necessary for oxygen activation, see Figure 3.9 steps 2 and 7. Introducing a hydrogen bond to the active site of NOS may alter the rate of reaction or stabilise an intermediate, as has been seen previously (95). Therefore a mutation was introduced converting an active site glycine to serine (G586S). This mutation was created in the nNOSoxy construct and characterised spectroscopically and crystallographically.

The G586S mutation was found, by stopped flow reactions following oxy-ferrous decay, to stabilise an intermediate, Figure 3.1.

Rates of decay for the novel intermediate were derived and can be seen in Figure 3.1. The intermediate does not resemble a simple overlaying of other states and decays with a single rate.

Intriguingly the intermediate was not observed if oxyferrous decay was performed with the redox inactive H_4B analogue 4-amino-H_4B (aH_4B). This allows us to position the intermediate within the putative mechanism for NOS. The intermediate would seem to be the product of the donation of an electron from H_4B to the oxyferrous heme. This would place the observed intermediate in the portion of the mechanism for which there is least information, that of the active oxygenating species. If the stabilised intermediate observed in G596S could be shown to be mechanistically active then it could prove a valuable tool in unraveling the mechanism of NOS. Further work was undertaken to understand how the introduced serine was stabilizing this intermediate.

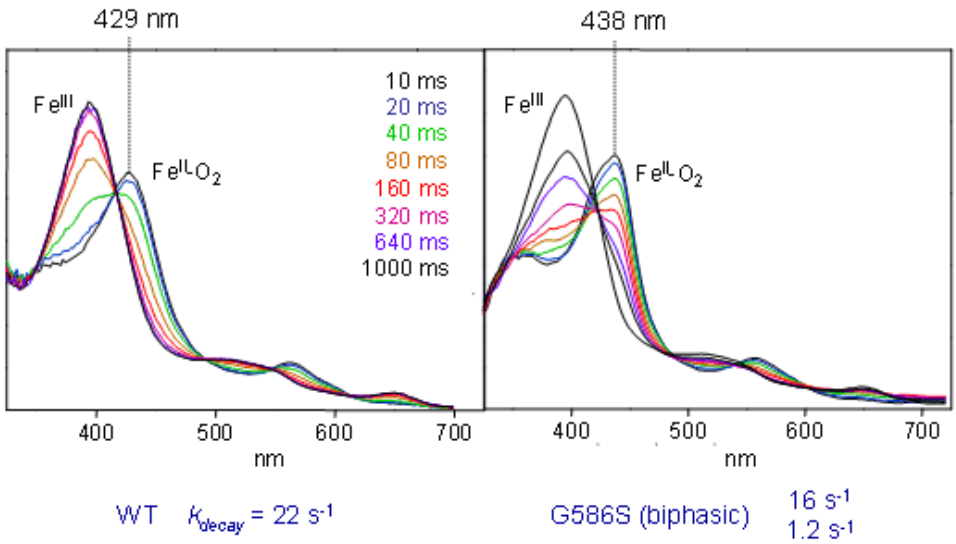

A

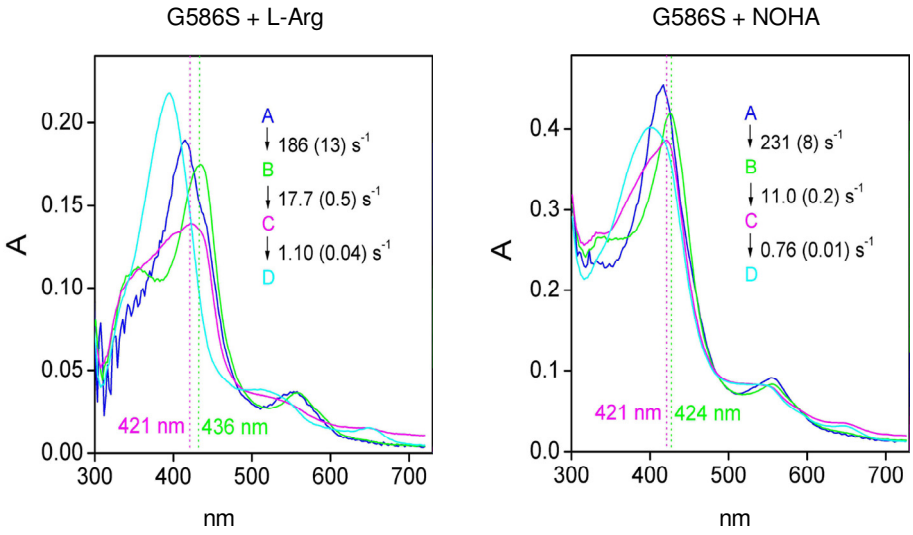

B

Figure 3.1- The G586S mutant was probed by stopped flow reaction of the reduced protein with oxygen. This forms the oxyferrous complex, and the decay of that species can be followed spectroscopically. A) Shows the spectra observed during oxyferrous decay of WT and G586S nNOSoxy, with L-Arg bound. Note the shift in the position of the oxyferrous peak in the mutant. B) During the decay of the oxy-ferrous species, green, in the G586S mutant a species previously unobserved, pink, in the WT is seen to form Dark blue is the ferrous heme, light blue the ferric heme. The intermediate was detected by fitting the observed data of oxyferrous decay to a triphasic mechanism. An extra intermediate is observed with either L-Arg or NOHA bound to G586S, with the same absorbance maximum. Spectra gathered at 10°C.

Affinity titrations showed that the introduced serine residue, likely due to the introduced hydroxyl on the side chain forming a hydrogen bond, stabilised the binding of arginine. Arginine affinity was increased by a factor of 10 in the G586S mutant, from 1.0μM in the WT enzyme to 0.1 μM. NOHA binding affinity was also increased from 0.9 μM in the WT to 0.5 μM. This shows a preference for arginine binding over NOHA in the mutant that is not present in the WT.

In WT nNOS the K_d of NO binding to the ferric heme in the absence of substrate was calculated as 2.5μM, decreasing to 6.9 μM and 20.3 μM in the presence of L-Arg and NOHA respectively. The introduced serine residue was not seen to significantly alter the binding of NO to the ferric heme of the mutant in the absence or presence of substrate, K_ds of 1.8, 3.2 and 2.2 μM were measured for G586S nNOSoxy substrate free, with L-Arg or NOHA respectively. The with-substrate binding affinities of diatomic ligands in the mutant are significantly higher than the WT enzyme however.

The binding of CO was used to probe the ferrous heme. Here either substrate was found to increase the binding affinity by ~10x in the mutant compared to WT. In summary the G586S mutation has little effect on the binding of diatomic ligands in the absence of substrate but increases the affinity with substrate. This suggests a substrate mediated interaction between diatomics bound to the heme and the introduced serine. It was suggested the stabilising of binding may be due to a repositioning of the substrate through interaction with the serine. A new interaction between heme binding diatomics and the guanidinium group of the substrate may have been introduced.

This was subsequently confirmed by x-ray crystallography which yielded a structure of 2.6 Å resolution (PDB 3FC5, unpublished paper). This structure, from a crystal grown

with protein prepared by the present author, showed no gross structural change in the enzyme. As Figure 3.2 shows the hydroxyl of the serine residue is indeed within bonding distance of the guanidinium group of arginine, with a distance of 2.9 Å. The extra hydrogen bond would account for the 10 fold increase in binding affinity for L-Arg. Modeling suggests that NOHA would also be able to support this hydrogen bonding. However, the additional hydroxyl that NOHA has could clash with the serine residue. This would account for the difference between the binding affinities of arginine and NOHA seen in the mutant. A crystal structure of the mutant with NOHA binding would clear up whether this is the case.

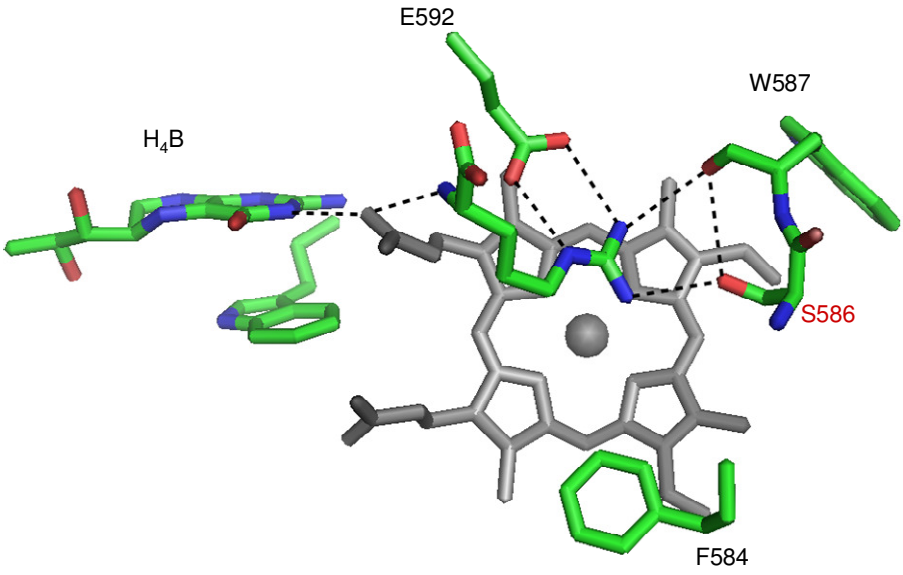

Figure 3.2- The active site of the G586S mutant with L-Arg bound. S586 is seen to contribute an extra hydrogen bond to the substrate, as predicted by binding affinities. It would also introduce an extra proton to the active site. (PDB 3FC5)

3.1.1 Aims

A major part of this project has been concerned with elucidating whether the mutant is catalytically competent to produce NO. As shall be seen this question has been solved and the role and identity of the stabilised intermediate can be theorised.

To confirm and add to the work already done on this mutant several experiments were required. A crystal structure of the mutant with NOHA bound was sought to confirm substrate orientation. EPR experiments were used to probe the active site interactions with a diatomic ligand bound at the heme. Finally a method of checking the catalytic competency of the mutant was required to understand the relevance and properties of the stabilised intermediate.

Results

3.2 Crystallographic studies of G586S

(With Laura Campbell, University of Edinburgh)

To aid in further understanding of the differences between the two monooxygenation steps of NOS, and specifically in the G586S mutant, a crystal structure of the G586S mutant with NOHA bound was sought to complement that already gained with L-Arg. Any differences in binding orientation detected in the crystal structure would aid in interpreting the data gained in binding affinities and other reactions.

Following purification of the G586S nNOSoxy and digest with trypsin to remove the mobile PDZ domain, as described in Materials and Methods, suitable protein for crystallography was collected. Using the conditions previously found (Unpublished data,

D. Papale and C. Bruckman) to suit crystallisation of the mutant with arginine several hanging drop trays were prepared around these conditions. 0.1M MES (2-(*N*-morpholino)ethanesulfonic acid) of pH ranging from 5.8-6.5 was used. Also varied in our trials was the concentration of polyethylene glycol, 3350Da, 20-25%. All other chemicals in each well were kept constant. These were 0.2M ammonium acetate, 2% isopropanol, 50mM Sodium Dodecyl Sulfate (SDS), and 50mM glutathione. 2µL of well solution was mixed with 2µL of protein (6-8 mg/ml) and placed upon a coverslip.

NOHA was added to the protein and the well solutions at a concentration of 150µM. This vast excess of substrate was used to ensure full occupancy of the active site and to facilitate dimerisation.

A crystal was found after 5 days of crystallisation, see Figure 3.3.

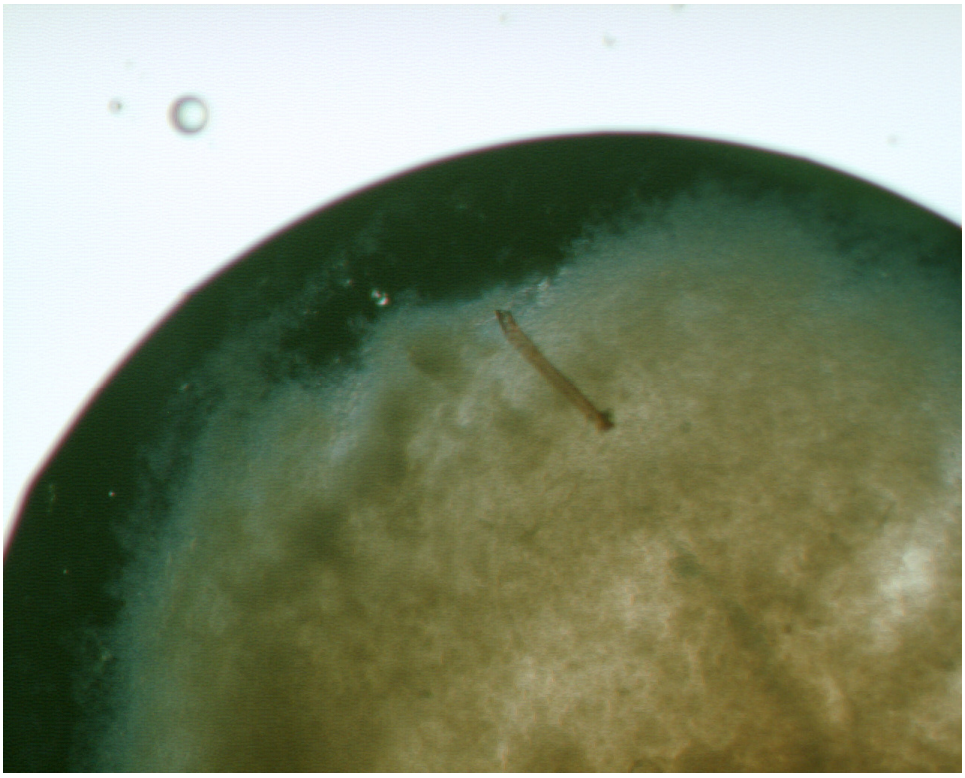

Figure 3.3- The rod shaped crystal gained for G586S nNOSoxy with NOHA.

The variable conditions used to grow this crystal were as follows. The protein concentration was 6 mg/ml, pH 6.5, 25% PEG. Unfortunately this crystal shattered as it was removed and frozen. Possible conditions for crystallisation have therefore been found. There was not sufficient time in this project to gain the crystal structure as to successfully grow a useable crystal would likely haven taken months of repeated attempts in varying conditions, as it did with the G586S with L-Arg crystal.

3.3 EPR studies of G586S

Without a crystal structure to supply information on the binding of NOHA in the active site an alternative experiment was sought to probe the active site interactions of the G586S mutant. EPR (Electron Paramagnetic Resonance) studies allow the probing of interactions of the ferrous heme-NO complex. The stability of this complex makes it ideal for these studies. The ferrous heme-NO complex is a good analogue of the oxyferrous complex and may point to important interactions between the substrate, active site residues and the diatomic ligands. Such studies allowed the probing of hydrogen bond networks in the active site by comparison of the WT enzyme with the G586S mutant, with and without substrates.

WT and G586S nNOSoxy protein was prepared to concentrations of 150 μM in a standard phosphate buffer (KPi 0.1M, pH 7.4, no Glycerol, no salt). The protein was then reduced carefully with sodium dithionite so as to leave no excess. After reduction of the protein sample NO gas was bubbled through the sample for several seconds and the

sample sealed. The protein was then flash frozen in liquid nitrogen and sent to Jerome Santolini and Pierre Dorlet (Institut de Biologie et de Technologies de Saclay, Saclay, France) who recorded the spectra shown in Figure 3.4. 9.4 GHz (X-band) EPR spectra were recorded on a Bruker ELEXSYS 500 spectrometer equipped with a standard TE cavity (Bruker) and an Oxford Instrument continuous flow liquid helium cryostat and a temperature control system. Simulations were performed by using the Easyspin software package. When required the substrates were added to the samples in excess. These results confirmed several predictions regarding the binding of substrates at the mutant active site. Figure 3.4 shows the main results of these studies.

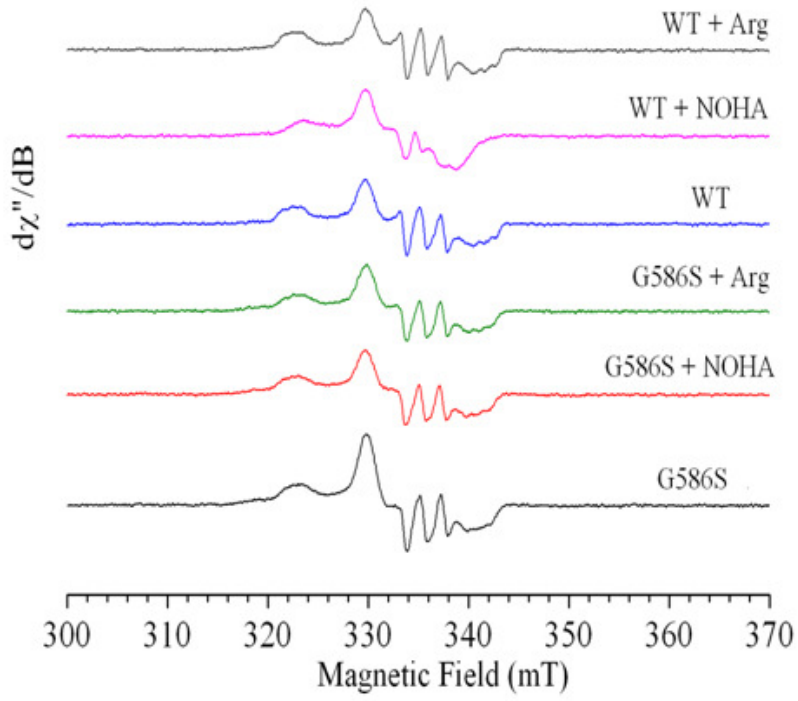

Figure 3.4- EPR results indicating the interactions of the ferrous heme-NO complex in WT and G586S nNOSoxy with various active site occupancies. Protein was 150 µM and substrate, if present, 300 µM.

These results closely resemble those previously gained for nNOS (86). As can be seen in Figure 3.4, and from the g –values in table 3.1, the binding of arginine does not greatly affect the profile of the ferrous-NO spectrum in either WT or mutant.

Protein Sample	g-values
WT (No substrate)	2.086, 2.005, 1.970
WT (Arginine)	2.085, 2.004, 1.970
WT (NOHA)	2.077, 2.005, 1.986
G586S (All conditions)	2.084, 2.005, 1.973

Table 3.1 – Table of g-values derived from EPR experiments on WT and G586S nNOSoxy (Ferrous-CO complex). Note only WT nNOSoxy with NOHA bound displays a markedly different spectrum. G586S nNOSoxy gave the same spectrum with either substrate, or none.

This suggests a very limited interaction between arginine and the heme-bound NO in both proteins, despite both proteins displaying a far greater affinity for NO when L-Arg is bound compared to substrate free. The binding of NOHA in the WT protein causes a large shift, 2.077 compared to 2.085 on L-Arg binding. This reflects an introduced H-bond network on NOHA binding that alters the ferrous-NO geometry (96). Interestingly this does not occur in the G586S mutant with NOHA, whose spectrum most resembles that of the G586S mutant with arginine. This can be explained by NOHA having a quite different binding orientation in the mutant than in the WT. As has been suggested in the introduction to this chapter, the introduced serine residue could clash with the NOHA hydroxyl group. It may be the interaction between this NOHA hydroxyl and the ferrous

heme-NO complex that leads to the different EPR spectrum in the WT. If there is a clash in the mutant, the NOHA would bind (since we know it does bind) in a different orientation. In this other orientation the NOHA hydroxyl may be orientated away from the heme. This would explain the seeming lack of interaction between NOHA and the ferrous heme-NO complex. It would be useful to have a crystal structure of the G586S mutant with NOHA bound to confirm this interpretation.

Catalytic competency of G586S

3.4 nNOSoxy peroxide shunt reactions

As mutagenesis of the full length enzyme to G586S proved difficult other experiments attempting to probe the catalytic competency of the mutant were attempted using just the oxygenase domain. The hydrogen peroxide driven 'Shunt' reaction is well known for P450 oxygenases. Hydrogen peroxide is thought to react with the ferric heme to form a peroxo-ferric species directly, bypassing several steps of the normal mechanism. The peroxo-ferric species then undergoes a heterolytic O-O bond cleavage to produce a Compound I intermediate that performs substrate oxidation (97).

Hydrogen peroxide has also been shown to be able to convert NOHA to citrulline in the presence of NOS (85) and so was used here to test catalytic competency of the mutant here.

Wild type and G586S nNOSoxy were tested for their ability to produce nitric oxide from NOHA using the peroxide shunt assay. Reaction of either enzyme with hydrogen

peroxide, but no substrate, gave no production of nitrite as judged by the Greiss reaction. Both enzymes proved capable of producing NO from NOHA by the shunt reaction. Both enzymes reached their maximum catalytic rate in the presence of approximately stoichiometric H_4B. Under these conditions wild-type and G586S nNOSoxy produced 0.142 ±0.011 and 0.154 ±0.005 mol of nitrite per mol enzyme respectively in 10 min assays as measured using the Greiss reaction for the detection of the breakdown products of NO (data not shown). In these assays, nitrite results from the production of NO, indicating that the mutant is as catalytically competent as the wild-type enzyme in performing nitric oxide synthesis under these conditions.

The qualification 'under these conditions' is important in reference to the 'shunt' reaction of NOS. Previous work has shown that the reaction is only capable of the second of the monooxygenation steps, which most researchers take as evidence that the two steps do not use the same mechanism. A second concern is the significant formation of cyano-ornithine, Figure 3.5, in this reaction (98). Cyano-ornithine has never been detected in normal turnover conditions and its presence as a significant product may raise doubts over whether the shunt reaction provides reliable data on catalytic competency. While NO is certainly being produced it is possible that the shunt reaction is not following the normal mechanistic pathway for NOS.

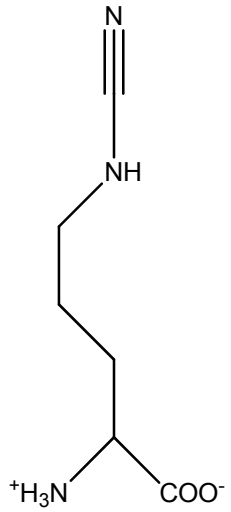

Figure 3.5- Cyanoornithine, a major byproduct of the peroxide shunt reaction of NOHA in NOS.

As well as these limitations it was also found that hydrogen peroxide and NOHA in the presence of hemoglobin is capable of producing NO, as judged by the Greiss reaction (data not shown). This suggests that the reaction is non-specific to the highly regulated environment of the nNOS active site, but capable of occurring at a non-specific heme. This ability of a non-NOS hemoprotein to support the peroxide shunt driven creation of NO from NOHA may offer further mechanistic insights, but requires more study than it has been possible to give in this work. The experiments of this reaction were limited and qualitative, but may be of interest.

3.5 Single turnover reactions

Single turnover reactions mimic exactly the conditions of normal turnover of the enzyme, but are capable of only single monooxygenations. That is, they can convert arginine to NOHA and NOHA to citrulline and NO. These reactions rely on the external delivery of

electrons, due to the absence of a reductase domain in this case as nNOSoxy was used for both WT and G586S experiments. Here sodium dithionite was used to reduce the heme by careful titration to ensure no excess dithionite provided excess electrons to the reaction. Once reduced the enzyme is then in the same state as it would be in normal turnover after the delivery of the first electron from the reductase domain (step 1 of the mechanism as shown in Figure 3.9). The protein is then exposed to oxygen, which binds to the heme. The reaction then continues using an electron donated from the pterin. The substrate should then be converted to the product of whichever monooxygenation step is being tested. L-Arg would be unable to undergo the second monooxygenation though as further electrons, normally reductase domain derived, would be unavailable. These single turnover reactions should therefore allow the complete probing of a catalytic cycle of the mutant enzyme and reveal competency.

To follow these reactions, as no NO would be produced by the first monooxygenation, product analysis of the amino acid substrates and products (l-Arg, NOHA and citrulline) by HPLC was used. To allow detection of the amino acids they were derivitised with OPA, as stated in the materials and methods. The following three Figures (figs. 3.6, 3.7, and 3.8) are representative of the results gained by HPLC analysis of the products of single turnover reactions of the WT and G586S enzymes.

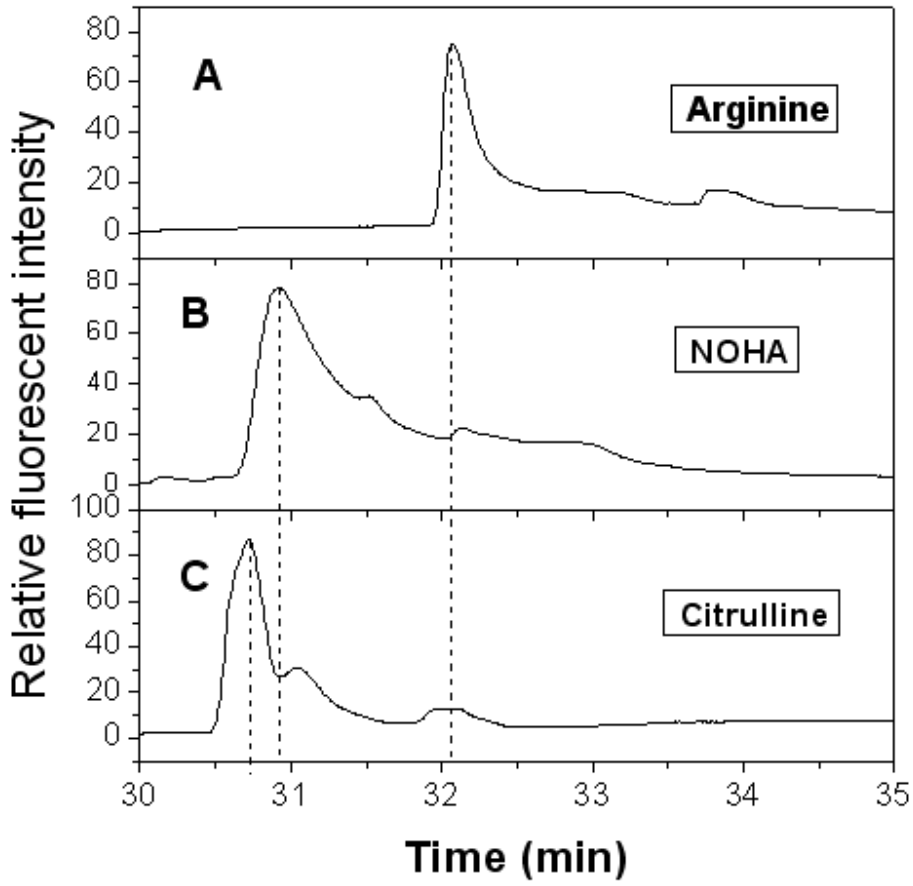

Figure 3.6- Fluorescence traces of the OPA-derivatives of L-Arg, NOHA and citrulline as they were eluted from the HPLC column as controls. Reaction mixtures were prepared (50 μM nNOSoxy, 150 μM amino acid, 1 μM H_4B), but not reduced by dithionite, and protein removed by centrifugal concentrator. 80 of the solution was mixed with 20 OPA solution, allowed to react for 1 minute. 20 of the derivitisation mix was injected into hypersil reverse phase column, running conditions in materials and methods. Product elution was detected by fluorescence at 455nm (excitation wavelength 360nm). Elution times for arginine (A), NOHA (B) and citrulline (C) were 32.2, 30.9 and 30.7 minute respectively.

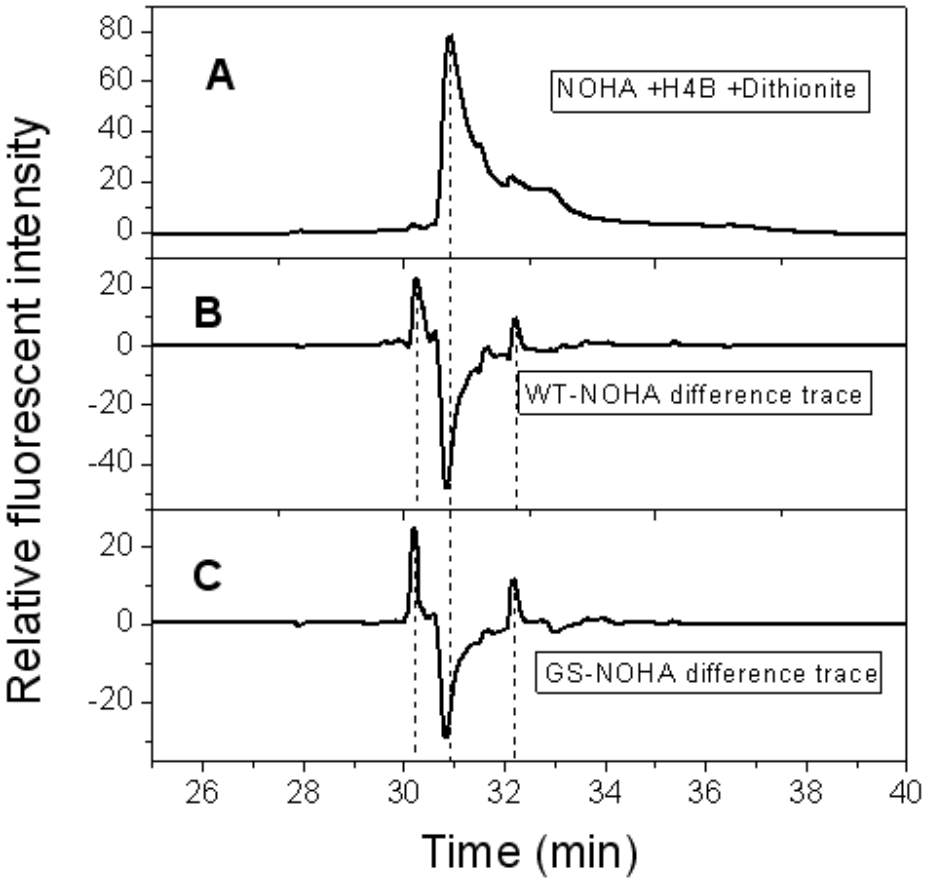

Figure 3.7- Single turnover results for WT and G586S with NOHA. A) The first trace shows the control elution trace for NOHA derivatised with OPA. B) The second trace shows the elution trace for the WT single turnover reaction minus the standard. The peaks at 30.1 and 32.1 min show amino acid products of the single turnover reactions. Citrulline appears to have been produced from NOHA by the WT enzyme. C) The third trace shows the elution trace for the G586S single turnover reaction minus the standard. The peaks at 30.1 and 32.1 min show amino acid products of the single turnover reactions. Citrulline appears to have been produced from NOHA by the G586S mutant. As separation of amino acids was not complete, to make the results clear the standard elution trace of NOHA was subtracted from the reaction product traces to easily view the product peaks. See text for full explanation.

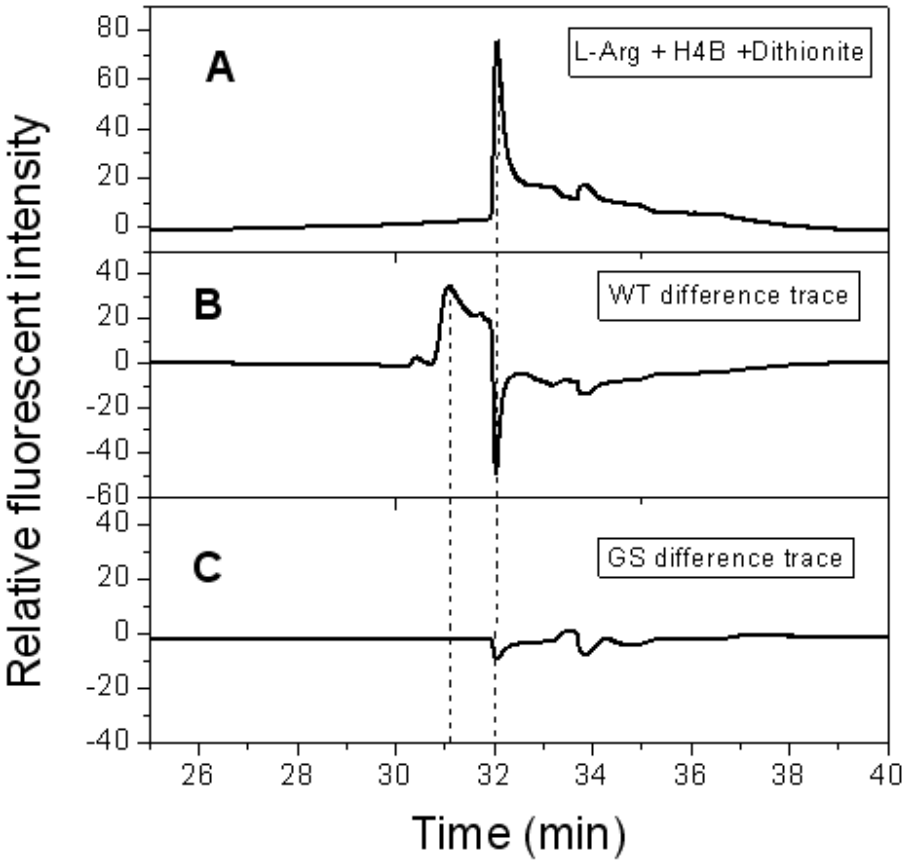

Figure 3.8- Single turnover results for WT and G586S with L-Arg. A)The first trace shows the standard elution trace for L-Arg derivatised with OPA. B) The second trace shows the elution trace for the WT single turnover reaction minus the standard. The peak at 31.1 min is characteristic of NOHA. NOHA appears to have been produced by the WT enzyme by these single turnover reactions. C) The third trace shows the elution trace for the G586S single turnover reaction minus the standard. The lack of any major peaks suggest the G586S was unable to react with arginine under single turnover conditions. See text for explanation. As separation of amino acids was not complete, to make the results clear the standard elution trace of NOHA was subtracted from the reaction product traces to easily view the product peaks. See text for full explanation.

As Figure 3.6 shows the separation of arginine, NOHA and citrulline was not completely resolved, with elution times of 32.2, 31.0, and 30.7 minutes respectively, but they were sufficiently separated to allow for analysis.

Figure 3.7 shows the traces recorded for the HPLC analysis of the reaction mixture, without enzyme, and the difference traces of the single turnover reactions of the G586S mutant and WT enzymes with NOHA, as followed by OPA derivitisation of amino acids in the reaction mix after the reaction. These reactions mimic the second monooxygenation step and were performed to confirm the previously gained results from the peroxide shunt mechanism. The difference traces were calculated by simply subtracting the trace of the reaction mixture from the trace recorded for the single turnover. This was done to allow ease of comparison due to the lack of complete separation. The difference trace for the single turnover reaction of WT enzyme with NOHA shows a negative peak at ~31min elution time, corresponding to NOHA consumption. This results from the consumption of NOHA in the single turnover reaction. The same is seen for the G586S mutant. A peak appears at 30.1 min, corresponding to citrulline. This suggests that NOHA has been converted to citrulline under these conditions by both the WT and mutant enzyme. It should be noted that there is a significant, though minor, extra product in the NOHA single turnover steps. It is unclear what this product may be, but it appears in both the WT and mutant reactions and should perhaps be seen as an artifact of the single turnover technique, much as cyano-ornithine is seen in the peroxide shunt reaction (though this minor product is at a much lower proportion than that of cyano-ornithine in those experiments) (98).

Figure 3.8 shows the traces for the HPLC analysis of the reaction mixture, without enzyme, and the difference traces of the single turnover reactions of the G586S mutant and WT enzymes with L-Arg. The difference trace for the WT enzyme shows a negative peak at ~32 min elution time corresponding to L-Arg, showing its consumption in the single turnover reactions. There is also a peak at ~31 min, suggesting the production of NOHA by the WT enzyme from NOS, as would be expected. However the difference trace for the G586S mutant shows no significant peaks, either negative or positive on the difference trace. This would be the case if no reaction had occurred.

By examination of the difference traces in Figures 3.7 and 3.8 it appears that under these conditions the WT enzyme is capable of both monooxygenation steps while the G586S mutant is competent of only the conversion of NOHA to citrulline. The G586S mutation seems to have uniquely disentangled the monooxygenation steps of the NOS reaction.

3.6 Discussion

For the purposes of this discussion it is useful to replicate the mechanism shown in the introduction, as it will be referred to throughout.

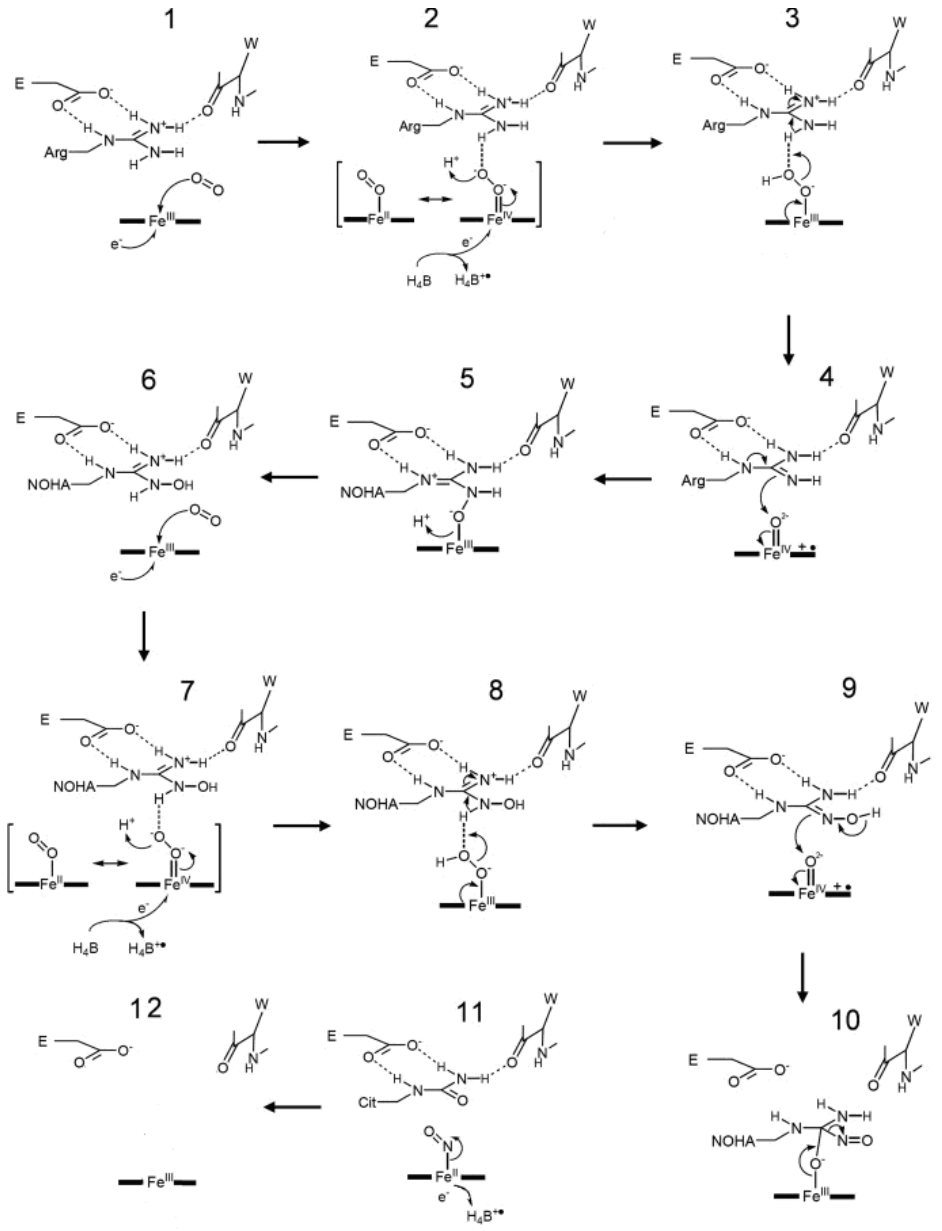

Figure 3.9- Proposed mechanism of NOS using a Compound I active species for both monooxygenations. Water is lost at steps 4 and 8.

Figure 3.9 shows a proposed mechanism, one of several (99, and references therein), for NOS. We must consider what the experiments performed here can reveal about this mechanism and the role of H_4B.

Peroxide driven shunt reactions proved useful as a first line test for catalytic activity in the G586S mutant. However this method of testing NOS catalysis is limited. The WT enzyme is incapable of supporting the full catalysis of NO and citrulline from arginine by the peroxide shunt reaction, only from NOHA. This inability intriguingly suggests that the two monooxygenation steps differ from each other in some fundamental way. However it may be that hydrogen peroxide only offers only a poor mimicry of what is actually occurring in normal turnover. It could be that NOHA is a rather promiscuous substrate, able to react in a number of ways to produce NO. This would certainly be evolutionarily favourable in the construction of a robust mechanism and would explain NOHA's presence as an intermediate. This peroxide shunt mechanism is fascinating but of limited use here, given the limitations mentioned. The results gained are insufficient on their own to reveal whether the G586S mutation will support complete turnover, as it can only provide information about the second monooxygenation step. Since the shunt reaction also shortcuts the reaction directly to step 8, Figure 3.9, it also reveals little of the activity of H_4B, since it misses the electron donation from the pterin. Other experiments were needed.

Construction of the full length mutant proved to be non-trivial for various reasons and so other methods were sought. These other methods arguably offer greater information than simple turnover assays. Had the full length mutant been unable to turnover, as we

can now say it would have, single turnover reactions would have proved necessary to understand which part of the reaction the mutant was incapable of performing.

Single turnover assays and subsequent product analysis supported, but added to, the findings of the peroxide shunt reactions. Single turnover reactions have shown that the G586S mutant is incapable of converting arginine to NOHA. This potentially provides further insight into the differences between the two monooxygenation steps that have so often been treated as identical for ease of description. This mutant has disentangled the two monooxygenation steps of NOS in a meaningful way and will now allow for further probing of the mechanism.

Limitations of OPA detection of amino acid products are several. For identification of amino acid products the method here described is of great use, if access to mass spec is limited. However for absolute quantification of amino acids there are three main problems. The length of time of derivitisation is key to getting reproducible data. The peaks for each amino acid are not all of the same broadness, requiring integration to determine the strength of the signal. There is also the problem of substrate and product remaining bound to the enzyme used in the reaction. It is therefore difficult to be absolutely sure of the stoichiometry of the reaction, but it is possible to identify products clearly. Given that, what can the single turnover reactions reveal about the NOS mechanism? We must pool all of the data we have on the G586S mutant.

Figure 3.9 shows only one of the possible mechanisms of NOS NO synthesis. While referring to it, it must be reconsidered in the light of the data gained here.

The comparison of the NOS mechanism to that of cytochrome P450s should not hide the fact that the reaction catalysed and the mechanism itself are unique. The production

of an NO radical from a stable molecule such as arginine is hard to understand, and the complexity of the proposed NOS mechanisms, is why NOSs are so well studied. Here the data provided by the G586S mutant studies will be used to shed light on the mechanism and the role of H_4B in it.

The two monooxygenation steps each activate a dioxygen molecule to perform a P450-like reaction. The P450 mechanism is widely thought to proceed via a Compound I intermediate, and Compound I has now been directly observed in, and found to be catalytically competent in, the P450 CYP119 (74). No such consensus on the active oxygenating species of NOS exists. Figure 3.9 shows a possible mechanism for NOS that uses a Compound I species for both steps of the reaction. Compound I formation in P450s requires single electron donation to an oxyferrous complex, followed by two protonations and the removal of a water molecule. The oxyferrous complex in NOS is hydrogen bonded to the substrate in the active site. It is likely that by interaction of the substrate guanidinium the oxygen on the heme will have a polarised character, with greater electron density on the distal oxygen. P450s lack the stabilising effect of the interaction and oxyferrous decay is typically faster than in NOS (101). The reduction of the oxyferrous complex NOS occurs with the transfer of an electron from H_4B, which, while close enough to the heme to allow very rapid electron transfer, is a possibly thermodynamically uphill reaction. In P450s the transfer of an electron is usually via a flavin or iron-sulphur cluster. The potentially unfavourable electron transfer from pterin to oxyferrous complex in NOS likely results in an equilibrium disfavouring reduction of the heme. Step two of Figure 3.9 shows a possible way for the electron, once transferred from the pterin, to be locked on the heme; the protonation of the peroxo ferric species

complex. Protonation of the peroxo ferric complex after reduction by H_4B may then be key to mechanism.

The G586S mutation stabilises two intermediates, both highlighting the role of H_4B in the mechanism. The mutant shows a red-shifted Soret band for the oxyferrous complex compared to the WT enzyme and the aH_4B-bound mutant. That a redox inactive pterin does not red-shift the spectrum of the oxyferrous complex shows that the mutant must be having an effect on H_4Bs role as an electron donor. The mutant has an extra hydrogen in the active site, due to the introduced serine. It is possible that introduced hydrogen bond, by strengthening interaction between the dioxygen and substrate guanidinium, shifts the electron transfer equilibrium from the pterin to the heme. Shifting the equilibrium to the heme would lend a significant peroxoferric (or hydroperoxoferric) character to the oxyferrous complex. Intriguingly the hydroperoxoferric complex of chloroperoxidase has a Soret peak similarly red-shifted (101). The hydroperoxoferric complex is a very unstable species and at room temperature decays much faster than it forms and so is difficult to detect.

The second intermediate stabilised by the G586S mutant is that observed following the decay of the oxyferrous species. The spectrum of this intermediate seems oddly undefined in its major absorbance band. This may lead to speculation that the intermediate is actually two species, possibly in rapid equilibrium. The intermediate decays with a single rate, where a mixture of species would be expected to decay with several rates. This intermediate forms after electron transfer from H_4B. An electron transfer from the pterin to the oxyferrous complex would therefore form the peroxoferric heme complex, steps 2 and 7 of the mechanism in Figure 3.9. By protonation of the

peroxoferric heme complex a hydroperoxoferric heme complex would form. Some researchers favour the hydroperoxoferric species as the active oxygenating species of NOS (102). The hydroperoxoferric species may abstract a proton from the substrate, and form a Compound I species, as shown in Figure 3.9. The intermediate stabilised by this mutant could then be the peroxoferric, hydroperoxoferric or Compound I species. Comparison of the spectrum of this intermediate with these species as observed in other heme-thiolate enzymes may be productive. The previously mentioned hydroperoxoferric species of chloroperoxidase has a sharply defined Soret peak at 449nm, that is quite unlike the intermediate observed here. Compound I is a very unstable species and usually only observed under extreme conditions and by freeze-quenching of reactions. To have stabilised a Compound I to the extent that the intermediate here is stabilised, milliseconds, would be unlikely in the extreme. The reported UV/VIS spectra of Compound I (102, 74) and ES (103) species have very little definition in the 500-600nm region. The intermediate observed in the mutant following oxyferrous decay shares this lack of definition. A Compound I species observed by flash photolysis of a Compound II species of cytochrome P450 119 resembles the intermediate seen here in the G586S mutant (104). The Compound I species reported by reaction CYP119 with *m*-chloroperbenzoic acid (74) has a Soret peak at ~370nm however, and is quite unlike the intermediate reported here, and unlike the spectrum produced by flash photolysis.

For several reasons it seems unlikely that direct comparison of NOS spectra with those of other heme-thiolate enzymes will give an exact match. The active site of NOS is unique. In nNOS Trp409 hydrogen bonds to the heme axial cysteine. This will directly affect the UV/VIS spectrum (105). Most uniquely the active site of NOS has a radical

cation pterin hydrogen bonded to a heme propionate. Comparison within the NOS family may be most revealing. Recently an intermediate with a similar spectrum has been observed in the W188H iNOS, which mutates the hydrogen bond to the axial cysteine donated by the Trp409 in nNOS. The W188H intermediate resembled that presented here, with a Soret peak at 421nm (95). That intermediate was found to hydroxylate L-Arg, unlike the intermediate observed here.

The identity of the intermediate formed by G586S nNOS during oxyferrous decay is therefore still an open question. However it seems likely that the intermediate stabilised here is the active oxygenating species and so will prove useful for future research. But it may be possible from the data here to deduce some of the characteristics of the active oxygenating species. The stabilisation of this species must be due to stabilisation of bound substrate by the introduced hydrogen bonds in the active site. The introduced serine hydroxyl group is 3.0 Å and 3.5 Å from the terminal N groups of the guanidinium ion of the substrate. It is also 2.7 Å from the peptide amide of Trp587. The serine hydroxyl can be seen then as both a hydrogen bond donor and acceptor, stabilising substrate binding as binding studies showed. Hydrogen bonding may be key.

The donation of an electron from the pterin to the heme may be unfavourable and require the reaction of the peroxo species with a proton to hold the electron on the heme. The stronger hydrogen bond between the substrate and the heme bound oxygen may slow this proton transfer.

While more work needs to be done to identify the intermediate stabilised by the G586S mutant it is possible to offer a hypothesis explaining the observations. De Visser and Tan (106) have used QM/MM calculations to discover the protonation state of the

substrate in NOS mechanism. That work suggests that the substrate in NOS is the donor of the proton required in step 2 of Figure 3.9. They calculate that this neutral, deprotonated, substrate L-Arg is able to undergo monooxygenation while the protonated L-Arg would not. The G586S mutant has an extra hydrogen bond in the active site via the serine hydroxyl. The introduced hydrogen bond also introduces an extra hydrogen to the active site. Steps 3 and 8 of the mechanism shown in Mechanism 3.1 require the deprotonation of the substrate. The introduced serine may be acting either to hinder deprotonation or actively reprotonating the substrate. The inability of the protonated L-Arg to undergo monooxygenation would explain the increased lifespan of the intermediate in the mutant (it persists until decaying by a non-normal turnover mechanism). This would fit with the single turnover data presented here, indeed the G586S mutant is unable to perform the monooxygenation of L-Arg. Harder to explain is the apparent ability of the mutant to perform the monooxygenation of NOHA to citrulline, whilst still showing accumulation of the intermediate in oxyferrous decay experiments. As EPR experiments suggest that the G586S serine has altered the orientation of the bound NOHA such that it does not interact with diatomic ligands bound at the heme. This alteration of orientation may cause the stabilisation of the intermediate.

It must acknowledged that it is possible the mutant is not forming citrulline in the single turnover reactions but some other amino acid that elutes at the same time citrulline under the HPLC conditions used. LC-MS may be of use in confirming whether this is the case.

Despite the mutant being unable to perform the hydroxylation of L-Arg an intermediate with the same absorbance maximum is observed with both substrates. With

NOHA the intermediate appears to lead to hydroxylation and citrulline formation. This suggests there is a key difference between the two monooxygenations, and they have been disentangled for the first time.

What then may be hypothesised about the G586S mutant? In the first monooxygenation step it seems likely that the mutant, via the extra proton present in the active site due to the introduced serine residue, encourages protonation of the arginine substrate. The protonated substrate is much less likely to undergo reaction. We observe no turnover of the mutant enzyme in single turnover reactions with arginine. The intermediate stabilised in this monooxygenation step may be the reactive species in normal turnover, stabilised by its inability to react with the protonated substrate. An intermediate is also observed in the second monooxygenation step with an absorbance maximum at 421nm, Figure 3.1. However the overall shape of the intermediate observed in the second monooxygenation step is somewhat different. That we observe the intermediate is likely due to the protonation state of the substrate again. However, single turnover experiments show NOHA being converted to a product with the same HPLC elution profile as citrulline. This can be explained if the protonated form of NOHA is able react with the stabilised intermediate, albeit at a decreased rate.

As to what the stabilised intermediate actually is, be it peroxoferric or compound II or some other species, further work needs to be undertaken.

Chapter four

Inter-pterin electron transfer

4.1 Introduction

As has been seen previously the mechanism of NOS is still hotly debated. What is known of the mechanism is that the final product of turnover is the ferric heme-NO complex. This state is thought to be the product of a rapid oxidation of a ferrous heme-NO by the radical pterin cation. Ferric heme-NO is a very weakly bound complex and rapidly releases NO (107). However the rate of reduction of the heme, via electrons delivered from the reductase domain, is of a similar order as the release of NO (40). If an electron is delivered from the reductase domain before the pterin radical cation oxidizes the heme the cation will be neutralized and be unable to oxidize the heme to ferrous-NO. This mistimed electron delivery from the reductase domain creates, particularly in nNOS, a significant amount of a ferrous heme-NO complex without a radical pterin cation to oxidize it as electrons from the reductase domain reduce the heme (108). Ferrous-NO has been called a dead-end complex due to the tightness of its binding. This complex blocks further turnover at the active site. Furthermore, the breakdown of the ferrous heme-NO complex does not lead to NO release. One mechanism for removing this complex is the direct reaction of the ferrous heme-NO complex with a molecule of dioxygen to generate nitrate and ferric heme (Figure 4.1), ready for another turnover.

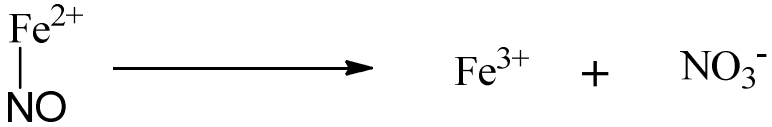

Figure 4.1 - Decay of the dead-end complex by reaction with molecular oxygen.

NOS then has one mechanism for the removal of the ferrous heme-NO complex. With reference to the mechanism in Figure 3.9, the initial product of NOS turnover is accepted to be the ferrous heme-NO complex. In normal turnover it is predicted that the ferrous heme-NO complex would be oxidized by the H_4B radical cation. When the pterin cofactor is in its neutral state it is unable to pull an electron off the heme to generate the unstable ferric heme-NO complex. It is then, with a neutral pterin bound, that the ferrous heme-NO complex may be referred to as dead-end. This dead-end state is what occurs if an electron from the reductase domain is delivered to the heme before NO release.

However, it has recently been suggested that electron transfer between the pterins at the dimer interface could provide an alternative mechanism for degradation of the ferrous heme-NO complex (99). This would add a further function to the pterin, in what is already a unique mechanistic use of a pterin. Figure 4.2 shows the proximity of the pterins, with the conjugated π-systems only 13Å apart, noting also the presence of two tryptophans which could aid in electron transfer between the pterins. If electron transfer is possible between the pterins, as protein electron transfer theory would suggest it is, then migration of the radical from one subunit's pterin to the other could oxidise the ferrous heme-NO complex leading to NO release.

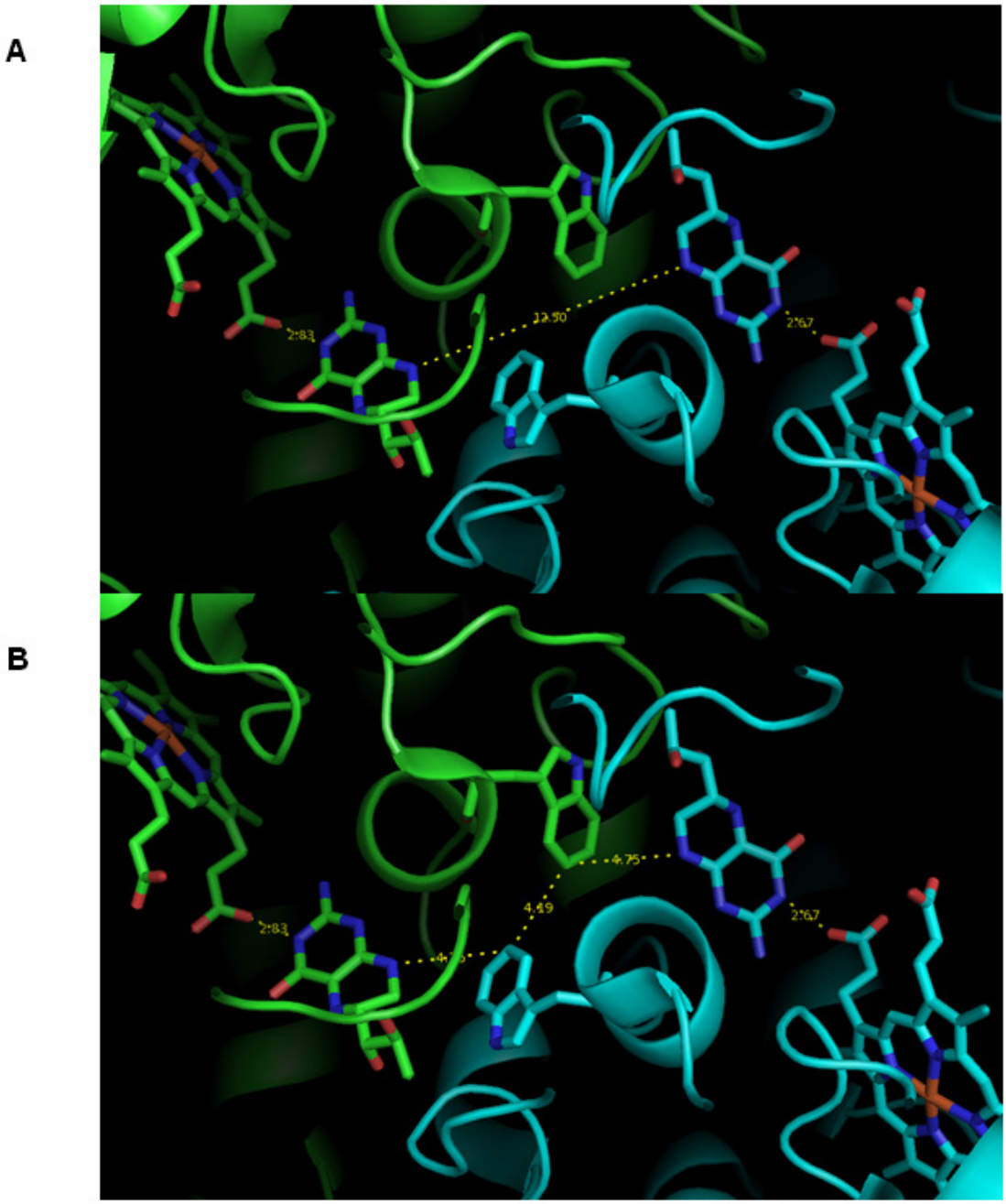

Figure 4.2- The position of the pterins at the nNOS dimer interface. The lower picture, B, shows two tryptophans that could aid in electron transfer between the pterins. Distances shown in Å. (PDB 1OM4)

If this electron transfer occurs between the pterins then a reaction such as shown in Mechanism 4.1 could be envisaged.

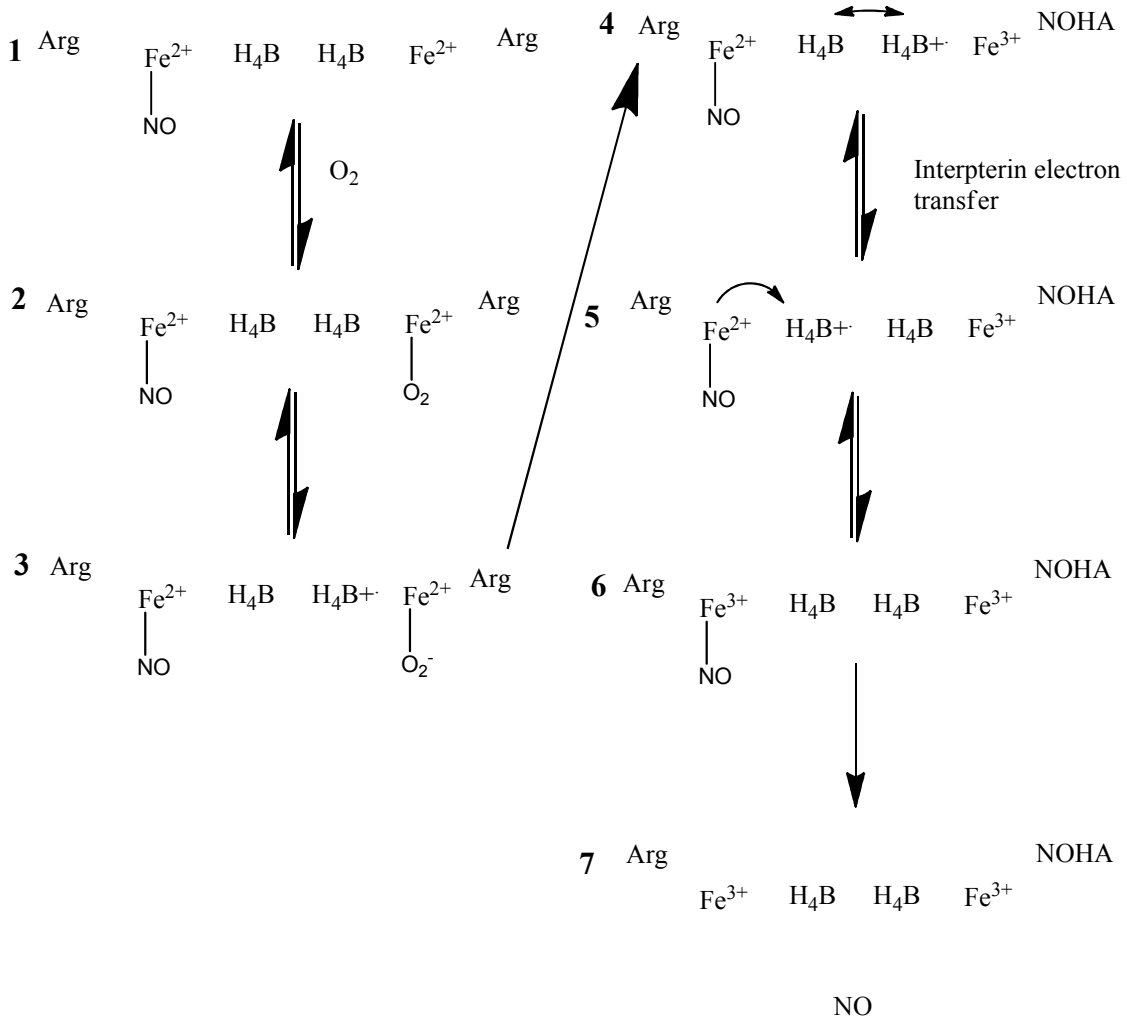

Mechanism 4.1- A proposed mechanism under which it would be possible for electron transfer between the pterins to recover enzyme function from the ferrous heme-NO complex with the release of NO. Mechanism discussed in text.

As mechanism 4.1 shows, electron transfer between the pterins offers a route for efficient recovery from the ferrous-NO state that also leads to NO production, rather than nitrate. The mechanism shown above starts with one heme of the dimer in the ferrous state, and the other as the ferrous heme-NO complex. In normal turnover this would not be an unusual condition, it is estimated that in normal turnover conditions 70-90% of nNOS hemes will be in a ferrous heme-NO complex, a huge proportion if accurate (96). The

rate of oxygen binding to the reduced heme is very rapid. The rate of ferrous heme-NO complex reaction with oxygen is at least three orders of magnitude slower than that of oxidation of the ferrous heme by oxygen. This would tend to leave us with one heme of the dimer in the ferrous heme-NO complex, and the other able to catalyse normal turnover. This will be referred to in this work as NO-heterodimeric (Fe^{II}-NO on one heme, and any other state on the other). An electron from H_4B will be rapidly transferred to the bound oxygen, forming the superoxy-ferrous species. Regardless of whether this is the ultimate reactive species or not the monooxygenation of arginine will occur to form NOHA at the relevant active site. After this reaction the dimer will contain one ferric heme and one ferrous-NO. It is under this situation that electron transfer between the pterins could allow for the recovery of the ferrous-NO heme. After this reaction one pterin has been left in the radical cation state. The hypothesis is that a rapid equilibrium will be set up such that electrons transfer rapidly between pterins. When the radical cation is on the pterin nearest the ferrous-NO heme it could pull an electron off the ferrous-NO heme, creating the ferric-NO complex. This is a very weakly bound complex, and NO will rapidly be released, leaving both hemes free to start another round of catalysis.

That, at least, is the simplified scheme that we have here probed by stopped flow reactions. The nNOSoxy domain was used to simplify matters, by removing the delivery of electrons from the reductase domain.

4.1.1 Aims

The potential for electron transfer between the hemes via the pterin cofactors was tested by monitoring the rate of decay of the ferrous-NO complex under various heme occupation states.

The ability of the pterin cofactors to transfer electrons between themselves would have mechanistic implications and those will be discussed.

Results

4.2 Titrations

Careful titration with sodium dithionite was required to produce reduced nNOSoxy (L-Arg bound), without leaving excess dithionite. Excess dithionite would affect the inter-pterin electron transfer we were looking to observe. Figure 4.3 shows the reduction of nNOSoxy with dithionite, the lack of increase in absorbance at ~350nm shows there was little to no excess dithionite.

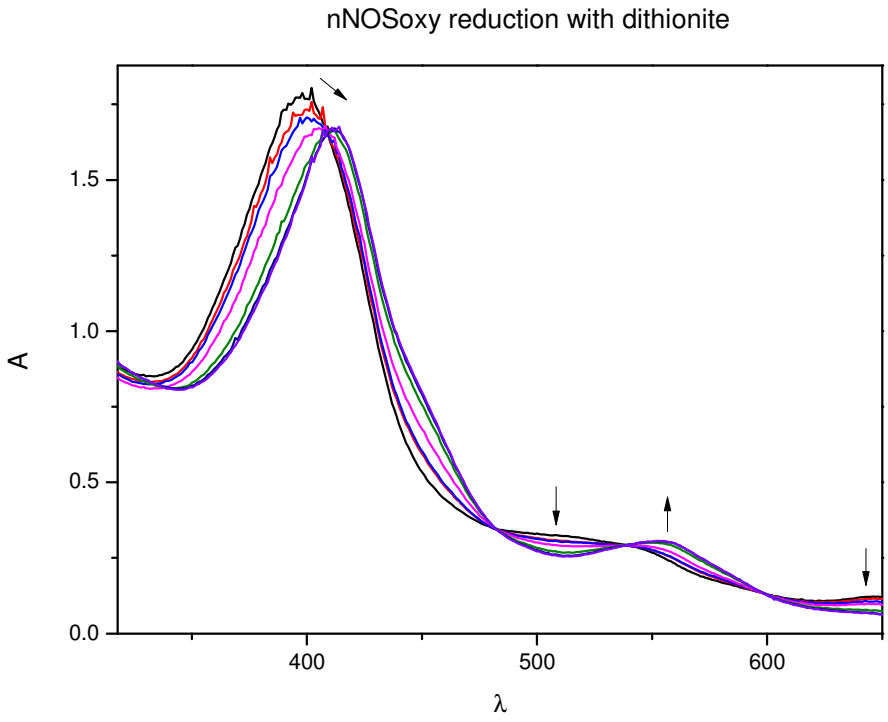

Figure 4.3- Titometric reduction of nNOSoxy with sodium dithionite. Complete reduction was judged by final Soret peak position and flattening of the band at 650nm. Qualitative titration of sodium dithionite was used to ensure complete reduction, but without addition of excess reducing agent.

NO will only bind non-transiently to the ferrous heme, with a dissociation constant of 0.17 nM with L-Arg also bound (109). Once reduced a saturated anaerobic solution of NO was used to titrate NO into the protein. This titration is shown, with spectral changes in Figure 4.4.

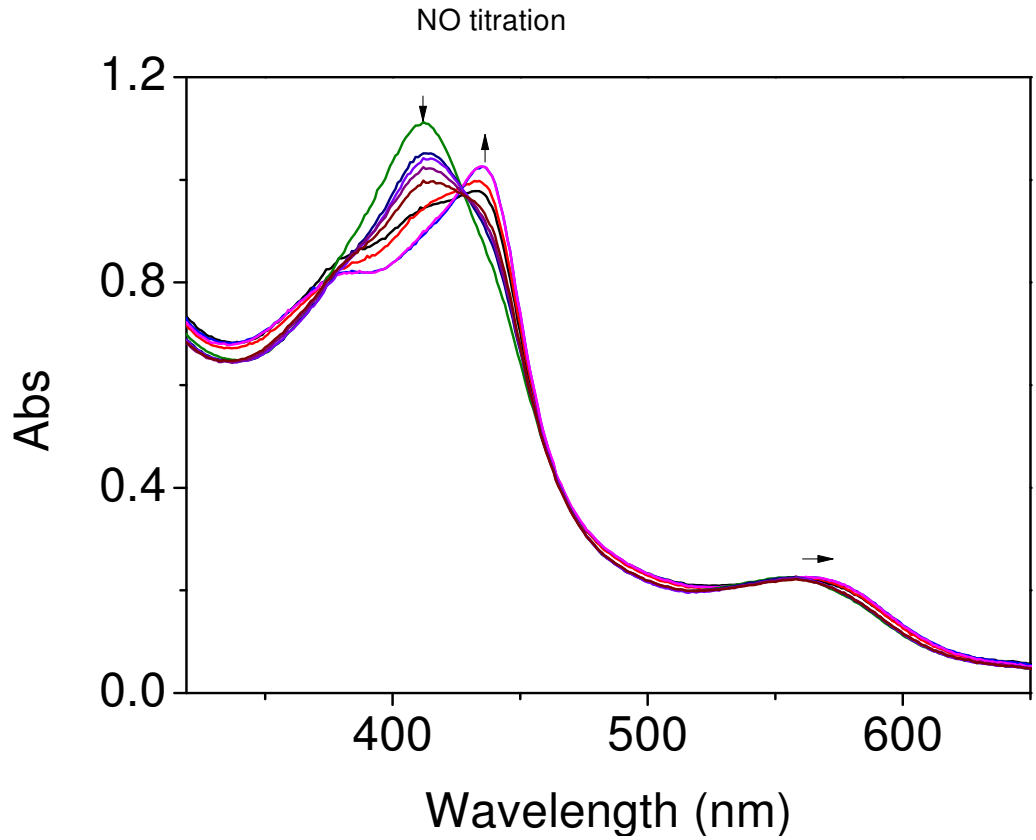

Figure 4.4- Spectral shifts associated with the binding of NO to ferrous nNOSoxy. Note the characteristic absorbance of ferrous-NO at 436nm.

By careful titration it was possible to create samples of nNOSoxy with differing proportions of ferrous-NO heme, so that at least some of the dimmers will be NO-heterodimeric (step 1, mechanism 4.1). These samples were then reacted with an oxygenated buffer and the spectral changes of the reaction followed. Following reaction with oxygen both the ferrous-NO and ferrous hemes will be oxidised to the ferric state. This can be seen in Figure 4.5.

4.3 Stopped flow

As stated in the introduction to this section, the reaction of the ferrous heme and the ferrous-NO hemes with oxygen will occur at vastly different rates. Figure 4.5 shows the spectral changes associated with oxyferrous decay and ferrous-NO decay and the very different timescales they occur on. Both reactions also progress from different starting spectra. This allows probing of this mechanism as analysis of the spectra gained can be fitted to allow for these two separate reactions. A confirmation of the hypothesis of effective inter-pterin electron transfer would have been the observation of a rate of ferrous-NO decay in the case of NO-heterodimers different from that recorded for the simple reaction of ferrous-NO complex heme with oxygen. By using samples with different proportions of ferrous-NO:ferrous heme it was possible to create samples with differing amounts of NO-heterodimer. In these experiments the amount of dimers in this state ranged from 36 to 50%. This is based on an assumed statistical distribution of the NO to the hemes. It is possible, though unlikely, that NO binds either cooperatively or anti-cooperatively. Table 4.1 shows the assumed NO distribution in the samples. Only in NO-heterodimers would inter-pterin electron transfer be detectable by our stopped flow method.

% Heme NO bound	Fe^{II}-NO/Fe^{II}-NO	Fe^{II}-NO/Fe^{II}	Fe^{II}/Fe^{II}
0	0	0	100
24	6	36	58
32	10	44	46
47	22	50	28
71	50	41	9
100	100	0	0

Table 4.1- Showing the simple statistical distributions assumed in the experiments of ferrous-NO decay. If there is cooperativity or anti-cooperativity then the distribution of NO amongst dimers will be altered, but there is no evidence this is the case.

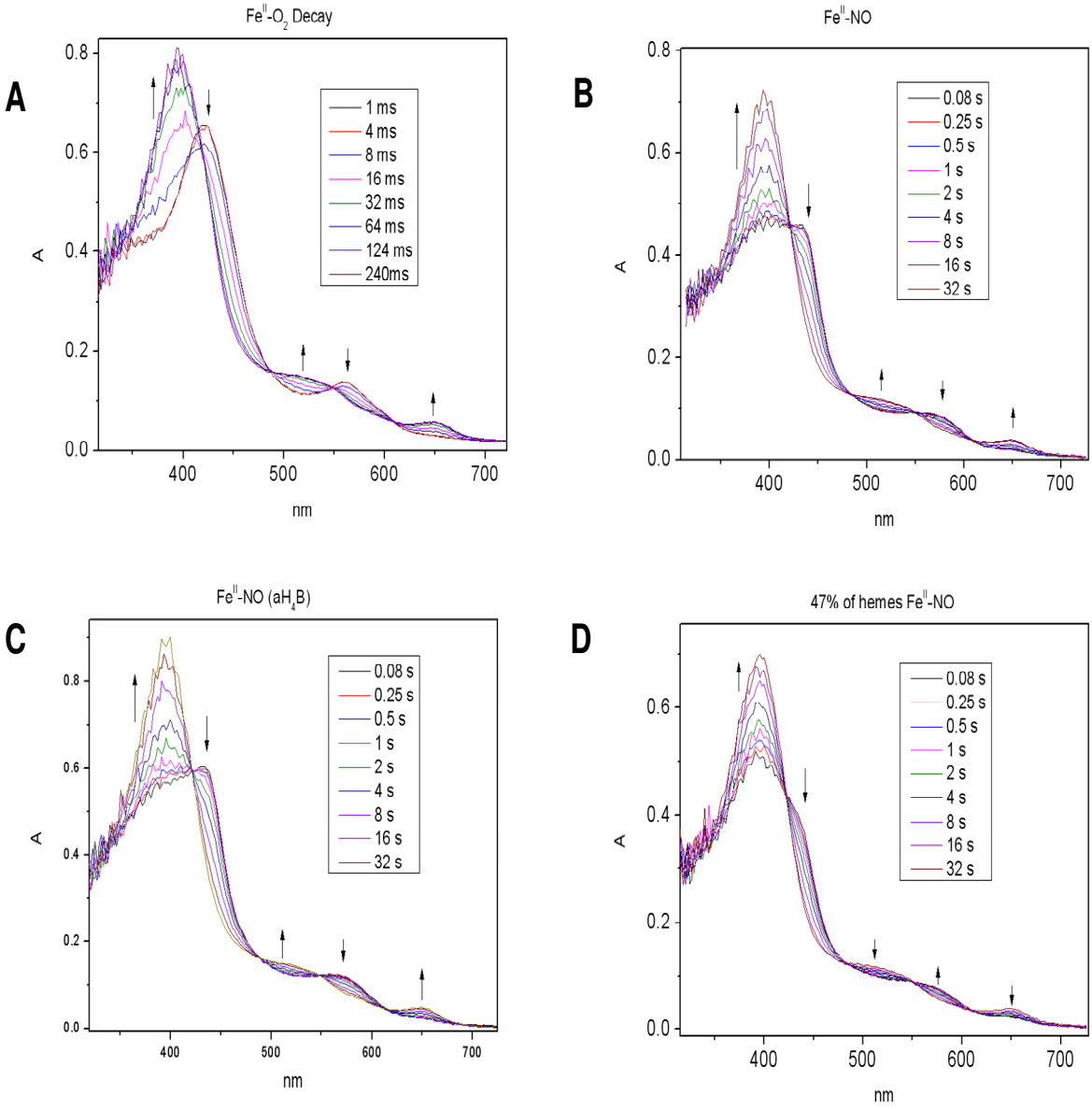

Figure 4.5 - Representative spectra for various stopped flow reactions. A) shows the spectral change on reaction of ferrous nNOS with O_2. In A can be seen the oxyferrous complex decaying to leave ferric heme. B) shows the reaction of Fe^{II}-NO nNOS (with natural pterin cofactor H_4B) with O_2. The Fe^{II}-NO reacts with oxygen to leave ferric heme and nitrate. C) shows the reaction of Fe^{II}-NO nNOS (with inactive pterin cofactor aH_4B) with oxygen. The Fe^{II}-NO reacts with oxygen to leave ferric heme and nitrate. D) shows the reaction of an nNOS sample with 47% of its hemes in the Fe^{II}-NO state, the other hemes are in the Fe^{II} state at the start of the reaction. Here two reactions occur. Fe^{II}-NO reacts with oxygen to leave ferric heme and nitrate. The Fe^{II} hemes react with oxygen to form the oxyferrous species. The oxyferrous species decays to leave the ferric heme. All reactions were carried out at 25˚C, against air saturated buffer (~200μM O_2).

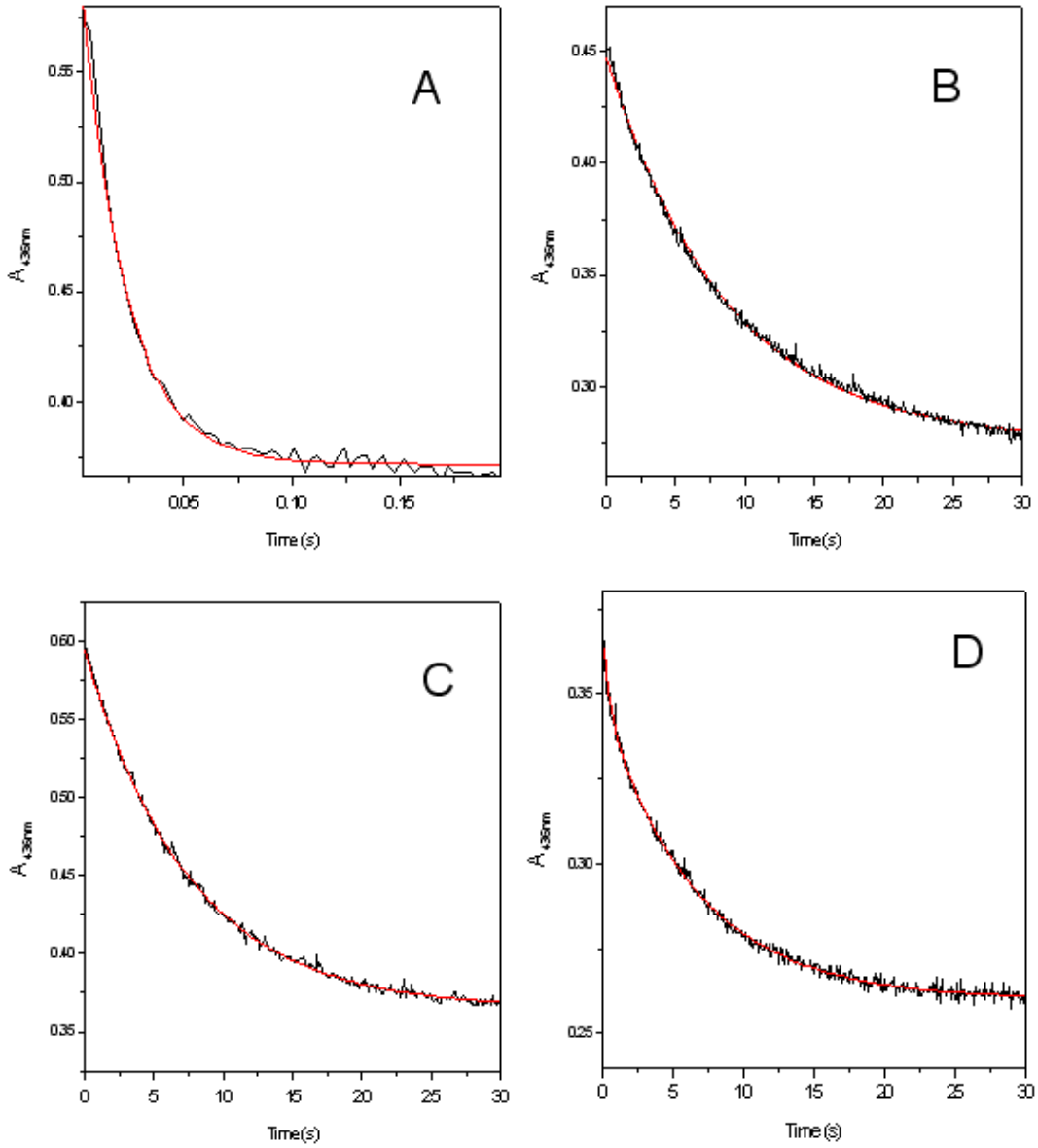

Figure 4.6 - Recorded and fit data at 436nm for: A) Decay of the oxyferrous complex formed by stopped flow reaction of reduced enzyme with oxygen, B) Decay of the ferrous-NO complex in protein with H_4B bound and all hemes in the ferrous-NO state, C) Decay of the ferrous-NO complex in protein with aH_4B bound and all hemes in the ferrous-NO state, D) Decay of the ferrous-NO complex in a protein (H_4B bound) sample with 47% NO occupation of heme. Rates from these calculations can be seen in table 4.2. All reactions carried out at 25˚C and as described in materials and methods (Section 2.7).

For any proportion of heme in the ferrous-NO state the rates observed fit well to a model of oxyferrous to ferric, and ferrous-NO to ferric, see table 4.2, using Pro-Kineticist 4.21 software (Applied Photophysics), Reactions 1 and 2. Under the conditions used here the rate of oxyferrous formation, k_1, was too rapid to be detected.

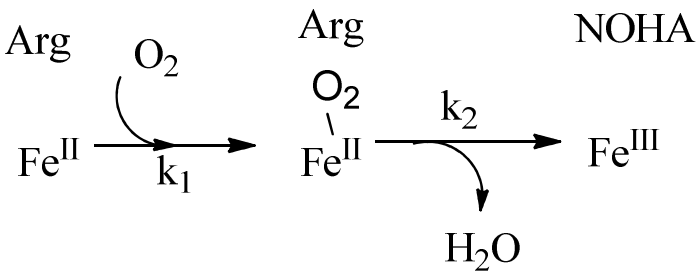

Reaction 1- The observable steps in stopped flow reaction of reduced nNOS with oxygen. k_1 is the rate of oxyferrous formation. k_2 is the rate of ferric heme formation, the intermediate steps being unobserved in this experiment, this occurs at the same rate as the formation of the pterin radical.

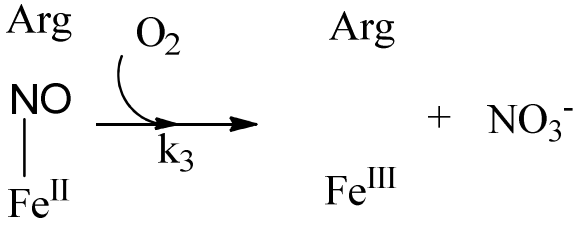

Reaction 2- The known pathway for ferrous-NO decay by reaction with molecular oxygen. k_3 is the rate of ferric heme formation by this reaction.

Ferrous-NO decay was unaffected by whether the dimer partner heme was not in the ferrous-NO state, table 4.2. We observed no evidence of inter-pterin electron transfer. Figure 4.6 shows representative decay traces for these samples.

Proportion of ferrous heme NO bound	Oxyferrous>Ferric k_2 Rate (s^{-1})	(±Errors)	Ferrous heme-NO>Ferric k_3 Rate (s^{-1})	(±Errors)
0	48.1	(0.4)	-	
0.24	35.0	(0.3)	0.12	(0.01)
0.32	35.1	(0.5)	0.12	(0.01)
0.47	34.0	(0.4)	0.12	(0.01)
0.71	29.4	(0.4)	0.12	(0.01)
1	-		0.12	(0.01)

Table 4.2- Rates of reaction for oxyferrous decay and ferrous-NO decay measured by stopped flow reaction at 25˚C. No change of rate for ferrous heme-NO decay was measured in rate for any proportion of the sample in the ferrous-NO state. The rate of oxyferrous decay was ~$32s^{-1}$ for all experiments. The models were fit to an A>B, C>B reaction (both the oxyferrous and ferrous heme-NO complex decay to the ferric state), except the first and last rows which were A>B reactions as they contained only one heme state to decay to ferric. These results match well with other studies (110).

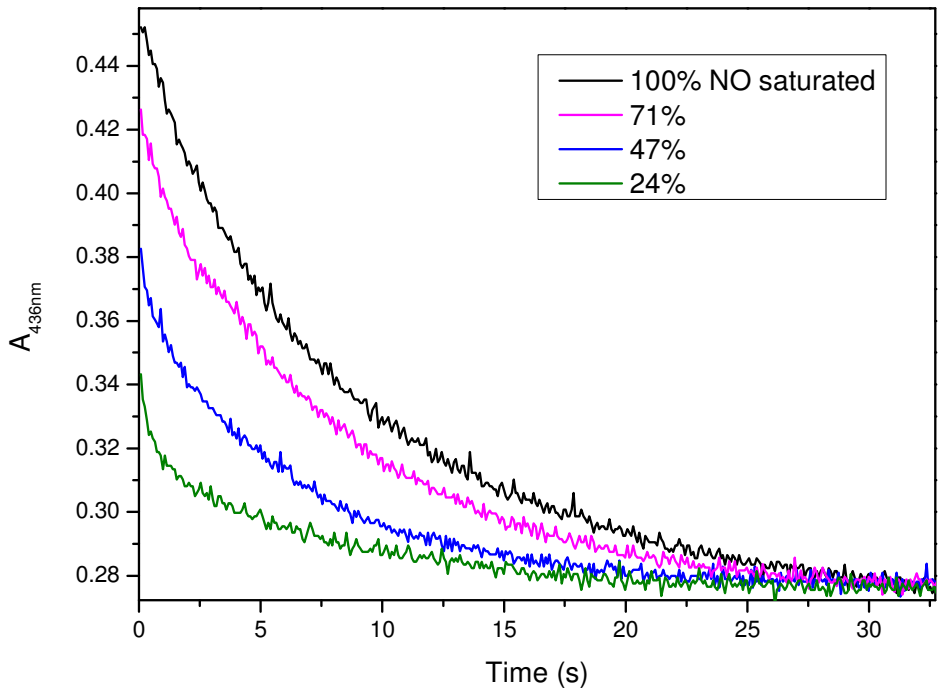

Figure 4.7- Comparing the decay data gained for different samples. After the first few seconds of reaction almost all the oxyferrous species will have decayed. This should leave curves of similar shape if there is no inter-pterin electron transfer, which is what we observed.

Can the pterins of an nNOSoxy dimer transfer electrons effectively between themselves?

Based on the evidence here presented the answer would appear to be no.

4.4 Discussion

Using simple statistical distributions it was trivial to predict what proportion of dimers were in the NO-heterodimeric state. While it would be possible to use any of these proportions to test the inter-pterin electron transfer a variety was used for a thorough examination. Confirmation of our titrations, of the amount of NO bound, was calculated graphically, see Figure 4.7. The amplitudes used in this graph were calculated from the reduced protein sample compared to the maximum absorbtion peaks of the two species. The more NO was bound, the less oxyferrous heme should have been generated, and that is what we see in Figure 4.8.

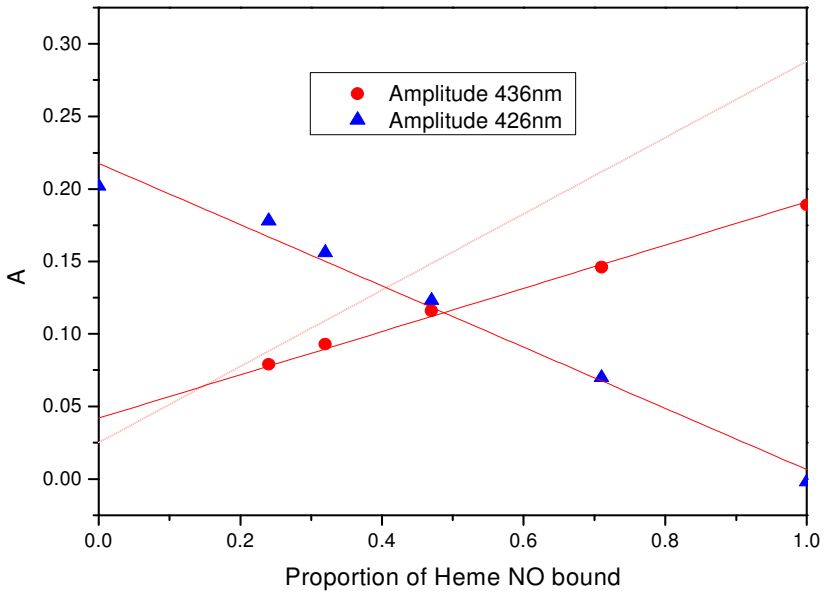

Figure 4.8 - How amplitude at 426nm (oxyferrous) and 436nm (ferrous heme-NO) change with the proportion of NO bound to the ferrous heme. These amplitudes represent the difference in absorbance at these wavelengths compared to the reduced protein sample. This graph confirms our interpretation of the amount of NO bound in each sample.

As we see no inter-pterin electron transfer we can say it is certainly not because we miscalculated the amount of ferrous heme-NO complexes.

Having discussed why inter-pterin electron transfer is likely how then can we account for not observing it? There are two possibilities; it is occurring and we have not observed it or it is not occurring. Here we will discuss which is the more likely scenario.

Mechanism 4.1 shows what we predicted would happen in a special circumstance. Here we created those special circumstances, under a range of conditions. At which stage of the proposed mechanism does the experimental data differ from prediction? We certainly formed at least some NO-heterodimers (dimers with only one of their hemes in the ferrous-NO state) as shown in step one. The formation of the oxyferrous complex occurs at 25°C at ~180 s^{-1} while ferrous heme-NO decays at a 0.12 s^{-1}, so step two is certainly likely to form in the majority of NO-heterodimers. Step three is the donation of an electron from the pterin to form the radical pterin cation (111). This is the accepted mechanism, and occurs at ~32 s^{-1}. Between steps 3 and 4 of the mechanism as shown in mechanism 4.1 occurs the monooxygenation of the substrate in normal turnover. It is assumed it occurs in these experiments. It is at this point that electron transfer was expected to occur between the pterins, leading to equilibrium, and allowing the release of NO. However the rate of ferrous heme-NO decay was the same in samples completely in the ferrous-NO state, and those in the NO-heterodimeric state, table 4.1.

13Å is within what is considered a reasonable distance for efficient electron transfer. What efficient means depends on whom one asks. It is generally held to be in the range of hundreds or thousands of electron transfers per second. Since the rate of ferrous heme-

NO complex decay is here measured at 0.12 s^{-1} it would seem that electron transfer is not occurring between the pterins.

The most reasonable explanation for not monitoring inter-pterin electron transfer is then that it does not occur under these conditions. The role of H_4B must therefore be reconsidered in the possibility that it is possible that the pterin radical is kinetically stabilised by undergoing some chemical transformation, for example deprotonation to form the neutral radical H_3B. Proton transfer from the pterin to the heme, as has been proposed before (100) may inhibit electron transfer between the pterins, Mechanism 4.2.

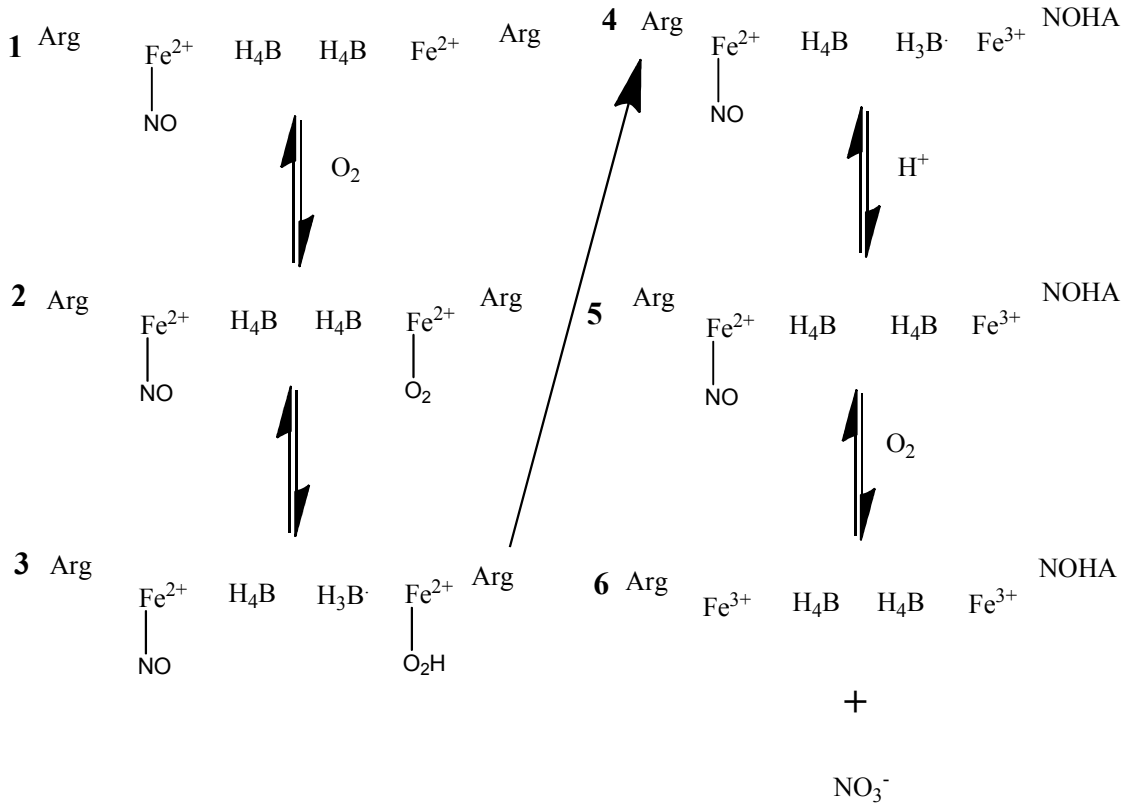

Mechanism 4.2- A proposed mechanism for the stopped flow reactions performed with NO-heterodimers showing proton transfer coupled with electron transfer from the pterin. Here electron transfer between the pterins would be unlikely as migration of the radical between pterins would require the formation of the anion radical form of H_4B, which would be heavily disfavoured.

A further possibility is that the widely accepted mechanism of the H_4B radical cation removing an electron from the ferrous heme-NO complex to induce NO release may not actually be occurring (84).

Pterin proton transfer is far more likely. There is already a putative proton transfer pathway from the pterin to the heme iron, Figure 4.9.

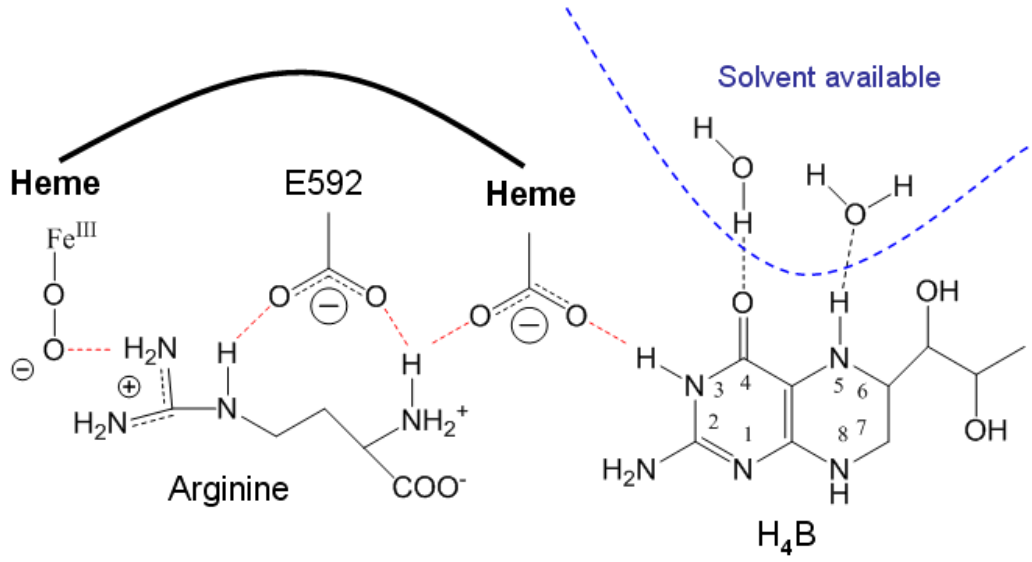

Figure 4.9 - The putative proton transfer pathway, via red hydrogen bonds, between H_4B and heme-oxy species (here peroxo ferric). The hydrogen on N5 is solvent accessible (100).

On the donation of an electron from H_4B there will be a shift in the hydrogen bond between N3 of the pterin and the heme propionate, towards the heme. The hydrogen on N5 is solvent accessible, and there is therefore a potential pathway through which solvent derived protons may be transferred to the heme oxy species.

The evidence presented in this chapter does not prove the putative proton donor role of H_4B. However there is no theoretical reason why electron transfer between pterins should

not occur. No evidence for electron transfer between the pterins has been observed. Electron transfer would be unlikely to occur if H_4B is also a proton donor as it would require the formation of a pterin anion.

Chapter five

Analogues of H_4B

5.1 Introduction

H_4B is an essential cofactor for several vital enzymes. It plays a key role in production of the neurotransmitters L-DOPA by tyrosine-3-hydroxylase and 5-hydoxytryptophan by tryptophan-5-hydroxylase (68). In this chapter, however, the role of H_4B in the mechanism of NOS will be addressed via reference to several novel analogues of H_4B.

The importance of the H_4B binding site as a drug target has only recently become clear. Mutations of the enzymes responsible for the synthesis of H_4B are thought to be the causal factor in diseases showing a severe depletion of serotonin and dopamine, such as hyperphenylalaninemia (112). Synthesis of H_4B from GTP requires the enzymes GTP cyclohydrolase I, 6-pyruvoyl-tetrahydropterin synthase and sepiapterin reductase. For H_4B to be regenerated from the dihydro-form requires pterin-4a-carbinolamine dehydratase and dihydropteridine reductase (113). A harmful mutation is possible in any of these enzymes and the effects of H_4B deficiency can be severe. The use of drugs to treat such a deficiency would be of great value, however the unstable nature of H_4B makes it of limited use as a drug, particularly if the underlying problem is in the enzymes required for regeneration. Treatments of 4-20 mg/kg of H_4B have been used in phenylketoneuria, and the cost is seen as prohibitive (114).

Previous work on analogues of tetrahydrobiopterin have tended to focus on them as possible inhibitors (107). Aside from one previously published structure, which is reexamined here, the only commonly known pterin analogue activator is the C5 methyl analogue, Figure 5.1 (91).

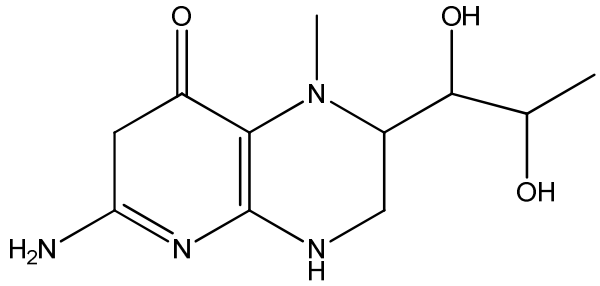

Figure 5.1 - The 5-methyl analogue of H_4B.

With all three mammalian isoforms of NOS requiring H_4B for catalysis and the vital nature of NO in the body it is clear that H_4B, or a compound mimicking its activity, could be of medical use. H_4B treatment for high blood pressure is effective, certainly in rats (115). Further work is necessary on the medical use of H_4B, but what is clear is the need for a more suitable delivery system for H_4B or a more stable analogue of H_4B.

Aside from use as a drug, an analogue capable of supporting NO production by NOS would be useful in elucidating the role of H_4B in the mechanism. As described in the introduction to this thesis the role of H_4B is subtle and still not entirely clear. We know that it acts as both an electron donor and acceptor, and forms a strongly oxidising radical. Debate hinges on whether H_4B is also a proton donor, as some have suggested (116). By testing a range of analogues of H_4B for activity it was hoped that a structure/function analysis could be performed that would offer insight into many of the still hazy parts of NOS mechanism.

5.1.1 Aims

With a potent inhibitor for NOS already known that targets the pterin binding site, aH_4B, it is in the search for activators that most research is focused.

Here dihydropterines blocked at the C7 position (Figure 5.2 for pterin numbering system) were trialed as active analogues, with hopes that the blocking would prevent reoxidation. In H_4B it is possible to get oxidation across the 6-7 bond forming an inactive dihydropterine form. By adding substituents to the C7 position it is possible to block this reaction. This blocking was performed to try and stabilize these analogues compared to H_4B. Here we test their ability to support NO synthesis in nNOS.

Results

5.2 Turnover assays

Analogues were synthesised by Craig McInnes at Strathclyde University, Figure 5.2. They were assayed for activity using the turnover assay described in Materials and Methods.

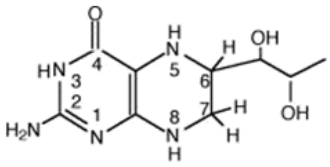

Tetrahydrobiopterin (H_4B)

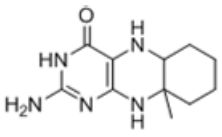

WSG1007

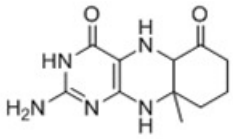

WSG1060

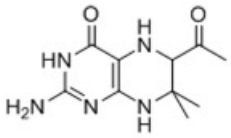

WSG1002

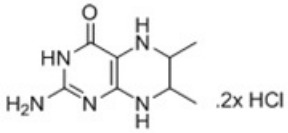

.2x HCl

WSG1010

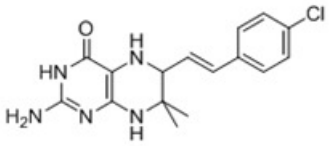

WSG1017

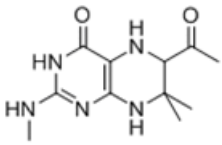

NMe1002

Figure 5.2- These analogues were found to give at least some activity *in vitro*, or to act as inhibitors. Shown at the top is pteridine with the ring numbering system used here to describe analogue structure.

All analogues were screened for activity by turnover assay (section 2.8) where NO production is detected by the conversion of oxyhemoglobin to methemoglobin, and the measurement of the spectral shift at 401nm that conversion causes. Those analogues with measurable activities were taken forward for more in depth analysis. Table 5.1 shows the activities derived for the analogues tested.

Compound	Rate (min^{-1}) (±Errors)
H_4B	~18 (1.1)
WSG1060	8.2 (0.3)
WSG1007	2.8 (0.4)
WSG1010	1.3 (0.4)
WSG1002	11.2 (0.9)
NMe1002	0.0 (0.0)
WSG1017	Inhibitor*

Table 5.1- The rate of activity derived from assays of the pterins with nNOS. All compounds were screened at 20μM, except WSG1002 where the v_{max} is given. * See text for discussion of WSG1017.

As can be seen from Table 5.1 the rates of turnover supported by the analogues varies greatly, at least at 20μM concentrations. Previous work on WSG1002 had shown it to have a K_d of 151μM (117). However, in this study analogues were being sought that could compete with H_4B in both binding affinity and activity so concentrations of 20μM were used in initial screening as a maximal concentration.

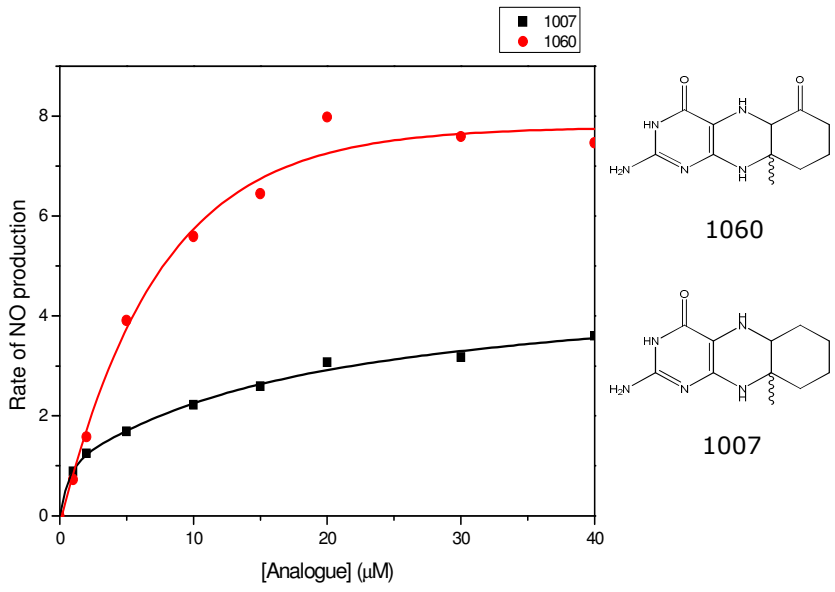

Figure 5.3- The activity curves derived for WSG1007 and WSG1060, fitted to the Michaelis equation by Origin 8.1 (OriginLab Corporation).

After screening, two analogues, WSG1060 and WSG1007, were chosen for further study. These two 6,7-cyclized pterins were thought the most interesting structurally, and being similar in structure would allow for greater structure/function analysis. Figure 5.3 shows how activity for these two analogues varies with concentration. This allowed for the calculation of K_d and V_{max}. These are shown in table 5.2, as well as those for WSG1002.

Pterin	K_d (μM) (±Errors)	Rate of NO production as % of H_4B
H_4B	<1	100
WSG1007	5.6 (1.0)	25
WSG1060	7.4 (1.6)	55

Table 5.2- Showing the K_ds for the two most active analogues, derived from fitting of activity curves to Michaelis equation by Origin 8.1 (OriginLab Corporation). K_d is used rather than K_m as the pterin is not the substrate of the enzyme, but a cofactor.

These novel, alloxazine-like, analogues (WSG1007 and WSG1060) had binding affinities similar to H_4B. However the rates at which they support catalysis are significantly lower. This was mechanistically interesting and so further studies were performed to ascertain whether the difference in catalytic rate was related to the ability of the analogues to donate electrons, a vital mechanistic step.

5.3 Stopped flow

When molecular oxygen is reacted with the reduced heme of NOS an oxy-ferrous species forms rapidly. This has a characteristic Soret peak at 426nm. With the donation of an electron from the pterin cofactor this species decays to the ferric heme. With a bound

substrate and H_4B this would lead to a normal monooxygenation. With aH_4B, an inactive pterin, this electron donation cannot occur and there is no turnover, see Figure 5.4, and the rate of oxyferrous decay is significantly slower.

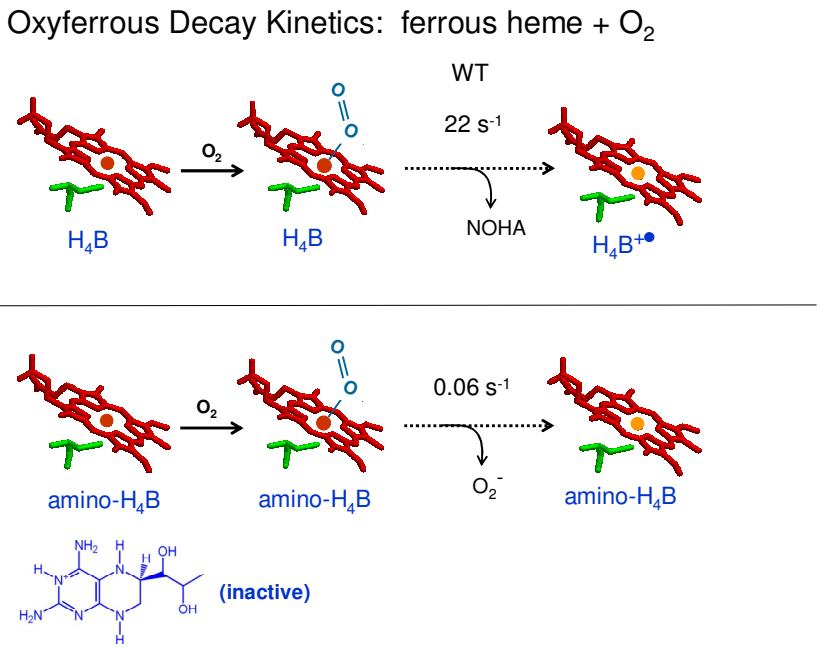

Figure 5.4- Showing the steps in stopped flow monitoring of oxyferrous decay, and associated rate, for H_4B and an inactive analogue of H_4B, aH_4B.

Figure 5.5 shows the decay of the oxy-ferrous species as followed by stopped flow spectrophotometry. This allows for a calculation of the rate of decay of the oxy-ferrous species, and therefore the rate of electron donation from the analogue.

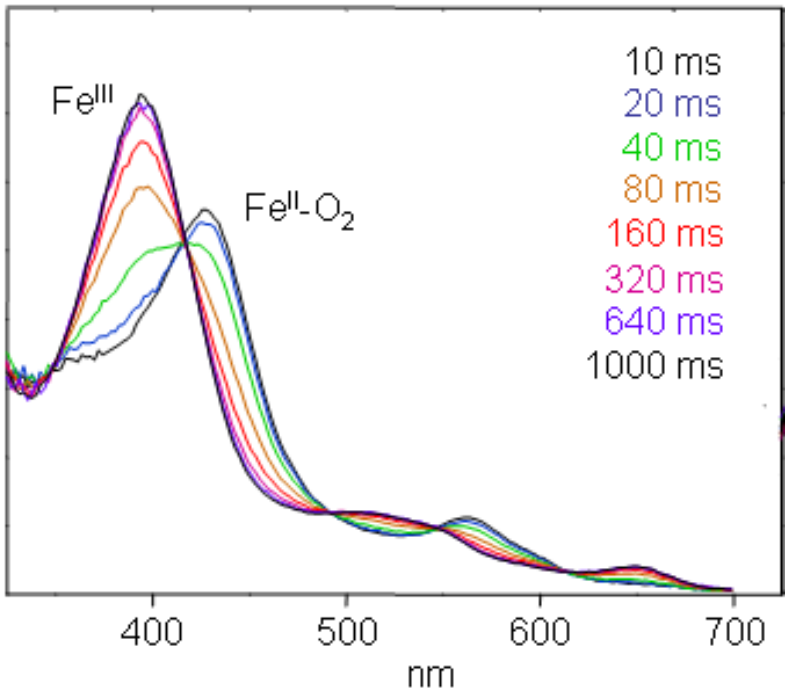

Figure 5.5- This Figure shows the spectral changes involved in the decay of the oxyferrous species in nNOS with H_4B. These changes allow the rate of electron donation from H_4B to be calculated. The reaction allows the rate of electron transfer from pterin analogues to be measured.

These rates were calculated for the five pterins, shown in table 5.3, as calculated by Pro-Kineticist 4.21, Applied Photophysics, software from the total spectra collected over 1s. Using a simple A>B (Oxyferrous to ferric) model rates of decay were arrived at. The rate of decay of the oxyferrous species being equal to the rate of donation of an electron from the pterin it gives a measure of the redox activity of the analogues. The rates for H_4B and aH_4B agree with previously published data.

Pterin	Fe^{II}-O_2 to Fe^{III} (s^{-1})	(±Errors)
WSG1002	25.2	(0.3)
WSG1007	24.5	(0.2)
WSG1060	24.7	(0.2)
aH_4B	<1s^{-1}	
H_4B	27.8	(0.2)

Table 5.3- The rate of oxyferrous decay, and therefore the rate of electron donation from the pterin, measured at 10°C and over the course of a second after mixing the reduced protein with an oxygenated buffer.

As table 5.3 makes clear all analogues tested were able to donate electrons to the heme at a rate similar to H_4B. The rate of oxy-ferrous decay with aH_4B was too slow to accurately measure over 1s, but over a longer timescale agreed well with the previously ascertained rate, 0.06s^{-1}. The rates of all three novel analogues tested were similar to each other and H_4B. This is somewhat puzzling as, table 5.2 shows, these analogues supported turnover of the enzyme at significantly different rate. It is likely that the difference in turnover rates is due to differences in the ability of these analogues to support the NOS dimer. This will be addressed further in the discussion.

5.4 Analogue decay

Working with these compounds it became clear that some of these blocked dihydropterine analogues of H_4B had problems of stability. When working with H_4B *in vitro* it is important to add a reducing agent such as DTT to the H_4B solution to stop

oxidation to the inactive dihydro-form (118). This is why DTT was a standard addition to the assays. With DTT added a solution of H_4B, kept on ice, maintains its activity for several hours. This was not neccessarily the case with these analogues.

All analogues were judged pure by NMR and HPLC following preparation (57). They were then exposed to a high vacuum to produce a stable solid and kept at -80°C. It became readily apparent that some change was occurring once the analogues were placed in solution, strong changes in colour occurred. It also became apparent that this change was related to a reduction in the ability of the analogues to support turnover. After 1hr in solution WSG1060 had lost approximately 40% of its activity. This occurred in the presence of DTT, and in aerobic or anaerobic solutions. Ascorbic acid was also tried to limit or recover activity in the analogues, but was ineffective. The following spectra show the change in absorbance of the analogues over time.

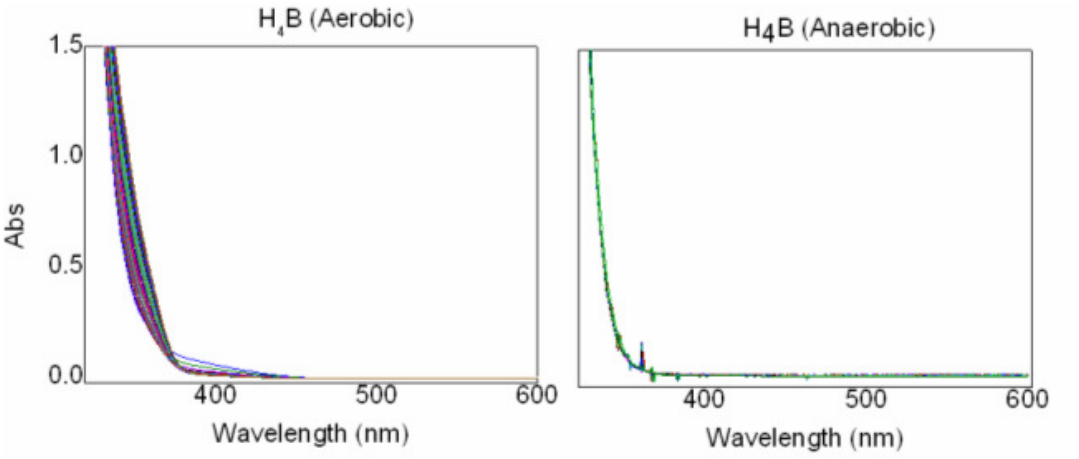

Figure 5.6- The spectral change recorded for a 5mM solution of H_4B, aerobically and anaerobically. Each line represents 5 minutes.

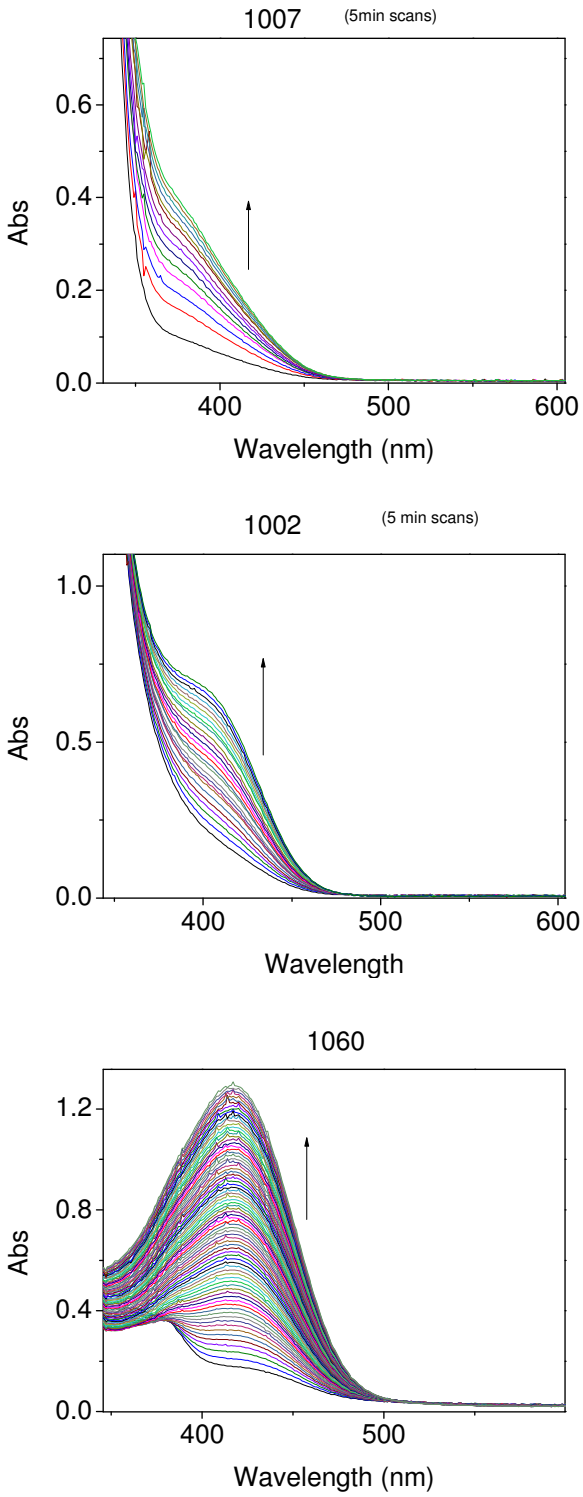

Figure 5.7- The spectral changes recorded, anaerobically, for WSG1002, WSG1007, and WSG1060. Each line represents 5 minutes.

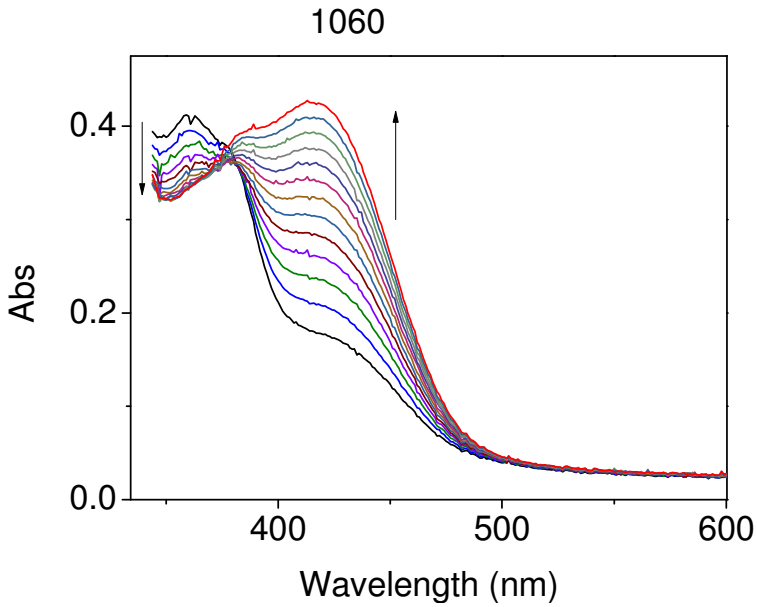

Figure 5.8- The spectral changes recorded for WSG1060 aerobically. Each line represents 1 minute. The build up of the colourful product occurs at a greater rate aerobically.

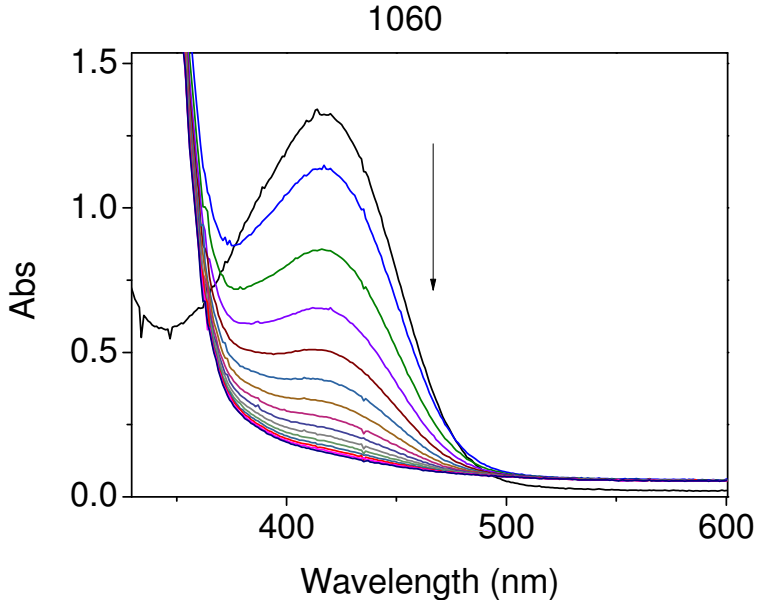

Figure 5.9- Spectral changes recorded for the colourful solution product of WSG1060 after the addition of sodium dithionite.

The formation of this broad peak at 417nm, Figures 5.7 and 5.8, in WSG1060 can be reversed by addition of dithionite. However the reduced 'colourful product' of WSG1060 decay, while losing its absorbance at 417nm, does not recover its activity. There would appear to be no simple way to undo whatever reaction is occurring on WSG1060 entering solution.

Interestingly a similar spectrum has been reported for another analogue of H_4B, 6-formyl-7,8-dihydropterin, Figure 5.10 (119). This may suggest the rearrangement of bonds that occurs when WSG1060 goes into solution.

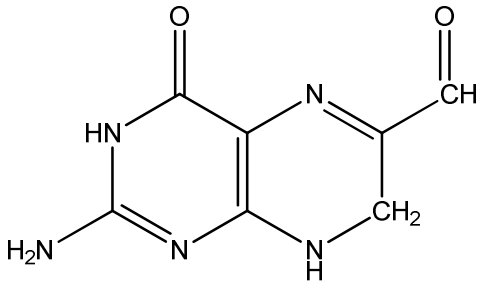

Figure 5.10- The structure of a pterin analogue, 6-formyl-7,8-dihydropterin, with a UV/VIS spectrum very similar to the colourful WSG1060 product.

If a direct comparison is useful it would suggest that a double bond has formed between the N5 and C6 of WSG1060, forming the conjugated π-system likely responsible for the absorbance in the 417nm region. However, sodium dithionite would not normally be able to reduce a double bond. It would also require an oxidizing agent to perform this double bond formation, something lacking in anaerobic conditions. It is possible that we are observing a keto-enol tautomerisation. However this would only be possible in the case of WSG1060, and the instability of the other analogues remains unexplained.

5.5 Crystallography

(With Laura Campbell, University of Edinburgh)

The binding mode of the pterin cofactor is an important factor in the electron transfer role of the pterin. Crystallographic study in therefore vital in the design of new analogues. For the analogues here presented the determination of the crystal structure of the nNOSoxy protein with analogue bound was attempted. The rearrangement of the residues which compose the pterin binding site would presumably be altered by the large extensions on the analogues. A crystal structure with an analogue would be useful in revealing whether the analogues disrupt the dimer interface.

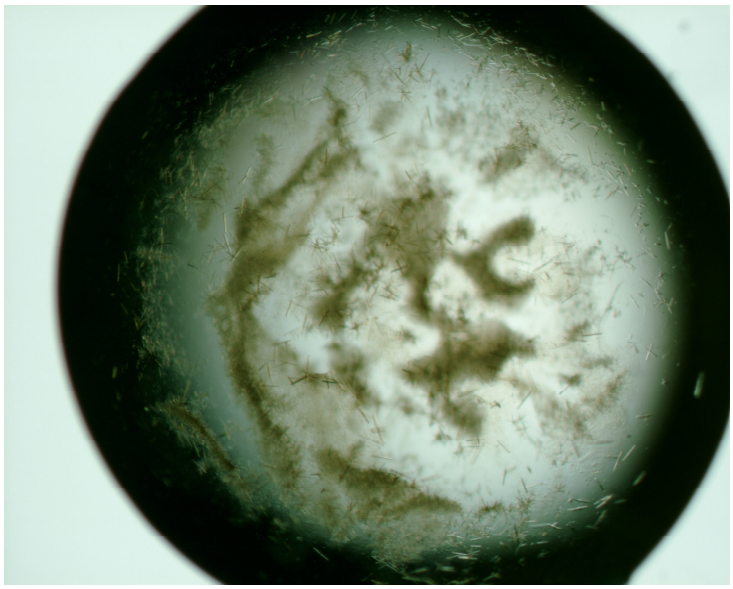

Figure 5.11 - Crystals of digested nNOSoxy with WSG1060.

The crystallographic approach was similar to that previously described for the G586S mutant nNOSoxy. The conditions which provided crystals were as follows: 0.1 M MES (pH 5.8/6.0), 22-24% PEG 3350, 0.2 M ammonium acetate, 25 mM L-Arg, 35 mM SDS,

5 mM GSH, 2% isopropanol. Crystal growth was attempted at 4°C and 17°C. Crystals became apparent after 2 days.

Crystals were readily grown with WSG1060 at 17°C, under most of the conditions trialled, as seen in Figures 5.11 and 5.12.

Figure 5.12- The shape of the crystals gained with WSG1060 was broadly similar to that of nNOSoxy with H_4B.

The crystals achieved by this method were similar in shape and colour to those previously gained for the WT oxygenase domain with H_4B. The crystals grown here were small, ~10μm in size. This made collection of single crystals difficult. The largest crystals were however collected and prepared for the data collection. The largest crystals shattered on freezing. Of the crystals that survived freezing none diffracted significantly. In view of the lack of stability of the analogues in water it seems unlikely that useful analogue-bound structures are obtainable.

5.6 Discussion

The binding site for H_4B is at the dimer interface of the NOS oxygenase domains (PDB 1OM4). The binding pocket can be seen in Figure 5.13 and shows the distal portion of the pterin binding site with which we shall be most concerned here.

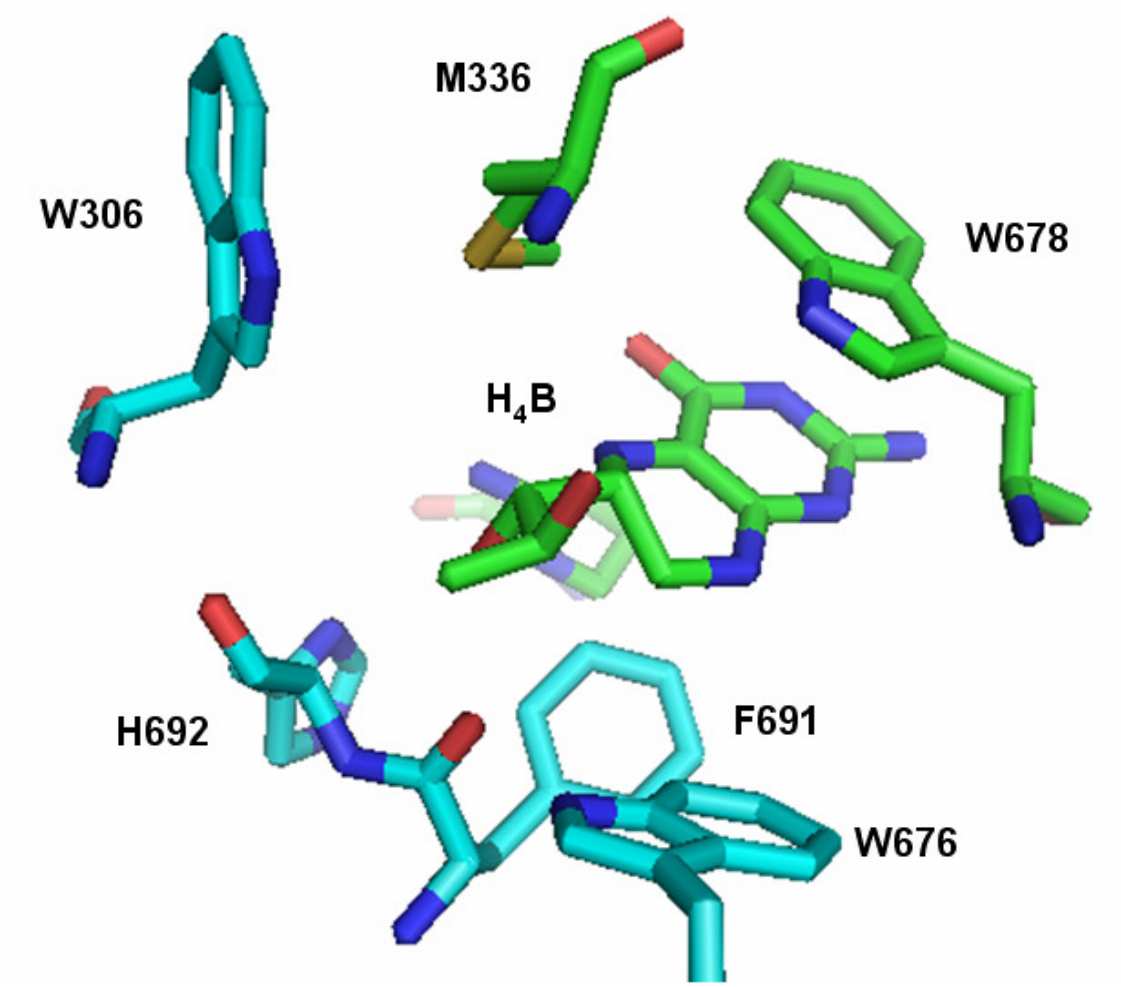

Figure 5.13 - The residues defining the distal portion of the pterin binding site. Both subunits supply several residues to the binding pocket. Not that both subunits are stongly present in this portion of the binding pocket. (PDB 1OM4, unpublished paper)
Subunit 1 = Trp306, Trp676, Phe691, His692, and Glu694
Subunit 2 = Ser334, Met336

This distal portion of the binding site offers more space for modification than does the heme-proximal portion. The heme proximal portion is also the 'business-end' of the molecule, involved in electron, and according to some researchers proton, transfer. This portion of the pterin must be held in the correct orientation to allow electron transfer, and must maintain a hydrogen bond to the heme propionate. Extension at these positions is

not well tolerated, even a methyl addition at the C2 position, shown here in the N-methyl analogue (NME1002), abolishes activity. The distal portion contains the sites of the interactions between the pterin and both subunits of the dimer. Dimerisation is vital to the activity of the enzyme as electrons pass from one subunit of the dimer to the other (120). As the modifications of the analogues here described are mainly at the C6 and C7 positions, possibly involved in dimerisation, we must consider the role of the analogues on dimerisation. First let us consider what can be learned from a structure/function analysis of the analogues we have tested.

5.7 Structure/Function Relationship

The first comparison to be made should be between the analogues WSG1007 and WSG1060, the 6,7 cyclized pterin and the 6,7 cyclo ketone pterin respectively, and WSG1002, the 6-acyl, 7,7 dimethyl pterin, and H_4B. Figure 5.2 compares these structures.

The K_ds for WSG1007, WSG1060, WSG1002 and H_4B are 5.6μM, 7.4 μM, 151Mm and ~1μM respectively. This shows that extension at the C7 position is well tolerated but will decrease binding affinity. Interestingly the larger extensions of the 6,7 cyclized pterins decrease binding affinity less than does the relatively small 7,7 dimethyl extension. This is difficult to explain. It is possible that the introduced ring structure, easily accommodated spatially, may favour binding of these analogues in the correct orientation by a stacking interaction with Trp676, Figure 5.12. The possible stacking interaction with Trp676 may also lead to increased dimer stabilisation. Without a crystal

structure of the protein with these analogues bound it is difficult to discuss binding modes or the rearrangement of residues necessary to allow their binding.

The keto groups of WSG1002 and WSG1060 might mimic a hydroxyl group on the C6 extension of H_4B. In iNOS the dihydroxypropyl side chain interacts with Ser104 or Phe462, depending on the diastereomer form of the pterin (95). If this keto oxygen is mimicking an interaction of the normal dihydroxypropyl group it does not give an increase of binding affinity here. The keto group does seem to increase the activity of the analogues however. One problem with discussing the binding affinity of these analogues has already been mentioned. Using an activity assay to assess the binding of analogues requires the analogues to still be active. As has been shown, on being placed in solution there is a rapid reaction forming a colourful, inactive, product. While efforts were made to work quickly with the analogues by necessity some time passed. This makes it impossible to accurately and absolutely gauge the concentration of active analogue present in the assay mix. The V_{max} of the analogues may be a better measure for analysis.

From the structures in Figure 5.2 we can clearly rank the analogues in terms of maximum turnover rate. H_4B has a V_{max} of ~18 min^{-1}. The 6-acyl WSG1002, with a keto group in place of the first hydroxyl of H_4B achieves a V_{max} of approximately 11 min^{-1}. The bulkier 6,7 cyclo-keto pterin, WSG1060, which shares this corresponding keto oxygen achieves a rate of 9 min^{-1}. The 6,7 cyclized pterin, WSG1007, lacks this keto group and has a V_{max} of approximately 7 min^{-1}. From these Figures we can suggest a role for an oxygen on the C6 extension of the pterin in maintaining the correct binding mode of the pterin. However, its presence is not an absolute requirement. Intriguingly having only a methyl group at the C6 position reduces activity greatly (WSG1010).

WSG1017 has the largest C6 extension of any of the analogues here tested. No activity was recorded of this analogue, with its chlorophenylacyl side chain. However it did act as a competitive inhibitor against H_4B. This suggests it binds in the pterin binding site, but probably not in the correct orientation. This may point to a maximum C6 extension size for active analogues.

Stopped flow data on oxy-ferrous decay shows no significant difference in the rate of electron transfer from the analogues to the heme. This could have been the source of the difference in turnover rates, though unlikely as the rate of turnover is closely linked to the rate of electron delivery from the reductase domain (121). The slower rates of turnover could have been explained if the rate of electron transfer was sufficiently slow to allow build up of a dead end complex. This is not the case. How then can we explain the difference in turnover rate between these pterins?

It is here that we must discuss dimerisation. Monomeric NOS is unable to produce NO as the electrons required for turnover are derived from the reductase domain of the dimer partner (122). An active H_4B analogue must be able to donate and accept electrons at a suitable rate, but must also stabilise the dimer.

The analogues tested by stopped flow, which all conserve the basic pterin structure, are able to donate electrons at a rate similar to H_4B. The rates are marginally slower, suggesting a slight increase in the distance of the analogue from the heme propionate compared to H_4B, as electron transfer rate is effected by distance. The slower rate of electron transfer may also be due to changes in the electronic potentials of the pterin induced by the modifications. However this work makes it seem likely that any analogue that conserves this basic structure and bind in approximately the correct orientation will

be able to fulfill the requirement of electron donor. However the analogues tested support NO production at markedly different rates. One possibility is that the alterations at the C6 and C7 positions are interfering with dimerisation of the enzyme.

With reference to the structures in Figure 5.2, we can see that these blocked dihydropterines are bulkier in the heme-distal portion than H_4B. Figure 5.13 shows the residues that form the distal pocket of the pterin binding site are contributed by both partners of the dimer. The extra size of the analogues in the distal portion could disrupt dimerisation by some extent, probably by displacing Trp676, Phe691, and His692. If the first hydroxyl of the sidechain of H_4B contributes to dimerisation by formation of a hydrogen bond, then the keto oxygen of WSG1060 and WSG1007 may also be able to. This would tend to stabilise the dimer. However the extra bulk of the analogues could disrupt the dimer. This could well explain the difference in turnover rates. WSG1007, the 6,7 cyclized analogue, lacks a corresponding oxygen to the H_4B hydroxyl. Its turnover rate is lower than WSG1060, giving further evidence to support a stabilising role for the keto oxygen. With the binding of these analogues there is likely to be some structural rearrangement of the residues of the pterin binding site. Without a crystal structure it is hard to judge how great this rearrangement is likely to be. However if the analogues are disrupting dimerisation it may be hard to gain a crystal structure as all structures of the NOS oxygenase domain so far gained have been of the dimer. Disruption of the dimer may have led to the formation of the smaller crystals gained here. It may also have caused heterogeneity in the crystals and blocked diffraction. Further work needs to be down to ascertain the effect of these analogues on dimerisation.

Another remaining possibility is that the analogues are less effective oxidising agents. The ability of the radical cation to pull an electron off the heme is vital in the release of NO as it converts the 'dead-end' ferrous heme-NO complex to the deeply unstable ferric heme-NO complex. Monitoring turnover assays for the build up of the ferrous heme-NO complex may shed light on this possibility.

The final possibility hinges on the hypothetical role of H_4B as a proton donor. A hydrogen bond network, linking N3 of H_4B to the substrate could allow passage of a proton. This is a common enough motif in biological mechanisms to be feasible. Unfortunately the analogues here tested reveal little about this possibility. Computer models of the analogues reveal no great difference in the likelihood of the N3 amino group to give up a proton, compared to H_4B. Analogue design focused on altering the acidity of that nitrogen may be mechanistically revealing.

Chapter six

Conclusions

NO is a vital and versatile biological molecule. The mechanism by which NO is produced by NOS is thought to follow the general mechanism for cytochromes P450. However NOSs are unique in their cofactors and the reaction they catalyse. The mechanism has been closely studied but the active oxygenating species has not been identified. The role of the pterin cofactor of NOS, tetrahydrobiopterin, is subtle and unique. It is so subtle and

unique that doubt still reigns over its exact role in the mechanism. The main aim of this project has been to further our knowledge of the role of H_4B in the NOS mechanism. What has been uncovered about the role of this interesting pterin has clarified some matters but also pointed to further work that must be done.

The G596S mutant stabilises an intermediate formed by electron donation from H_4B to the oxyferrous complex capable of the monooxygenation of NOHA to produce NO, but incapable of the hydroxylation of L-Arg. This is the first time that the two monooxygenations have been separated in reactions mimicking normal turnover. There are three possibilities to explain this result: the two steps of the NOS mechanism are different in their active species, or the mutant stabilises L-Arg to such an extent that that the active species decays before it has a chance to react, or that the stabilised intermediate is not the active species of normal catalysis but one still capable of the second monooxygentation. This is the first NOS mutant reported that can catalyse only one of the two monoxygenations. This is not sufficient evidence to suggest that the two monooxygenations proceed via different intermediates as the reactivity of the substrates may be different. Stabilisation of L-Arg, probably by protonation from the introduced serine hydroxyl, is supported by DFT calculations showing the protonated substrate to be less reactive. The final possibility is that the intermediate stabilised here is not the reactive species. Spectral changes in the mutant oxyferrous complex hint at that electron transfer from the pterin is favoured in this mutant compared to the WT enzyme. It may be that by stabilisation of the active species, if it is a Compound I, that an extra electron is pulled from the pterin to the heme to form a Compound II. It is then possible that NOHA

is able to react with this Compound II, while L-Arg is not. Further work must be done to confirm which of these hypothesises is correct.

Further work must be undertaken to ascertain what this mutation can tell us about the role of H_4B in NO synthesis. Further work should be done to identify the stabilised intermediate. This could be achieved by double mixed stopped flow reactions with various oxidising and reducing agents to probe the reductive potential of the intermediate. Freeze quenching EPR experiments would allow us to test whether the stabilised intermediate is the product of a second electron being pulled off the pterin, forming a Compound II species, $Fe_{(IV)}$=O.

H_4B is a very complex molecule with redox states ranging from biopterin to dihydrobiopterin to tetrahydrobiopterin and stabilised radical states as seen in the NOS mechanism. It is used by a range of enzymes for a range of reactions. Only in NOS does it play a sublime role as oxidising and reducing agent over the course of a single turnover. With these roles for the pterin cofactor in mind, and in some cases still poorly understood, we sought to test a further possible role.

The ferrous heme-NO complex is considered a dead end complex. In normal turnover it is thought that the radical pterin cation oxidises the heme to the less stable ferric heme-NO complex, and so releases NO at the end of each turnover. However if an electron from the reductase domain is delivered before this oxidation by H_4B, then the dead-end ferrous heme-NO complex will accumulate. Since H_4B is considered to rescue the enzyme from this dead end complex in normal turnover in this way we sought to test whether electron transfer between the pterins would allow it to rescue ferrous heme-NO

build up caused by premature reduction from the reductase domain. The H_4B molecules in the nNOS dimer are bound 13Å apart. This distance is within the range of what has previously been designated as allowed for efficient electron transfer in a protein medium. Two identical molecules within this distance should set up a rapid equilibrium if one is oxidised, as electrons will transfer between them. The possibility of electron transfer between the pterins in the nNOS enzyme offered a route of recovery for the enzyme from the dead-end ferrous heme-NO complex. This was probed by stopped-flow reactions involving NO-heterodimers of the enzyme with only one of the hemes in the dimer in the ferrous heme-NO complex. Monitoring decay rates for the ferrous heme-NO complex found no difference between the rate of these NO-heterodimers, and dimers with both hemes in the ferrous heme-NO complex. This suggests either no electron transfer between the pterins, or electron transfer between the pterins is unable to rescue a heme from the dead-end complex. There is no easy explanation as to why there would not be electron transfer between the pterins, but no easy way of absolutely confirming it. One tantalising possibility is that the pterins role in the mechanism also involves proton transfer, which would slow down interpterin electron transfer. The hypothesis tested by these experiments hinged on the presumed role of H_4B as the oxidising agent in normal turnover of the ferrous heme-NO complex. If this assumption is incorrect it would allow for electron transfer to occur but the migrated radical cation would be unable to rescue the dead-end complex. If H_4B is not the oxidising agent of the ferrous heme-NO complex it would change much of our understanding of the NOS mechanism. Further work is required.

H_4B is so valuable a molecule due to its role in the synthesis of NO that its binding site represents a major drug target. NO is involved in vital physiological processes ranging from immune responses to blood vessel relaxation to angiogenesis. Antibiotics, erectile dysfunction and cancer bring pharmacology companies billions. The search for H_4B analogues that are functional in NO synthesis but also more stable and druggable is an important one. Most importantly H_4B analogues will allow the probing of the role of H_4B in NOS mechanism.

The extension with two hydroxyls on the C6 position of H_4B is not functionally necessary. All analogues that showed activity were altered in this position. More work is required to probe the role of substituents on this part of the molecule however. It may play some role in determining the tightness of pterin binding.

While none of the analogues tested in this work seem suitable as drugs, lacking the stability we sought, the binding and catalytic features of the molecules have been tested. A large range of extensions are possible in the C6 and C7 positions that allow binding of the pterin in the correct orientation and give activity. A six membered ring at the C6 and C7 position gives analogues with K_ds $<10\mu M$, showing the volume of extensions allowable in this position. An inhibitor of NOS activity with a very large and mobile chlorophenyl side chain on the six position hints at the upper limit for extension. Blocking at the C6 and C7 positions to the dihydropterine form does not abolish activity of these analogues. This offers scope for further analogue design that may lead to druggable compounds as trapping in an active dihydropterine form should remove the need for analogues to be regenerated by dihydropterine reductase.

Adding a carbonyl group next to the pterin does not affect the ability of the pterin to donate electrons. This suggests that the electronic configuration of the pterin will be able to withstand additions next to the pterin and still fulfil its redox functions.

The decay of the several of the analogues to an inactive form in solution requires further study if progress is to be made in the search for druggable active pterins. The is potential in NMR studies of the analogues in solution to uncover in what way they are becoming inactive.

For the analogues to be of further use in unravelling the role of H_4B more work must be done. The binding mode of the analogues must be probed. The electrostatic interaction of the analogues with the enzyme must also be probed. To allow this a crystal structure of NOS with the analogue bound would be most useful. The work on crystallisation should hopefully prove trivial with the basis of work here presented. The key question as yet unanswered about these analogues is why, when they all transfer electrons at rates comparable to tetrahydrobiopterin, the rates of enzyme turnover are significantly slower. That extensions to the C6 and C7 of the pterin may in some way be impairing dimerisation seems the most likely explanation.

In summary the results in this thesis have shown that:

-The two steps of NOS catalysis can be disentangled by mutagenesis of the active site residues.

-That interpterin electron transfer does not occur during the oxygen activation process.

-That large substituents can be added to the C6 and C7 positions of pterin analogues while retaining activity.

All of these results offer novel insights into the role of H4B in NOS and point to future areas of investigation.

References

1- E. Faassen, and A. F. Vanin
Radicals for life: the various forms of nitric oxide (2007)
Published by Elsevier, Netherlands

2-Ignarro LJ, Buga GM, Wood KS, Byrns RE, Chaudhuri G.

Proc Natl Acad Sci U S A. 84:9265-9. (1987)

3- Furchgott RF, Khan MT, and Jothianandan D.

Federation proceedings 46:385 (1987)

4-Ignarro L.J., Harbison R.G., Wood K.S., Kadowitz P.J.

J Pharmacol Exp Ther. 237:893-900. (1986)

5-Mannick J.B., Schonhoff C.M.

Free Radic Res. 38:1-7.(2004)

6- Gaston, B. M., Carver, J., Doctor, A., Palmer, L. A.

Mol. Interv. 3 **,** 253–263. (2003)

7- Lima B., Forrester M.T., Hess D.T., Stamler J.S.

Circ Res. 106:633-46. (2010)

8- Chen K., Popel A.S.

Biorheology. 46:107-19. (2009)

9- Foster M.W., Hess D.T., Stamler J.S.

Trends Mol Med. 15:391-404 (2009)

10- D.P. Ballou, Y. Zhao, P.E. Brandish, M.A. Marletta

PNAS, 99:19, 12097-12101 (2002)

11- Lincoln T.M.

Pharmacol Ther. 41:479-502. (1989)

12- O'Dell T.J., Hawkins R.D., Kandel E.R., Arancio O.

Proc Natl Acad Sci U S A. 88:11285-9. (1991)

13- L.J. Ignarro, J.M. Fukuto, J.M. Griscavage, N.E. Rogers, R.E. Byrns

Proc Natl Acad Sci U S A. 90: 8103–8107 (1993)

14- Kominami S. Yamazaki T., Koga T., Hori H.

J Biochem. 126:756-61. (1999)

15- Moser, C. C., Keske, J. M., Warncke, K., Farid, R. S., & Dutton, P. L.

Nature 355, 796-802, (1992)

16- Buhks E., Jortner J.

FEBS letters 109:1 (1980)

17- C. C. Moser, C. C. Page, X. Chen and P. L. Dutton

Journal of inorganic biological chemistry, 2;393-398 (1991)

18- Moser, C. C., Keske, J. M., Warncke, K., Farid, R. S., & Dutton, P. L.

Nature 355, 796-802, (1992)

19- J. N. Betts, D. N. Beratan, J. N. Onuchic,

J. Am. Chem. Soc. 114; 4043 (1992)

20- Stuehr D.J.

Biochim Biophys Acta.; 1411:217-30. (1999)

21- C. Giroud, M. Moreau, T.A. Mattioli, V. Balland, J. Boucher, Y. Xu-Li, D.J. Stuehr, J. Santolini.

Journal of Biological Chemistry 285; 7233-7245. (2010)

22- J. O. Lundberg, E. Weitzberg, M. T. Gladwin

Nature Reviews Drug Discovery 7; 156-167 (2008)

23- Cosby K., Partovi K.S., Crawford J.H., Patel R.P., Reiter C.D., Martyr S., Yang B.K., Waclawiw M.A., Zalos G., Xu X., Huang K.T., Shields H., Kim-Shapiro D.B., Schechter A.N., Cannon R.O., Gladwin M.T.

Nat Med. 9;1498-505. (2003)

24- J. O. Lundberg, E. Weitzberg

Am J Physiol Heart Circ Physiol 295: 477-478 (2008)

25- Nagababu, E., Ramasamy, S., Abernethy, D. R. & Rifkind, J. M.

Journal of Biological Chemistry 278; 46349–46356 (2003).

26- Rassaf, T.

Circ. Res. 100; 1749–1754 (2007)

27- Godber, B. L.

Journal of Biological Chemistry 275, 7757–7763 (2000)

28- Carlsson, S., Wiklund, N. P., Engstrand, L., Weitzberg, E. & Lundberg, J. O.

Nitric Oxide 5, 580–586 (2001)

29- Gago, B., Lundberg, J. O., Barbosa, R. M. & Laranjinha, J.

Free Radic. Biol. Med. 43, 1233–1242 (2007)

30- Lundberg, J. O., Weitzberg, E., Lundberg, J. M. & Alving, K.

Gut 35, 1543–1546 (1994)

31- Presta, A., Siddhanta, U., Wu, C., Sennequier, N., Huang, L., Abu-Soud, H.M., Erzurum, S., Stuehr, D.J.

Biochemistry 37; 298-310 (1998)

32- Spratt, D. E., Newman, E., Mosher, J., Ghosh, D.K., Salerno, J.C., Guillemette, J.G.

FEBS Journal 273 (2006)

33- E.D. Garcin, C.M. Bruns, S.J. Lloyd, D.J. Hosfield, M. Tiso, R. Gachhui, D.J. Stuehr, J.A. Tainer, E.D. Getzoff
Journal of Biological Chemistry 279; 37918–37927 (2004)

34- Zhou, L., Zhu, D.

Nitric Oxide 20; 223-230. (2009)

35- Garcin, E.D., Bruns, C.M., Lloyd, S.J., Hosfield, D.J., Tiso, M., Gachhui, R., Stuehr, D.J., Tainer, J.A., Getzoff, E.D.

J.Biol.Chem. 279: 37918-37927 (2004)

36- C.R. Nishida, P.R.O. Montellano

Journal of Biological Chemistry 274; 14692-14698 (1999)

37- A. Welland, S. Daff

FEBS Journal 277; 3833–3834 (2010)

38- S. Fuziwara, I. Sagami, E. Rozhkova, D. Craig, M.A. Noble, A.W. Munro, S.K. Chapman, T. Shimizu

Journal of Inorganic Biochemistry 91; 515-526 (2002)

39- K. Knight, N.S. Scrutton

Biochem J. 367; 19–30. (2002)

40- Sagami, I., Sato, Y., Noguchi, T., Miyajima, M., Rozhkova, E., Daff, S. and Shimizu, T.

Coord. Chem. Rev. 226, 179-186 (2002)

41- Abu-Soud H.M., Yoho L.L., Stuehr D.J.

J Biol Chem 269, 32047–32050. (1994)

42- Deng Z., Aliverti A., Zanetti G., Arakaki A. K., Ottado J., Orellano E. G., Calcaterra N. B., Ceccarelli E. A., Carrillo N., Karplus P. A.

Nat. Struct. Biol. 6:847–853 (1999)

43- K. Panda, M.M. Haque, E.D.Garcin-Hosfield, D. Durra, E.D. Getzoff, D.J. Stuehr.

Journal of Biological Chemistry 281, 36819-36827. (2006)

44- K. Yamamoto, S. Kimura, Y. Shiro, T. Iyanagi.

Archives of Biochemistry and Biophysics 440; 65-78 (2005)

45- Lowe P.N., Smith D., Stammers D.K., Riveros-Moreno V., Moncada S., Charles I., Boyhan A.

Biochem J. 314: 55-62. (1996)

46- H. Kuboniwa, N. Tjandra, S. Grzesiek, H. Ren, C.B. Klee, A. Bax

Nature Structural Biology 2; 768 - 776 (1995)

47- R.C. Venema, H.S. Sayegh, J.D. Kent, D.G. Harrison

The Journal of Biological Chemistry, 271, 6435-6440 (1996)

48- C. Feng, L. Roman, J. Hazzard, D. Ghosh, G. Tollin, B. Masters

FEBS Letters, 582; 2768-2772 (2008)

49- Qie Q. W., Cho H., Kashiwabara Y., Baum M., Weidner J. R., Elliston K., Mumford R., Nathan C.

Journal of Biological Chemistry 269:28500–28505. (1994)

50- Roman L. J., Miller R. T., de La Garza M. A., Kim J. J., Siler Masters B. S.

Journal of Biological Chemistry 275:21914–21919. (2000)

51- Roman L. J., Martasek P., Miller R. T., Harris D. E., de La Garza M. A., Shea T. M., Kim J. J., Masters B. S.

Journal of Biological Chemistry 275:29225–29232. (2000)

52- L.J. Roman, B.S. Masters

Journal of Biological Chemistry, 281; 23111-23118. (2006)

53- D.H. Craig, S.K. Chapman, S. Daff

Journal of Biological Chemistry, 277; 33987-33994 (2002)

54- S.L. Delker, H. Ji, H. Li, J. Jamal, J. Fang, F. Xue, R.B. Silverman, T.L. Poulos

J. Am. Chem. Soc. 132; 5437–5442 (2010)
55- Deng Z., Aliverti A., Zanetti G., Arakaki A. K., Ottado J., Orellano E. G., Calcaterra N. B., Ceccarelli E. A., Carrillo N., Karplus P. A.

Nat. Struct. Biol. 6:847–853 (1999)

56- Doukov, T., Li, H., Soltis, M., Poulos, T.L.

Biochemistry 48; 10246-10254 (2009)

57- McInnes, C.R., Suckling, C.J., Gibson, C.L., Morthala, R., Daff, S., Gazur, B.

Pteridines 20; 27-35 (2009)

58- H.J. Cho, E. Martin, Q. Xie, S. Sassa, C. Nathan

Proc. Natl. Acad. Sci. USA 92; 11514-11518 (1995)

59- K. Pant, B.R. Crane

Journal of Molecular Biology 352; 932-940 (2005)

60- Davis M.D., Kaufman S., Milstien S.

Eur J Biochem. 173; 345-51 (1998)

61- Stoll S., NejatyJahromy Y., Woodward J.J., Ozarowski A., Marletta M.A., Britt R.D.

J Am Chem Soc. 132:11812-23. (2010)

62- D.K. Menyhárd

Chemical Physics Letters 392, 439-443 (2004)

63- P.F. Fitzpatrick

Annual Review of Biochemistry 68: 355-381 (1999)

64- K. Teigen, K.K. Dao, J.A. McKinney, A.C.F. Gorren, B. Mayer, N.Å. Frøystein, J. Haavik, A. Martínez

J. Med. Chem. 47 (24), 5962–5971 (2004)

65- Andersen, O.A., Stokka, A.J., Flatmark, T., Hough, E.

J.Mol.Biol. **333:** 747-757 (2003)

66- Bigham E.C., Smith G.K., Reinhard J.F., Mallory W.R., Nichol C.A., Morrison R.W.

J Med Chem.;30(1):40-5. (1987)

67- United States Patent 5874433

68- Frantom P.A., Seravalli J., Ragsdale S.W., Fitzpatrick P.F.

Biochemistry. 45: 2372-9. (2006)

69- P.R.O. Montellano, J. J. De Voss

Nat. Prod. Rep., 19, 477–493 (2002)

70- Paul R. Ortiz de Montellano

Cytochrome P450: structure, mechanism, and biochemistry (available online)

71- Sono M., Roach M.P., Coulter E.D., Dawson J.H.

Chem Rev. 96: 2841-2888. (1996)

72- S. Modi, M.J. Sutcliffe, W.U. Primrose, L. Lian, G.C.K. Roberts

Nature Structural Biology 3; 414 - 417 (1996)

73- M. Newcomb, R. Zhang, R. E.P. Chandrasena, J.A. Halgrimson, J.H. Horner, T.M. Makris, S.G. Sligar

J Am Chem Soc. 128; 4580–4588 (2006)

74- J. Rittle, M.T. Green

Science 330; 933-937 (2010)

75- Ogliaro, F., Harris, N., Cohen, S., Filatov, M., Visser, S.P. de, Shaik, S.

J. Am. Chem. Soc., 122, 8977-8989 (2000)

76- R. Davydov, T.M. Makris, V. Kofman, D.E. Werst, S.G. Sligar, B.M. Hoffman

J. Am. Chem. Soc., 123; 1403–1415 (2001)

77- D. Hamdane, H. Zhang, P. Hollenberg

Photosynth Res., 98; 657–666. (2008)

78- A. Presta, A.M. Weber-Main, M.T. Stankovich, D.J. Stuehr

J. Am. Chem. Soc., 120; 9460–9465 (1998)

79- Abu-Soud H.M., Ichimori K., Presta A., Stuehr D.J.

J Biol Chem. 275; 17349-57. (2000)

80- Gao Y.T., Panda S.P., Roman L.J., Martásek P., Ishimura Y., Masters B.S.

J Biol Chem. 282; 7921-9. (2007)

81- R. Davydov, R. Kappl, J. Hüttermann, J. A. Peterson

FEBS letters 295; 113-115 (1991)

82- Hurshman A.R., Krebs C., Edmondson D.E., Huynh B.H., Marletta M.A.

Biochemistry. 38; 15689-96. (1999)

83- Ost T.W., Daff S.

J Biol Chem. 280; 965-73. (2005)

84-Wei C.C., Wang Z.Q., Tejero J., Yang Y.P., Hemann C., Hille R., Stuehr D.J.

J Biol Chem. 283; 11734-42. (2008)

85- Woodward J.J., Chang M.M., Martin N.I., Marletta M.A.

J Am Chem Soc. 131; 297-305. (2009)

86- R. Davydov, A. Ledbetter-Rogers, P. Martásek, M. Larukhin, M. Sono, J.H. Dawson, B.S. Masters, B.M. Hoffman

Biochemistry, 41; 10375–10381 (2002)

87- Goloubinoff, P., Gatenby, A.A and Lorimer, G.H.

J. Inher. Metab. Dis. 17; 661–663. (1989)

88- R.A. Pufahl, J.S. Wishnok, M.A. Marletta

Biochemistry, 34; 1930–1941 (1995)

89- V. M. Ivanov

J. of analytical chemistry. 59; 1002-1005, (1979)

90- Sorlie M., Gorren A.C., Marchal S., Shimizu T., Lange R., Andersson K.K., May G.

J Biol Chem. 278; 48602-10. (2003)

91- H.M. Abu-Soud, A. Presta, B. Mayer, D.J. Stuehr

Biochemistry, 36; 10811–10816 (1997)

92- Robinet, J. J., Cho, K-B. and Gauld, J. W

J. Am. Chem. Soc. 130; 3328-3334. (2008)

93- Martin, N.I., Woodward, J.J., Winter, M.B., Marletta, M.A.

Bioorganic & Medicinal Chemistry Letters 19; 1758-1762. (2009)

94- Vidakovic M., Sligar S.G., Li H., Poulos T.L.

Biochemistry. 37; 9211-9. (1998)

95- Tejero, J., Biswas, A., Wang, Z., Page, R.C., Haque, M.M., Hemann, C., Zweier, J.L., Misra, S., Stuehr, D.J.

Journal of Biological Chemistry 283; 33498-33507 (2008)

96- C.T. Migita, J.C. Salerno, B.S. Masters, P. Martasek, K. McMillan, M. Ikeda-Saito

Biochemistry 36: 10987-92. (1997)

97- Sliger, S.G.

Science 330; 924-925 (2010)

98- M. J. Clague, J. S. Wishnok, M. A. Marletta

Biochemistry, 36, 14465–14473 (1997)

99- S. Daff

Nitric Oxide 23; 1-11. (2010)

100- Gorren A.C., Mayer B.

Biochim Biophys Acta. 1770; 432-45. (2007)

101- I.G. Denisov, J.H. Dawson, L.P. Hager, S.G. Sligar

Biochem Biophys Res Commun. 363; 954–958. (2007)

102- S.R. Bell, J.T. Groves

J. Am. Chem. Soc., 131; 9640–9641 (2009)

103- Spolitak, T., Dawson, J. H. and Ballou, D. P.

Journal of Biological Chemistry 280, 20300-20309. (2005)

104- Sheng, X., Homer, J. H. and Newcomb, M.

J. Am. Chem. Soc. 130; 13310-13320. (2008)

105- H.L. Voegtle, M. Sono, S. Adak, A.E. Pond, T. Tomita, R. Perera, D.B. Goodin, M. Ikeda-Saito, D.J. Stuehr, J.H. Dawson

Biochemistry, 42; 2475-2484 (2003)

106- De Visser, S. P. and Tan, L. S.

J. Am. Chem. Soc. 130, 12961-12974 (2008)

107- Abu-Soud H.M., Wu C., Ghosh D.K., Stuehr D.J.

Biochemistry. 37; 3777-86. (1998)

108- H.M. Abu-Soud, J. Wang, D.L. Rousseau, J.M. Fukuto, L.J. Ignarro, D.J. Stuehr

Journal of biological chemistry 270; 22997–23006 (1995)

109- V. M. Ivanov

J. of analytical chemistry. 59; 1002-1005 (1995)

110- J. Tejero, J. Santolini, D.J. Stuehr

FEBS J. 276; 4505–4514. (2009)

111- C. Wei, Z. Wang, Q. Wang, A.L. Meade, C. Hemann, R. Hille, D.J. Stuehr

Journal of biological chemistry 276; 315–319, (2001)

112- Ayling J.E., Bailey S.W., Boerth S.R., Giugliani R., Braegger C.P., Thöny B., Blau N.

Mol Genet Metab. 70; 179-88. (2000)

113- W. Shi, C.J. Meininger, T.E. Haynes, K. Hatakeyama, G. Wu

Cell biochemistry and biophysics, 41; 415-433, (2006)

114- C.O. Harding

Biologics. 4; 231–236. (2010)

115- E. Podjarny, G. Hasdan, J. Bernheim, G. Rashid, J. Green, Z. Korzets، J. Bernheim

Nephrology Dialysis Transplantation 19; 2223-2227. (2005)

116- Gorren A.C., Sørlie M., Andersson K.K., Marchal S., Lange R., Mayer B.

Methods Enzymol. 396; 456-66. (2005)

117- Suckling C.J., Gibson C.L., Huggan J.K., Morthala R.R., Clarke B., Kununthur S., Wadsworth R.M., Daff S., Papale D.

Bioorg Med Chem Lett.;18(5):1563-6. (2008).

118- http://www.schircks.com/pteridines/data/data_sheet_11.209.htm

119- M.L. Dántola, A.H. Thomas, E. Oliveros, C. Lorente

Journal of Photochemistry and Photobiology A: Chemistry 209; 104-110 (2010)

120- K. Panda, S. Ghosh, D.J. Stuehr

Journal of biological chemistry 276; 23349 –23356 (2001)

121- C.R. Nishida, P.R.O. de Montellano

Journal of biological chemistry 273; 5566 –5571, (1998)

122- U. Siddhanta, A. Presta, B. Fan, D. Wolan, D.L. Rousseau, D.J. Stuehr

Journal of biological chemistry 273; 18950 –18958, (1998)

Appendix 1: nNOS sequence

From *Rattus norvergicus*

Amino acid sequence

```
        10         20         30         40         50         60
MEENTFGVQQ IQPNVISVRL FKRKVGGLGF LVKERVSKPP VIISDLIRGG AAEQSGLIQA
        70         80         90        100        110        120
GDIILAVNDR PLVDLSYDSA LEVLRGIASE THVVLILRGP EGFTTHLETT FTGDGTPKTI
       130        140        150        160        170        180
RVTQPLGPPT KAVDLSHQPS ASKDQSLAVD RVTGLGNGPQ HAQGHGQGAG SVSQANGVAI
       190        200        210        220        230        240
DPTMKSTKAN LQDIGEHDEL LKEIEPVLSI LNSGSKATNR GGPAKAEMKD TGIQVDRDLD
       250        260        270        280        290        300
GKSHKAPPLG GDNDRVFNDL WGKDNVPVIL NNPYSEKEQS PTSGKQSPTK NGSPSRCPRF
       310        320        330        340        350        360
LKVKNWETDV VLTDTLHLKS TLETGCTEHI CMGSIMLPSQ HTRKPEDVRT KDQLFPLAKE
       370        380        390        400        410        420
FLDQYYSSIK RFGSKAHMDR LEEVNKEIES TSTYQLKDTE LIYGAKHAWR NASRCVGRIQ
       430        440        450        460        470        480
WSKLQVFDAR DCTTAHGMFN YICNHVKYAT NKGNLRSAIT IFPQRTDGKH DFRVWNSQLI
       490        500        510        520        530        540
RYAGYKQPDG STLGDPANVQ FTEICIQQGW KAPRGRFDVL PLLLQANGND PELFQIPPEL
       550        560        570        580        590        600
VLEVPIRHPK FDWFKDLGLK WYGLPAVSNM LLEIGGLEFS ACPFSGWYMG TEIGVRDYCD
       610        620        630        640        650        660
NSRYNILEEV AKKMDLDMRK TSSLWKDQAL VEINIAVLYS FQSDKVTIVD HHSATESFIK
       670        680        690        700        710        720
HMENEYRCRG GCPADWVWIV PPMSGSITPV FHQEMLNYRL TPSFEYQPDP WNTHVWKGTN
       730        740        750        760        770        780
GTPTKRRAIG FKKLAEAVKF SAKLMGQAMA KRVKATILYA TETGKSQAYA KTLCEIFKHA
       790        800        810        820        830        840
FDAKAMSMEE YDIVHLEHEA LVLVVTSTFG NGDPPENGEK FGCALMEMRH PNSVQEERKS
       850        860        870        880        890        900
YKVRFNSVSS YSDSRKSSGD GPDLRDNFES TGPLANVRFS VFGLGSRAYP HFCAFGHAVD
       910        920        930        940        950        960
TLLEELGGER ILKMREGDEL CGQEEAFRTW AKKVFKAACD VFCVGDDVNI EKPNNSLISN
       970        980        990       1000       1010       1020
```

```
DRSWKRNKFR LTYVAEAPDL TQGLSNVHKK RVSAARLLSR QNLQSPKFSR STIFVRLHTN
      1030       1040       1050       1060       1070       1080
GNQELQYQPG DHLGVFPGNH EDLVNALIER LEDAPPANHV VKVEMLEERN TALGVISNWK
      1090       1100       1110       1120       1130       1140
DESRLPPCTI FQAFKYYLDI TTPPTPLQLQ QFASLATNEK EKQRLLVLSK GLQEYEEWKW
      1150       1160       1170       1180       1190       1200
GKNPTMVEVL EEFPSIQMPA TLLLTQLSLL QPRYYSISSS PDMYPDEVHL TVAIVSYHTR
      1210       1220       1230       1240       1250       1260
DGEGPVHHGV CSSWLNRIQA DDVVPCFVRG APSFHLPRNP QVPCILVGPG TGIAPFRSFW
      1270       1280       1290       1300       1310       1320
QQRQFDIQHK GMNPCPMVLV FGCRQSKIDH IYREETLQAK NKGVFRELYT AYSREPDRPK
      1330       1340       1350       1360       1370       1380
KYVQDVLQEQ LAESVYRALK EQGGHIYVCG DVTMAADVLK AIQRIMTQQG KLSEEDAGVF
      1390       1400       1410       1420
```

```
ISRLRDDNRY HEDIFGVTLR TYEVTNRLRS ESIAFIEESK KDADEVFSS
```

DNA Sequence

1 atggaagaga acacgtttgg ggttcagcag atccaaccca atgtaatttc
51 tgttcgtctc ttcaaacgca aagtgggagg tctgggcttc ctggtgaagg
101 aacgggtcag caagcctccc gtgatcatct cagacctgat tcgaggaggt
151 gctgcggagc agagcggcct tatccaagct ggagacatca ttctcgcagt
201 caacgatcgg cccttggtag acctcagcta tgacagtgcc ctggaggttc
251 tcaggggcat tgcctctgag acccacgtgg tcctcattct gaggggccct
301 gagggcttca ctacacatct ggagaccacc ttcacagggg atggaacccc
351 caagaccatc cgggtgaccc agcccctcgg tcctcccacc aaagccgtcg
401 atctgtctca ccagccttca gccagcaaag accagtcatt agcagtagac
451 agagtcacag gtctgggtaa tggccctcag catgcccaag gccatgggca
501 gggagctggc tcagtctccc aagctaatgg tgtggccatt gaccccacga
551 tgaaaagcac caaggccaac ctccaggaca tcggggaaca tgatgaactg
601 ctcaaagaga tagaacctgt gctgagcatc ctcaacagtg ggagcaaagc
651 caccaacaga gggggaccag ccaaagcaga gatgaaagac acaggaatcc
701 aggtggacag agacctcgat ggcaaatcgc acaaagctcc gcccctgggc
751 ggggacaatg accgcgtctt caatgacctg tgggggaagg acaacgttcc
801 tgtggtcctt aacaacccgt attcagagaa ggaacagtcc cctacctcgg
851 ggaaacagtc tcccaccaag aacggcagcc cttccaggtg cccccgtttc
901 ctcaaggtca agaactggga gacggacgtg gtcctcaccg acaccctgca
951 cctgaagagc acactggaaa cggggtgcac agagcacatt tgcatgggct
1001 cgatcatgct gccttcccag cacacgcgga agccagaaga tgtccgcaca
1051 aaggaccagc tcttccctct agccaaagaa tttctcgacc aatactactc
1101 atccattaag agatttggct ccaaggccca catggacagg ctggaggagg
1151 tgaacaagga gattgaaagc accagcacct accagctcaa ggacaccgag
1201 ctcatctatg gcgccaagca tgcctggcgg aacgcctctc gatgtgtggg
1251 caggatccag tggtccaagc tgcaggtgtt cgatgcccga gactgcacca
1301 cagcccacgg catgttcaac tacatctgta accatgtcaa gtatgccacc
1351 aacaaaggga atctcaggtc ggccatcacg atattccctc agaggactga
1401 cggcaaacat gacttccgag tgtggaactc gcagctcatc cgctacgcgg
1451 gctacaagca gccagatggc tctaccttgg gggatccagc caatgtgcag
1501 ttcacggaga tctgtataca gcagggctgg aaagccccaa gaggccgctt
1551 cgacgtgctg cctctcctgc ttcaggccaa tggcaatgac cctgagctct
1601 tccagatccc cccagagctg gtgctggaag tgcccatcag gcaccccaag
1651 ttcgactggt ttaaggacct ggggctcaaa tggtatggcc tccccgctgt
1701 gtccaacatg ctgctggaga tcgggggcct ggagttcagc gcctgtccct
1751 tcagcggctg gtacatgggc acagagatcg gcgtccgtga ctactgtgac
1801 aactctcgat acaacatcct ggaggaagta gccaagaaga tggatttgga
1851 catgaggaag acctcgtccc tctggaagga ccaagcactg gtggagatca
1901 acattgctgt tctatatagc ttccagagtg acaaggtgac catcgttgac
1951 caccactctg ccacggagtc cttcatcaaa cacatggaga atgaataccg
2001 ctgcagaggg ggctgccccg ccgactgggt gtggattgtg cctcccatgt
2051 cgggcagcat cacccctgtc ttccaccagg agatgctcaa ctatagactc
2101 accccgtcct ttgaatacca gcctgatcca tggaacaccc acgtgtggaa

2151 gggcaccaac gggaccccca cgaagcggcg agctatcggc tttaagaaat
2201 tggcagaggc cgtcaagttc tcagccaagc taatggggca ggccatggcc
2251 aagagggtca aggcgaccat tctctacgcc acagagacag gcaaatcaca
2301 agcctatgcc aagaccctgt gtgagatctt caagcacgcc ttcgatgcca
2351 aggcaatgtc catggaggag tatgacatcg tgcacctgga gcacgaagcc
2401 ctggtcttgg tggtcaccag cacctttggc aatggagacc cccctgagaa
2451 cggggagaaa ttcggctgtg ctttaatgga gatgaggcac cccaactctg
2501 tgcaggagga gagaaagagc tacaaggtcc gattcaacag cgtctcctcc
2551 tattctgact cccgaaagtc atcgggcgac ggacccgacc tcagagacaa
2601 ctttgaaagt actggacccc tggccaatgt gaggttctca gtgttcggcc
2651 tcggctctcg ggcgtacccc cacttctgtg cctttgggca tgcggtggac
2701 accctcctgg aggaactggg aggggagagg attctgaaga tgagggaggg
2751 ggatgagctt tgcggacagg aagaagcttt caggacctgg gccaagaaag
2801 tcttcaaggc agcctgtgat gtgttctgcg tgggggatga cgtcaacatc
2851 gagaaggcga acaactccct cattagcaat gaccgaagct ggaagaggaa
2901 caagttccgc ctcacgtatg tggcggaagc tccagatctg acccaaggtc
2951 tttccaatgt tcacaaaaaa cgagtctcgg ctgctcgact cctcagccgc
3001 caaaacctgc aaagccctaa gtccagccga tcgaccatct tcgtgcgtct
3051 ccacaccaac gggaatcagg agctgcagta ccagccaggg gaccacctgg
3101 gtgtcttccc cggcaaccac gaggacctcg tgaatgcact cattgaacgg
3151 ctggaggatg caccgcctgc caaccacgtg gtgaaggtgg agatgctgga
3201 ggagaggaac actgctctgg gtgtcatcag taattggaag gatgaatctc
3251 gcctcccacc ctgcaccatc ttccaggcct tcaagtacta cctggacatc
3301 accacgccgc ccacgcccct gcagctgcag cagttcgcct ctctggccac
3351 taatgagaaa gagaagcagc ggttgctggt cctcagcaag gggctccagg
3401 aatatgagga gtggaagtgg ggcaagaacc ccacaatggt ggaggtgctg
3451 gaggagttcc cgtccatcca gatgccggct acacttctcc tcactcagct
3501 gtcgctgctg cagcctcgct actactccat cagctcctct ccagacatgt
3551 accccgacga ggtgcacctc actgtggcca tcgtctccta ccacacccga
3601 gacggagaag gaccagtcca ccacggggtg tgctcctcct ggctcaacag
3651 aatacaggct gacgatgtag tcccctgctt cgtgagaggt gcccctagct
3701 tccacctgcc tcgaaacccc caggtgcctt gcatcctggt tggcccaggc
3751 actggcatcg cacccttccg aagcttctgg caacagcgac aatttgacat
3801 ccaacacaaa ggaatgaatc cgtgccccat ggttctggtc ttcgggtgtc
3851 gacaatccaa gatagatcat atctacagag aggagaccct gcaggccaag
3901 aacaagggcg tcttcagaga gctgtacact gcctattccc gggaaccgga
3951 caggccaaag aaatatgtac aggacgtgct gcaggaacag ctggctgagt
4001 ctgtgtaccg cgccctgaag gagcaaggag gccacattta tgtctgtggg
4051 gacgttacca tggccgccga tgtcctcaaa gccatccagc gcataatgac
4101 ccagcagggg aaactctcag aggaggacgc tggtgtattc atcagcaggc
4151 tgagggatga caaccggtac cacgaggaca tctttggagt caccctcaga
4201 acgtatgaag tgaccaaccg ccttagatct gagtccatcg ccttcatcga
4251 agagagcaaa aaagacgcag atgaggtttt cagctcctaa